EVOLUTION OF KARST IN THE LOWER SUWANNEE RIVER BASIN, FLORIDA

By

CAN DENIZMAN

A DISSERTATION PRESENTED TO THE GRADUATE SCHOOL
OF THE UNIVERSITY OF FLORIDA IN PARTIAL FULFILLMENT
OF THE REQUIREMENTS FOR THE DEGREE OF
DOCTOR OF PHILOSOPHY

UNIVERSITY OF FLORIDA

1998

To the memory of my brother, Levent Denizman.
Nous sommes du soleil.

ACKNOWLEDGEMENTS

I would like to express my sincere thanks to my supervisor, Dr. Anthony Randazzo, for his guidance and encouragement during various stages of this study. I am also grateful to my other committee members for their assistance and input, especially to Dr. Dan Spangler from whom I learned much of my knowledge on the hydrogeology of Florida.

Acknowledgements for assistance in data collection are extended to Ron Ceryak from the Suwannee River Water Management District and Jonathan Arthur from the Florida Geological Survey.

I am grateful to David Reed from the St. Johns River Water Management District (SJRWMD) for his generous assistance and creative ideas regarding many GIS operations performed in this study. Thanks are also due to Palmer Kinser and Marc Minno from the SJRWMD for their understanding and encouragement.

Additional thanks go to Yasar Yesilcay and Fuat Sener for their assistance in the application of statistical techniques. I am also grateful to Ron Ozbun from the Geology Department office of the University of Florida for his effort and time spent in resolving many complicated issues regarding my appointment as a research assistant.

Very special thanks to my wife, Isik, for her love, support and patience.

Finally, to John McLaughlin and many others for the music.

TABLE OF CONTENTS

page

ACKNOWLEDGEMENTS iii

LIST OF TABLES vii

LIST OF FIGURES ix

ABSTRACT xii

CHAPTERS

1 INTRODUCTION 1

Climate 4
Physiographic Setting 4
Geologic Structure 7
Geological Setting 10
Hydrogeologic Setting 12
Karst in Florida 15

2 MORPHOMETRIC AND SPATIAL DISTRIBUTION PARAMETERS OF KARSTIC DEPRESSIONS 21

Prospectus 21
Background 22
Methodology 26
Results 29
  Depression Density 29
  Planimetric Shape 37
  Mean Diameter 40
  Depth of Karstic Depressions 41
Discussion 43

3 FACTORS AFFECTING DEPRESSION MORPHOMETRY AND DISTRIBUTION 46

Prospectus 46
Methodology 50

Results........52
Lithology of the Vadose Zone........52
Thickness of the Overburden Material........54
Floridan Aquifer Potentiometric Level Fluctuation........60
Soil Type........64
Depth to Water Table........68
Photolineaments and Orientation of Depressions........73
Topographic Slope........76
Reported Sinkholes........78
Discussion........88

4 KARSTIC EROSION RATE CALCULATIONS........97

Prospectus........97
Background........98
Methodology........100
Results........106
Discussion........112

5 EVOLUTION OF KARST IN THE SUWANNEE RIVER AREA........115

Prospectus........115
Background........116
Methodology........118
Results........120
Morphometric Evolution of Karstic Depressions........120
Depression area........123
Mean depression diameter........126
Planimetric shapes and allometry of depressions........128
Evolution of the Spatial Distribution of Depressions........136
Discussion........144
Conceptual Model of Karst Evolution........148

6 SUMMARY AND CONCLUSIONS........158

APPENDICES

A DEPRESSION AREA AND LENGTH-WIDTH RELATIONSHIP FOR TOPOGRAPHIC QUADRANGLES........164

B DEPRESSION LENGTH AND WIDTH RELATIONSHIPS FOR TOPOGRAPHIC QUADRANGLES........177

C FLOW DURATION CURVES........190

D ALLOMETRIC RELATIONSHIPS FOR ELEVATION RANGES AND MARINE TERRACES 193

E LENGTH-WIDTH RATIO AND AREA RELATIONSHIP WITHIN ELEVATION RANGES 201

LIST OF REFERENCES 205

BIOGRAPHICAL SKETCH 214

LIST OF TABLES

Table page

2.1. Morphometric and spatial distribution parameters for topographic quadrangles. 30
2.2. Statistical summary of morphometric parameters 44
2.3. Depression density and nearest neighbor statistics for various karst areas 45
3.1. Percentages of areas corresponding to depression density ranges for the vadose zone lithologies. 52
3.2. Percentages of areas corresponding to depression density ranges for the zones of the overburden thickness 57
3.3. Percentages of areas corresponding to depression density ranges for the zones of Floridan aquifer potentiometric level fluctuations. 60
3.5. Percentages of areas corresponding to depression density ranges for the zones of the depth to water table. 71
3.6. Summary of the mean morphometric parameters and the clay content within the zones of the overburden thickness 93
3.7. Summary of the mean morphometric parameters and the clay contents within the zones of the depth to water table 95
4.1.Statistical summary of hydrologic and chemical parameters for the Santa Fe River basin. 109
4.2. Statistical summary of hydrologic and chemical parameters for the Upper Suwannee River basin 110
4.3.Statistical summary of hydrologic and chemical parameters for the Lower Suwannee River basin 111
4.4. Published erosion rates of different geographic locations 113
5.1. Statistical summary of depression area (m^2) within the ranges of elevation 124
5.2. Statistical summary of the depression area (m^2) within the marine terraces. 125
5.3. Statistical summary of mean depression diameter (m) within the ranges of elevation 126
5.4. Statistical summary of the mean diameter (m) within the marine terraces. 127
5.5. Statistical summary of the length/width ratio within the ranges of elevation. 128
5.6. Statistical summary of the circularity index within the ranges of elevation 129
5.6. Statistical summary of the length/width ratio within the marine terraces 130
5.7. Statistical summary of the circularity index within the marine terraces. 131
5.8. Allometric relationships in elevation ranges. 132
5.9. Allometric relationships within marine terraces 133
5.10. Statistical summary of depression density within elevation ranges 137
5.11. Statistical summary of depression density within marine terraces. 138

5.12. Statistical summary of mean nearest neighbor distance (m) within the elevation ranges. 139
5.13. Statistical summary of nearest neighbor distance (m) within marine terraces. 140
5.14. Summary of mean spatial parameters. 141
5.15. Summary of mean morphometric parameters. 148

LIST OF FIGURES

Figure page

1.1. The study area. 3
1.2. Physiographic regions. 5
1.3. Structural features of Florida 8
1.4. Hydrostratigraphic column for the Suwannee River Basin 13
1.5. Drawdown doline initiation in the subcutaneous (epikarstic) zone 19
2.1. Names and location of topographic quadrangles within the study area. 27
2.2. Histogram of depression density distribution. 31
2.3. Distribution of depression density. 32
2.4. Histogram of nearest neighbor index. 34
2.5. Distribution of nearest neighbor index within the study area. 35
2.6. Percent frequency of nearest neighbor distance.......... 36
2.7. Cumulative percentage of nearest neighbor distance. 36
2.8. Percent frequency of L/W ratio. 38
2.9. Cumulative percentage of L/W ratio.......... 38
2.10. Percent frequency of circularity index.......... 39
2.11. Cumulative percentage of circularity index. 39
2.12. Percent frequency of mean diameter. 40
2.13. Cumulative percentage of mean diameter. 40
2.14. Cumulative percentage of depression area. 41
2.15. Depth-frequency distribution for the depressions. 42
3.1. Distribution of the vadose zone lithology within the study area.......... 53
3.2. Distribution of depression density within the vadose zone lithologies.......... 54
3.3. Distribution of overburden thickness within the study area. 55
3.4. Changes in depression density within the zones of the overburden thickness 56
3.5. Changes in vadose zone lithology with the thickness of the overburden. 58
3.6. Changes in mean depression area with the overburden thickness.......... 58
3.7. Changes in mean depression diameter with the overburden thickness.......... 59
3.8 Changes in mean length/width ratio with the overburden thickness. 59
3.9. Fluctuation of the Floridan aquifer potentiometric level. 61
3.10. Changes in mean depression density with the potentiometric fluctuation. 62
3.11. Changes in mean depression area with potentiometric fluctation. 63
3.12. Changes in mean depression diameter with potentiometric fluctation. 63
3.13. Changes in mean length/width ratio with potentiometric fluctation. 64
3.14. Distribution of soil types within the study area. 65
3.15. Changes in mean depression density with soil types. 66
3.16. Changes in mean depression area with soil types. 67

3.17. Changes in mean depression diameter with soil types.. 67
3.18. Changes in mean length/width ratio with soil types.. 68
3.19. Distribution of depth to water table within the study area..................................... 69
3.20. Changes in mean depression density with depth to water table............................. 70
3.21. Changes in vadose zone lithology with depth to water table................................. 70
3.22. Changes in mean depression area with depth to water table.................................. 72
3.23. Changes in mean depression diameter with depth to water table........................... 72
3.24. Changes in mean depression length/width ratio with depth to water table............. 73
3.25. Map of photolinears and karstic depression density within the study area.............. 74
3.26. Histogram of depression major axis orientations.. 75
3.27. Histogram of nearest neighbor directions.. 76
3.28. Map of topographic slope within the study area.. 77
3.29. Histogram of topographic slope distribution within the study area........................ 78
3.30. Distribution of reported sinkholes within the study area.. 79
3.31. Changes in reported sinkhole frequency with vadose zone lithology...................... 81
3.32. Changes in mean diameter with vadose zone lithology for reported sinkholes........ 81
3.33. Changes in mean depth with vadose zone lithology for reported sinkholes. 83
3.34. Changes in mean length/width ratio with vadose zone lithology for reported sinkholes.. 83
3.35. Changes in reported sinkhole frequency with potentiomeric level fluctuation of the Floridan aquifer.. 84
3.36. Changes in mean diameter with potentiomeric level fluctuation of the Floridan aquifer for reported sinkholes.. 84
3.37. Changes in mean length/width ratio with potentiometric level fluctuation of the Floridan aquifer for reported sinkholes.. 85
3.38. Changes in mean depth with potentiometric level fluctuation of the Floridan aquifer for reported sinkholes.. 85
3.39. Changes in reported sinkhole frequency with depth to water table......................... 86
3.40. Changes in mean diameter with depth to water table for reported sinkholes. 86
3.41. Changes in mean length/width ratio with depth to water table for reported sinkholes.. 87
3.42. Changes in mean depth with depth to water table for reported sinkholes................ 87
3.43. Changes in reported sinkhole frequency with the thickness of the overburden material.. 89
3.44. Changes in mean depth with the thickness of the overburden material for reported sinkholes.. 89
3.45. Changes in mean diameter with the thickness of the overburden material for reported sinkholes.. 90
3.46. Changes in mean length/width ratio with the thickness of the overburden material for reported sinkholes.. 90
3.47. Changes in reported sinkhole frequency with the soil type.................................... 91
3.48. Changes in mean length/width ratio with the soil type.. 91
3.49. Changes in mean diameter with the soil type for reported sinkholes...................... 92
3.50. Changes in mean area with the soil type for reported sinkholes............................ 92

4.1. Location map of flow and water quality stations.............................. 101
4.2. Discharge – hardness relationship for the Upper Suwannee River basin. 103
4.3. Discharge – hardness relationship for the Santa Fe River basin. 103
4.4. Discharge – hardness relationship for the Lower Suwannee River basin................ 104
4.5. Discharge – mass flux relationship for the Upper Suwannee River basin. 104
4.6. Discharge – mass flux relationship for the Santa Fe River basin. 105
4.7. Discharge – mass flux relationship for the Lower Suwannee River basin............... 106
4.8. Annual dissolved load carried by different flows in the Upper Suwannee River basin... 108
4.9. Annual dissolved load carried by different flows in the Santa Fe River basin. 108
4.10. Annual dissolved load carried by different flows in the Lower Suwannee River basin... 109
4.11. Seasonal changes of the flow and mass flux for the Upper Suwannee River basin. 110
4.12. Seasonal changes of the flow and mass flux for the Santa Fe river basin.............. 111
4.13. Seasonal changes of the flow and mass flux for the Lower Suwannee River basin. 111
5.1. Map of elevation.. 121
5.2. Map of the marine terraces within the study area. 122
5.3. Changes in mean depression area with elevation. 124
5.4. Changes in depression area with marine terraces. 125
5.5. Changes in mean depression diameter with topography. 127
5.6. Changes in mean depression diameter with marine terraces.................................. 127
5.7. Changes in mean length/width ratio with topography... 129
5.8. Changes in mean circularity index with topography. 129
5.9. Changes in mean length/width ratio with marine terraces..................................... 131
5.10. Changes in mean circularity index with elevation. 131
5.11. Changes in allometric growth rate (a) with elevation. 134
5.12. Changes in allometric growth rate (a) with marine terraces................................ 136
5.13. Changes in depression density with elevation... 138
5.14. Changes in depression density with marine terraces. 139
5.15. Changes in mean nearest neighbor distance with elevation. 140
5.16. Changes in mean nearest neighbor distance with marine terraces. 141
5.17. Changes in pitting index with distance from the Cody Escarpment...................... 142
5.18. Zones of equal distance from the Cody Escarpment.. 143
5.19 (a-f). Evolution of karst in the Suwannee river area, Late Oligocene to recent. 150

Abstract of Dissertation Presented to the Graduate School
of the University of Florida in Partial Fulfillment of the
Requirements for the Degree of Doctor of Philosophy

EVOLUTION OF KARST IN THE LOWER SUWANNEE RIVER BASIN, FLORIDA

By

Can Denizman

May 1998

Chairman: Anthony F. Randazzo
Major Department: Geology

This study represents an application of Geographic Information Systems to examine the morphometric and spatial distribution of karstic depressions and the factors controlling the karst development in the Lower Suwannee River basin. Because of the generally unconfined or semiconfined hydrogeologic conditions of the Floridan aquifer, the Lower Suwannee River basin presents an extraordinary set of karst features illustrating a complex evolutionary history. Analysis of the morphometric and spatial distribution parameters of karstic depressions reveals that the Florida karst is represented by broad, shallow depressions with an average density of 6.07 depressions/km^2 and an average pitting index of 14.5. A simple morphoclimatic classification of karst landforms is precluded by the great variation of morphometric and spatial ditribution parameters of karstic depressions within the Lower Suwannee River basin.

Comparison of morphometric and spatial distribution parameters of depressions with geologic and hydrogeologic factors such as potentiometric level fluctuation of the Floridan aquifer, thickness of overburden material above the Floridan aquifer, depth to water table, soil type, and the vadose zone lithology suggests that all of the factors examined in this study collectively affect the morphometric characteristics and spatial distribution of karstic depressions. Analysis of depression major axis orientations does not show a structural control on the karst development

Application of the mass flux technique to available data indicates that the best estimate of the net karstic dissolution rate in the Lower Suwannee River basin is 40 m^3/km^2/year. This is equal to a denudation rate of 40 mm/1000 years.

Morphometric and spatial distribution characteristics of karstic depressions suggest that the last phase of the post-Miocene karstic evolution within the Lower Suwannee River basin has been controlled by the retreat of the Pleistocene sea level stands. During the Pleistocene, as interglacial seas retreated, marine terraces were formed by sequential sea level lowstands and the total period of subaerial exposure diminished towards the sea. Consequently, geomorphologically younger karst landforms formed as the elevation of marine terraces decreased. This evolutionary pattern of karst landforms has resulted in the development of more frequent and/or larger and more complex depressions at higher elevations.

CHAPTER 1
INTRODUCTION

Karst can be defined as a terrain with distinctive hydrology and landforms formed by a combination of high rock solubility and well developed secondary porosity (Ford and Williams, 1989). Approximately 20 percent of the earth's land surface consists of karstic terrains and about 25 percent of the global population supplies its water from wells and springs in karst aquifers (Ford and Williams, 1989; White et al., 1995). The highly complicated surficial and underground karst network of the subtropical Florida karst not only hosts one of the most productive aquifers of the world, but also reveals a variety of karst features such as caves, dolines, uvalas, poljes, sinking streams and dry valleys which are world-famous. The Suwannee River basin presents an extraordinary set of karst features of Florida. Here, the generally unconfined or semiconfined hyrogeologic conditions of the Floridan aquifer have resulted in a fascinating collection of karst depressions illustrating a complex evolutionary history.

The Florida Platform, on which extensive carbonate deposition took place for much of the Mesozoic and Cenozoic, has been variously subject to periods of extensive karstification resulting from the glacio-eustatic fluctuations. Numerous studies on the hydrogeochemical, structural, diagenetic and hydrogeologic characteristics of the Florida karst have provided a great deal of information which may serve as a basis for understanding the karstic evolution of the Suwannee River basin (Vernon, 1951; White, 1958; Ceryak et al., 1983; Randazzo and Bloom, 1985; Scott, 1997). Yet, a detailed geomorphologic approach with particular emphasis on the analysis of the spatial and temporal characteristics of karstic depressions and studies on karst has rarely been attempted. Despite considerable study on the classification and formation mechanisms of sinkholes in the Florida Platform, much confusion still exists as to the evolution of karst in the Suwannee River basin. Better understanding of the karstic evolution of the Suwannee River basin requires recognition of paleoenvironments and associated karstic dissolution rates, identification of glacio-eustatic controls on the karst base level changes, evaluation of the influence of paleokarst phases, and particularly assessment of spatial and temporal distribution of sinkholes.

This study integrates morphometric techniques and karstic erosion rate studies in an attempt to describe the subtropical Suwannee River karst area and to address the post-Miocene evolution of karst. The study area is located in the Suwannee River basin, northwest peninsular Florida, where sinkhole (doline) karst dominates (Figure 1.1). The hypothesis to be tested is that the post-Miocene evolution of karst in the study area has been predominantly controlled by the sea level changes represented by marine terraces at various elevations and by changes from confined to water table aquifer conditions of the Floridan aquifer. It is further hypothesized that the fluvial erosion of the overlying impermeable siliciclastic deposits is responsible for the post-Miocene karstic evolution.

The morphometric and spatial distribution parameters of karstic depressions were determined based on a Geographic Information System database created by delineating depressions on twenty-four 7.5 minute topographic maps of 1:24,000 scale along the Suwannee River (Chapter 2). The effect of geologic, structural, and hydrogeologic variables on the morphometry and spatial distribution of depressions are discussed in

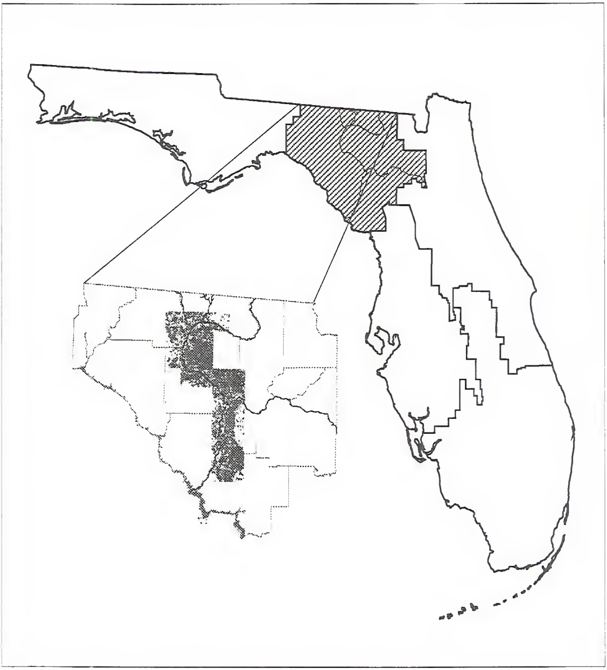

Figure 1.1. The study area.

Chapter 3. Factors addressed within this context include; fluctuation of the Floridan aquifer potentiometric level, thickness of the overburden material, depth to water table, type of soil media, lithological conditions of the vadose zone, and regional and local fracture traces. Chapter 4 includes a thorough discussion of karstic dissolution rate evaluation and its seasonal changes within the lower Suwannee River drainage basin. Chapter 5 describes the substitution of space for time to address the problem of post-Miocene karstic evolution in the study area by addressing how depression morphology and distribution pattern have changed through time, that is, on surfaces of successively greater age.

Climate

Humid subtropical climate prevails in the study area. Average annual temperature varies between 68° - 72° F. Mean annual precipitation is 1422 mm. Most rainfall occurs as localized thunderstorm activities in the summer months from June through August. In winter, convectional systems provide rainfall of longer duration and uniform spatial distribution (Fernald and Patton, 1985). Average evapotranspiration rate estimated for the area is 1092 mm per year (Fisk, 1977; Ceryak et al., 1983).

Physiographic Setting

The Northern Highlands and the Gulf Coastal Lowlands constitute the major physiographic provinces in the area (Figure 1.2) (Schmidt, 1997). As one of the most distinct physiographic features in Florida, the Northern Highlands occupies most of the

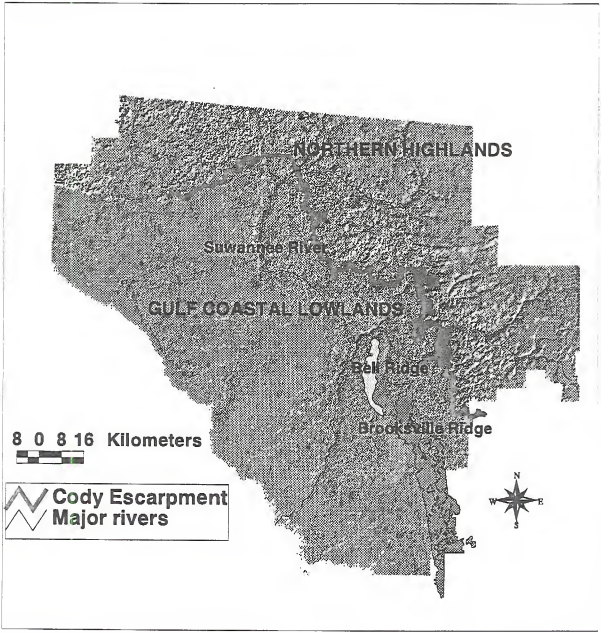

Figure 1.2. Physiographic regions.

north and east of the study area. Elevations for the Northern Highlands range between 100 - 240 feet (30.5 – 73.2 m) asl within the study area. The plateau, which originally covered the entire study area has been eroded by headward erosion through surface drainage as well as by karstic dissolution within the underlying carbonate units (Scott, 1997). The Cody Escarpment, which is described as "…the most persistent topographic break in Florida" (Puri and Vernon, 1964, p. 11), separates the Northern Highlands from the Gulf Coastal Lowlands. The scarp generally coincides with the 100-foot topographic contour except when it is interrupted by rivers such as the Suwannee, Withlacooche, and Santa Fe.

Hydrologically, the Northern Highlands contains a thick confining unit of Hawthorn Group sediments and represents confined conditions of the Floridan aquifer. Occasionally, cover collapse doline development takes place near the margin of the plateau (e.g., Devil's Millhopper). In general, karstic depressions in this zone are marked by low relief slumpage and erosional infilling due to thick cover sediments.

The Gulf Coastal Lowlands, covering large areas within the study area, consists of both erosional and depositional features. Broad plains of a series of Pleistocene surfaces and shorelines are pitted with karstic depressions within the limestones at or near land surface. It represents a typical mature karst terrane with a thin mantle of permeable marine terrace deposits. Because of the low topographic relief and rapid infiltration of rainfall by diffuse recharge to the karst aquifer, surficial runoff is limited to major rivers. Remnants of the Northern Highlands occur as outlier hills and sinkhole fill. Important remnant features in the Gulf Coastal Lowlands are the Bell and Brooksville ridges (Figure 1.2). The coastal swamps consist of muddy and silty deposits which support a growth of both fresh water and saltwater marshes.

The transition zone or "Marginal Zone" between the Gulf Coastal Lowlands and the Northern Highlands is an active zone of extensive karstification caused by allogenic recharge from the covered karst terrains of the Northern Highlands. Because of their highly acidic chemical properties, the waters of these allogenic streams rapidly dissolve the carbonates and disappear underground along the Cody Escarpment. The area is represented by numerous sinking streams, sinkholes of various sizes, closed karst praires (poljes), karst resurgences, and extremely complicated surface water-ground water interactions. Point recharge to the Floridan aquifer occurs via discrete conduits connected to well-developed phreatic cave systems of anastomotic pattern. The hydrogeologic and geomorphologic structure of the karst system is further complicated by paleokarst horizons developed during low sea-level stands (Hunn and Slack, 1983).

Geologic Structure

Despite its relatively stable geologic history on the passive margin of the North American Plate, the Florida Platform is considered to have been subject to tectonic activities occurring in the Caribbean and Gulf of Mexico (Randazzo, 1997; Scott, 1997; Safko and Hickey, 1992). Structural features associated with these tectonic forces are explained by possible fault and fracture systems, folding, uplift and subsidence.

Major structural features of the Suwannee River basin are the Ocala "Uplift", Peninsular Arch, and the Suwannee Straits (Figure 1.3). The term "Ocala Uplift" was first used by O.B. Hopkins in the USGS press release in 1920 to describe the Eocene limestone outcrops in the western peninsular Florida. Vernon (1951, p.55), generally agreeing with Hopkins, described this feature as having "....developed in Tertiary sediments as a gentle

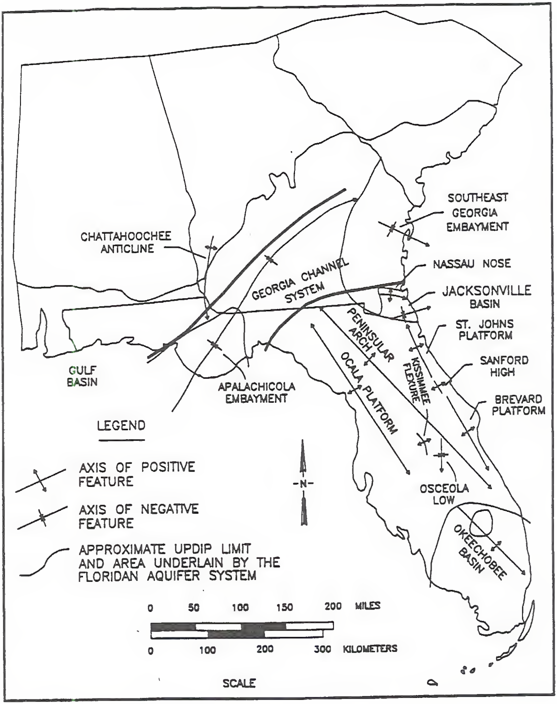

Figure 1.3. Structural features of Florida (from Scott, 1997).

flexure, 230 miles long, and 70 miles wide where exposed in central peninsular Florida." He suggested that the "uplift" consists of two well-defined shallow folds trending northwest-southeast formed by tectonic activities occurring from Late Eocene through Early Miocene. Noting that the rocks older than Middle Eocene were not affected by the proposed Ocala "uplift", Winston (1976) suggested that this feature was not an uplift but was formed by a thickening of the Lake City Formation and the eastward tilting of the Florida Peninsula (Ceryak et al, 1983). In this study, the term "Ocala Platform" will be used in order to avoid any generic connotation of this feature whose origin is yet to be clearly defined. Regardless of its origin, the Ocala Platform has significantly affected the Neogene deposition and the karstic evolution of the area. Miocene sediments once covering the whole area are much thinner on the Ocala Platform. Fluvial and karstic erosion of the Hawthorn Group sediments exposed the Eocene carbonates along the crest of the Ocala Platform (Scott, 1997).

The Peninsular Arch is approximately 275 mile long subsurface feature trending northwest-southeast and forming the axis of the Florida peninsula (Applin, 1951). Its crest is formed by the pre-Mesozoic rocks which were topographically high during the Early Cretaceous (Puri and Vernon, 1964) and intermittently positive during the Cenozoic (Miller, 1986). Based on the maps by Miller (1986), Scott (1997 p.58) states that the Peninsular Arch has affected sedimentation as late as Oligocene, but "…did not affect deposition of Neogene to Holocene sediments."

The Suwannee Channel located to the north of and adjacent to the Upper Suwannee River basin was a topographically low feature separating the Florida Platform from the continental landmass. It is described as an approximately 200 miles long and 20 to 30 miles wide channel developed on top of the Cretaceous rocks (Hull, 1962). The Suwannee current flowing within the channel has isolated the Florida carbonate Platform from the influence of siliciclastic sedimentation until the Late Oligocene (Scott, 1997).

Geologic Setting

After its separation from the African plate during the Jurassic, the Florida Platform has been a depocenter for thick carbonate sediments and minor amounts of evaporite throughout the Paleogene (Randazzo, 1997). The carbonate factory of the warm, shallow seas was effectively isolated from the northerly siliciclastic sediment transport by the Gulf Trough and the Suwannee Channel in which the Suwannee current was active until the Late Oligocene. Encroachment of siliciclastic transport onto the Florida Platform began to suppress carbonate deposition when the Suwannee current ceased to occur following a major sea level drop in the Oligocene. Siliciclastic sediments covered the entire Platform by mid-Pliocene and continued to be predominant except for the southernmost Florida, where carbonate sedimentation took over during the Late Pliocene (Randazzo, 1987; Scott, 1997).

Surrounded by submarine escarpments on both east and west, the Florida Platform consists of a thick sequence of limestone and dolomite deposited during the Tertiary period. Carbonate deposition in the warm, shallow seas of the Paleocene formed the Cedar Keys Formation. It was overlain by the Oldsmar, Avon Park, and Ocala carbonate sequences (Eocene) and Suwannee Limestone (Oligocene). Repeated sea level fluctuations during the Eocene have brought about short episodes of nondeposition and subaerial erosion within the carbonate rock sequence as evidenced by numerous unconformities (Randazzo, 1997). The oldest unit exposed in the study area is the Ocala Limestone.

In general, Miocene Hawthorn Group deposits are comprised of siliciclastics interbedded with carbonates. Phosphate is abundant in the Hawthorn Group sediments of the study area. The siliciclastic content increases in the younger sediments (Scott, 1997). On the lithology of the Hawthorn Group sediments Scott and MacGill (1981 p. 23) reported that the "...most predominant lithology in the study area is a silty, sandy, phosphatic dolomite, ...and comprises approximately 90% of the volume of sediments." Thickness of the Hawthorn Group increases to the north and east within the study area. It is virtually absent throughout the Gulf Coastal Lowlands physiographic province whereas its thickness may exceed 200 feet (61 m) in the northeasternmost part of the study area.

Ceryak et al. (1983) used the term "Undifferentiated Marine Terrace Deposits" for the Plio-Pleistocene clastic materials which overlie the Hawthorn Group sediments, where present, and the carbonate rocks of the Gulf Coastal Lowlands. These terrace deposits are formed by the Plio-Pleistocene eustatic sea level fluctuations and are composed of fine-to medium-grained quartz sand with minor amounts of organic material, clay, and heavy minerals.

Hydrogeologic Setting

Three aquifer systems are located in the study area. A surficial (water table) aquifer and an artesian "intermediate" aquifer exist in the Northern Highlands (Figure 1.4). The Floridan aquifer underlies the whole peninsular Florida and the panhandle, displaying both artesian and water table conditions.

The surficial aquifer is an unconfined aquifer consisting of Miocene and younger sediments. Its thickness varies between 20 to 150 feet (6 to 45.7 m). Ground water is recharged directly from precipitation. In the study area, due to the greater hydraulic head of the surficial aquifer, part of the percolating water leaks downward through confining beds to recharge the intermediate and the Floridan aquifer system. Because of the complex interbedding of aquifer material, the permeability and transmissivity of the surficial aquifer are extremely variable (Miller, 1997).

The intermediate aquifer system occurs between the surficial aquifer and the Floridan Aquifer. Lithologically, the aquifer material contains phosphatic sands, clays, and carbonates. Its thickness and depth varies with the lateral and vertical continuity of hydraulic conductivity. Thickness increases from the west to the northeast ranging from 80 feet to 234 feet (24.3 to 71.3 m). Confined hydraulic conditions occur except locally where overlying impermeable units are thin through erosion. Most recharge to the intermeadiate aquifer occurs as downward leakage through the confining unit (Ceryak et al., 1983)

Era	Period	Epoch		Group/Formation	Hydrogeologic Unit
Cenozoic		Holocene		undifferentiated	Surficial Aquifer
		Pleistocene		undifferentiated	
	Neogene	Pliocene			
		Miocene	Middle	Hawthorn Group	Intermediate Aquifer/ Confining Layer
			Lower		
	Paleogene	Oligocene		Suwannee Limestone	Upper Floridan Aquifer
		Eocene	Upper	Ocala Limestone	
			Middle	Avon Park Formation	
			Lower	Oldsmar Formation	Lower Floridan Aquifer
		Paleocene		Cedar Keys Formation	Lower Confining Unit
Mesozoic	Cretaceous			undifferentiated	

Figure 1.4. Hydrostratigraphic column for the Suwannee River Basin (after Hirten, 1996).

As one of the most productive karst aquifers of the world, the Floridan aquifer is the principal aquifer in the study area. It consists of a thick sequence of Tertiary carbonate rocks. Because of the highly variable lateral and vertical hydraulic conductivity of the aquifer material, there are zones of high productivity and low transmissivity within the Floridan aquifer system. Its vertical extension is determined by the relative permeability difference between the aquifer and the upper and lower boundaries of the system. The permeability of the aquifer material is at least one order of magnitude greater than that of the upper and lower confining units. Naturally, this permeability difference does not correspond everywhere to a particular lithologic unit. In general, massive anhydrite beds of the Lower Cedar Key Formation constitute the base of the aquifer. The top of the Ocala Limestone, or Suwannee Limestone, where present, marks the upper limit of the aquifer. In the study area, the most productive zones of the Floridan aquifer occur within the Suwannee Limestone and Ocala Limestone.

The Floridan aquifer system exhibits both confined and unconfined conditions. Overlain by the thick impermeable zones of the Hawthorn Group, the aquifer acts as an artesian system within the Northern Highlands physiographic region. Recharge to aquifer is maintained through slow leakage through the confining unit or as point recharge through collapse depressions breaching the impermeable layers of the overlying Hawthorn Group. In areas where the Hawthorn Group has been eroded, the Floridan aquifer is unconfined and represents water table conditions. This situation occurs over a great portion of the study area within the Gulf Coastal Lowlands physiographic province (Western Karst Plain). Here, diffuse recharge takes place through a thin blanket of terrace deposits covering the karst aquifer.

Because of the relatively high primary porosity coupled with extensive karstic dissolution conduits within the carbonate rocks of the Floridan aquifer, ground water storage and flow take place through a complex system of intergranular openings and cavities. Both diffuse and conduit ground water flows occur. Preferential ground water flow along solutionally enlarged joints, fractures, and bedding planes have been documented by numerous studies (e.g., Rosenau et. al, 1977; Hunn and Slack, 1983; Beck and Arden, 1983). Unlike deep karst ground water flow in south Florida, most of the ground water circulation in the study area occurs within the 200 to 300 feet (60 to 90 m) of saturated limestone. Most of the cave systems are reported to have formed at the contacts between the Hawthorn Group-Suwannee Limestone or Ocala Limestone-Suwannee Limestone (Beck, 1986). Rapid ground water flow takes place within the complex cave systems from recharge areas to major karst springs along the Suwannee River. Because of the complicated interaction between the surface water and ground water, recharge and discharge areas show strong temporal variations. Numerous ground water tracing studies were carried out to better understand the ground water-surface water interactions and to delineate ground water catchment areas for karst springs in the area (Hisert, 1994; Kincaid, 1994; Hirten, 1996).

Karst in Florida

Sea level is the absolute base level of karstification and its changing positions have played an important role in the vertical extension of karst processes, giving rise to repeated shifts of vadose and phreatic zones. Numerous subaerial exposures and accompanying dissolution processes caused by sea level fluctuations have extensively karstified the thick Tertiary carbonate rocks of the Florida Platform, resulting in a multi-cyclic, complex network of karst development (White, 1958; Hanshaw and Back, 1979; Randazzo and Bloom, 1985; Upchurch, 1989). Dissolution of carbonate rocks has been prevalent especially along the unconformities, marked by paleokarst horizons or extensive phreatic cave systems. In accordance with the sea level fluctuations, shifts in the sea water-fresh water mixing zone caused significant diagenetic changes in the carbonate rocks (Randazzo and Bloom, 1985; Back et. al, 1986). Various hydrochemical processes including dolomitization, dissolution and precipitation of carbonate minerals have taken place in the Floridan aquifer (Hanshaw and Back, 1979).

Sea level fluctuations have also brought about changes in recharge and discharge zones of the Floridan Aquifer. Most of the springs discharging from the Floridan Aquifer have sinkhole morphologies with shallow conduit networks. They represent previous point recharge locations to the Floridan Aquifer and currently function as discharge points due to rising sea levels (Ceryak et al, 1983).

Karst in Florida has developed in a relatively stable tectonic setting and is covered by either thick, impermeable siliciclastics or thin layers of Pleistocene terrace deposits. Therefore, structural control on karst development can not be readily observed. Nevertheless, preferential karst development along joints, fractures, and photolineaments were reported by White (1958), Pirkle and Brooks, (1959), and Littlefield et al (1984). Regardless of the existence of structural control on the karst development, major dissolution of carbonate rocks occurs at shallow depths of recharge areas with soil cover where water is undersaturated with respect to calcite, or within the sea water-fresh water mixing zone where undersaturation results from mixing of two different water bodies (Back et al, 1986; Randazzo, 1997). Major conduit development has also been observed within the zones of potentiometric level fluctuation (Ceryak et al, 1983).

Unlike tectonically deformed, uplifted, bare karst of the temperate Mediterranean region where almost all the drainage takes place underground, or tropical karst with positive features surrounded by polygonal doline fields, the Florida karst displays a gently rolling topography with shallow depressions. However, this gentle topographic relief and relatively low depression density in Florida represent a muted surficial expression of much denser doline network covered by at least several meters of soil material or as much as hundreds of meters of impermeable confining layer. In other words, karst in Florida is much more extensive and complicated than it is observed on the ground surface. Karstification has occurred as a multisequential process through which vertical and lateral dissolution zones associated with different sea level stands have been superimposed to form a complex three dimensional network of conduits throughout the thick carbonate rock sequence of the Florida Platform (Davies and Legrand, 1972; Randazzo, 1997).

Sinkholes (dolines) are the ubiquitous landform in the temperate karst of Florida. Beck (1986) classifies them into three types: ponors (swallets, stream-sinks), subsidence sinkholes, and cenotes. Most of the sinking streams represent allogenic recharge to the Floridan aquifer in an area confined to the transition zone between the Northern Highlands and the Coastal Lowlands physiographic provinces. He further relates these ponors to the paleokarst dissolution pipes reactivated by the erosion of the cover material.

Ponors, as described by Beck (1986), corresponds to the solution sinkholes of Ford and Williams (1989). They subclassify solution sinkholes into point recharge and drawdown sinkholes. Point recharge sinkholes form as the overlying material on an undeformed carbonate rock sequence is eroded by fluvial erosion. Points of high fissure frequency are attacked by chemically aggressive allogenic runoff. Once the connection between the input and output is established by a proto-cave system, then the removal of carbonate material is maintained by the focused recharge. Removal of rock mass is greater at the center of depressions than their sides. More water is focused as a result of increasing drainage areas and a positive feedback mechanism is established. Density of point recharge sites is increased by the continued erosion of the overlying material and by more sinkhole initiation at the expense of reduced drainage areas of individual depressions.

Drawdown sinkholes can be observed in uplifted and previously karstified areas where the overburden material has long been eroded. Focused corrosion is established not by point recharge, but by drawdown within the epikarstic (subcutaneous) aquifer (Figure 1.5). Williams (1983) has shown that diffuse recharge through the soil cover forms a perched water table in the extremely karstified epikarstic zone by virtue of the relatively low permeability of the underlying bedrock. However, preferred vertical paths of dissolution develop within this zone because of the initial variabilities in permeability. Further development of these paths brings about a cone of depression in the overlying epikarstic water table, resulting in focused corrosion and initiation of drawdown sinkhole development in the epikarstic zone with no requirement for a caprock point recharge. Once the positive feedback is established, zones of focused corrosion are represented by topographic depressions whose diameters are controlled by epikarstic water table drawdown cone (Williams, 1983).

In discussing the origin of solution sinkholes Ford and Williams (1989, p.402) point out that there is a "…necessity to distinguish (a) between doline initiation where there has been no proto-cave development and that where a ready made, permeable vadose zone is inherited from an earlier phase of karstification, and (b) between doline corrosion focused by point recharge as opposed to that focused by epikarstic drawdown." They further suggest that both successive caprock stripping and formation of secondary drawdown within a major epikarstic drawdown can account for the formation of different generations of sinkholes (parent and daughter, primary and secondary).

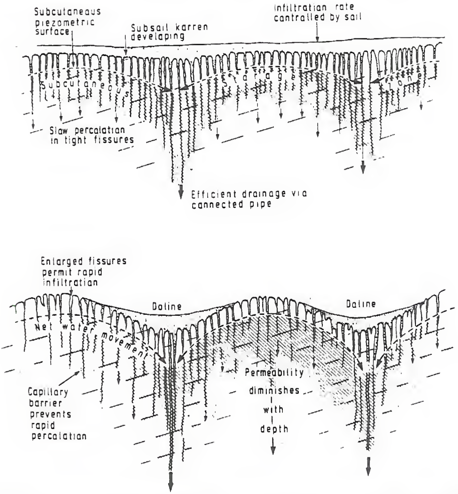
Subcutaneous piezometric surface
Subsoil karren developing
Infiltration rate controlled by soil
Subcutaneous storage zone
Slow percolation in tight fissures
Efficient drainage via connected pipe
Enlarged fissures permit rapid infiltration
Doline
Doline
Net water movement
Capillary barrier prevents rapid percolation
Permeability diminishes with depth

Figure 1.5. Drawdown doline initiation in the subcutaneous (epikarstic) zone (Williams, 1983).

Solution sinkholes constitute the predominant sinkholes type in the study area where a thin blanket of soil material overlies the carbonate rocks of the unconfined or semiconfined Floridan aquifer. Within the transition zone between the Northern highlands and the Gulf Coastal Lowlands where overlying siliciclastic material has been constantly eroded along the Cody Escarpment, focused corrosion by point recharge of allogenic runoff forms solution sinkholes of different generations. Epikarstic drawdown sinkholes are also expected to occur within the Gulf Coastal Lowlands, where the caprock has long been eroded and a paleokarst template is available to be reactivated by focused corrosion. After the initiation of sinkholes, their development is further encouraged by the increased aggresiveness of water as it percolates through thick soils accumulated in the bottoms of depressions. In some cases, accumulation of low permeability material within depressions may retard the sinkhole development, forming ponds and lakes. A majority of lakes in Florida has formed within karstic depressions lined by impermeable material.

CHAPTER 2
MORPHOMETRIC AND SPATIAL DISTRIBUTION PARAMETERS OF KARSTIC DEPRESSIONS

Prospectus

In light of the morphoclimatic approach to karst geomorphology, much research has been directed towards a better understanding of karst landform evolution in different climatic regions. Numerous attempts have been made to relate different karst landform patterns and corresponding dissolution rates to climate (Corbel, 1957; Lehman, 1964; Jakucs, 1973). It has been argued that variations in karst landforms were caused by different karst processes related to climatic variations in soil and vegetation types, and amounts and patterns of runoff. These early applications of a morphoclimatic approach to karst were based upon visual comparisons of karst landforms formed in contrasting climates, and on assertions, rather than measurements, of differences in erosion processes (Smith and Atkinson, 1976). Nevertheless, the morphoclimatic approach to karst processes and landforms has given rise to new perspectives in understanding the operation of karst systems. Its application to various karst regions has also brought the necessity for an objective system of karst landform description and analysis.

An objective and quantitative description of karst landforms is achieved by karst morphometry. It has been widely applied to a variety of karst regions and proved to be a very effective technique to describe and characterize karst landforms, especially depressions (e.g. Williams, 1972; White and White, 1979; Day, 1983; Troester et al., 1984). Evolution of karst landforms was also addressed by using morphometric and spatial distribution parameters of karstic depressions (e.g. Drake and Ford, 1972; Kemmerly and Towe, 1978; Kemmerly, 1982).

Smith and Atkinson (1976, p. 403) explain the importance of morphometric techniques and erosion rate calculations as ".... the tools of process studies and morphometric analysis, when used together, may prove powerful enough to unravel the interaction of lithology (or Structure), erosion rate and distribution (Process), and time (Stage) in sculpting the complex variety of landscapes found in limestone regions."

Despite its variety of karst landforms, the subtropical karst of Florida has rarely enjoyed a morphoclimatic approach with special attention to its morphometric parameters and erosion rates. The few studies on depression morphometry and spatial distribution were of local scale with small depression populations. In this study, morphometric analysis of a relatively large portion of the Suwannee River karst area was made possible by using the Geographic Information Systems.

Background

Morphometry can be defined as the measurement and mathematical analysis of the configuration of the Earth's surface and of the shape and dimensions of its landforms (Bates and Jackson, 1987).

Based on hundreds of field measurements, Cvijic (1893) classified dolines according to their side slope angles and depth-diameter ratios. He described them as bowl, funnel-, and well-shaped depressions. His quantitative approach was continued by Cramer

(1941), who summarized statistical results of previous workers and presented morphometric information for diverse karst regions of the world.

Other important contributions to karst morphometry were brought by Williams's (1966, 1971) works on the temperate and tropical karst of Yorkshire and New Guinea, respectively. Considering dolines as the smallest drainage basins, he mapped topographic divides, summits, channels and stream sinks on the polygonal karst of New Guinea. He applied Strahler's (1957) channel ordering system to depressions and classified them based on their drainage characteristics. Williams (1971) not only introduced a hydrological perspective to karst morphometry, but also drew attention to the spatial distribution patterns of karstic depressions. Following methods developed by plant ecologists, he applied Clark - Evans' (1954) index on the nearest neighbor distances as a measure of randomness in depression distribution (Williams, 1971, 1972).

The nearest neighbor analysis is used to describe a pattern with a nearest neighbor index that compares the actual nearest neighbor distance (L_a) with the average expected distance (L_e). The expected nearest neighbor distance in a randomly distributed depression population is given by;

$L_e = 1/(2\sqrt{D})$ where D is the depression density.

The nearest neighbor index R, described as the ratio of L_a / L_e, ranges from 0 for maximum clustering to 2.149 for a regular pattern in which depressions are as evenly and widely spaced as possible. A nearest neighbor index value of 1 indicates random distribution (Williams, 1972).

Drake and Ford (1972) applied morphometry to karst landform evolution. Using quadrat analysis, they verified the existence of two generations of dolines in the Mendip

Hills, UK. It was concluded that an average of four daughter depressions cluster around randomly distributed mothers.

Statistically comparing two random samples of karstic depressions based on the absence or presence of natural ponds, Kemmerly (1976) used morphometric measures such as long-axis orientation, length of long axis versus mean depression width. He concluded that the two random depression samples in Tennessee are not from the same population. He further analyzed a contagious karst mechanism and constructed a conceptual model for depression initiation and development by defining the parent and daughter depressions with different spatial characteristics (Kemmerly, 1982, 1986).

White and White (1979) performed a comprehensive statistical analysis on parameters of karst development such as relief factor, drainage factors, size and shape factors, carbonate rock fractions, measures of doline development, and measures of internal drainage. They described relationships between sinking stream catchment area and stream length, area of internal drainage into depressions and number of depressions, and also compared morphometric measures of karst with different rock type.

Among the more recent studies, Magdalena and Alexander (1995) analyzed sinkhole distribution in Minnesota. They applied nearest neighbor analysis to a sinkhole data set consisting of field-located karstic depressions. The randomness of sinkhole distribution was also tested by comparing it with artificially created random data sets. The observed sinkhole locations were found to be significantly different from a random spatial distribution. Rather they tend to occur in clusters, in which new sinkhole development is observed.

Despite an apparent absence of systematic application of morphometric techniques to karstic depressions of Florida, there are several important studies characterizing the subtropical Florida karst. Most research of karstic depressions in Florida is based on the sinkhole database compiled by the Florida Sinkhole Research Institute. The database consists of information on reported sinkholes. Therefore, distribution of sinkholes is strongly biased towards highly populated areas where sinkhole occurrence was detected and reported to the Institute. Nevertheless, studies based on this database may provide a better understanding of sinkhole-prone areas. One exception to these studies is the work of Troester et al. (1984) in which doline depth distribution was examined for two tropical and four temperate karst areas including Florida, based on data obtained from topographic maps of various scales. Considering the depth information as the most useful parameter in distinguishing temperate and tropical karst, they produced depth frequency plots for karstic depressions. For all areas considered in the study, the depth distribution was approximately exponential with different values of the exponential coefficient. Unlike tropical karst regions of Puerto Rico and Dominican Republic, the low relief Florida karst was represented by broad, shallow depressions.

Sinkhole density maps for old and new sinkholes were created by Bahtijarevic (1989) for a highly karstified area in central Florida. In order to classify areas based on their sinkhole densities she performed a terrane evaluation on the overall sinkhole population.

Wilson (1995) studied the surficial and buried sinkhole densities and new sinkhole frequencies in Peninsular Florida. Based on data obtained by ground penetrating radar studies, derived from topographic maps and from the database of new sinkholes he provided statistical information on old, new and buried sinkhole densities. He stressed the importance of buried sinkhole density information on assessing the vulnerability of the Floridan aquifer to ground water contamination.

Methodology

Morphometric and spatial distribution parameters of karstic depressions in the Suwannee River basin were evaluated in Geographical Information Systems (GIS) environment, using ArcInfo 7.0. In this study, morphometric analysis of 24,757 karstic depressions in an area covered by twenty-four 7.5 minute standard USGS topographic quads were made possible by the powerful and rapid analytical capabilities of the GIS. The procedure followed in obtaining morphometric data discussed in this chapter consists of extensive manual and computer work.

The first stage of the study involves detailed topographic map analysis. All the natural depressions depicted by hachured closed contours on topographic maps along the Suwannee River were delineated on transparent papers. The following topographic quadrangles were analyzed in this study: Lee, Ellaville, Fort Union, Hillcoat, Madison SE, Fallmouth, Live Oak West, Day, Dowling Park, Mayo, Mayo SE, Mayo NE, O'Brien, O'Brien SE, Branford, Hildreth, Hatchbend, Bell, Wannee, Fourmile Lake, Suwannee River, Trenton, Manatee Springs, and Chiefland (Figure 2.1).

All the depressions delineated on topographic quads were transferred one by one to ArcInfo (GIS) environment. Digital maps (coverages) of depressions were produced. In order to utilize GRID functions of ArcInfo, vector coverages of depressions were

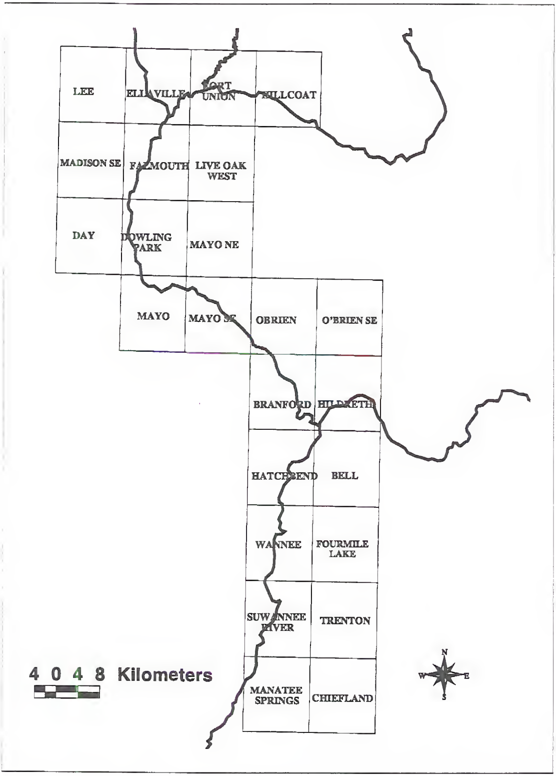

Figure 2.1. Names and location of topographic quadrangles within the study area.

converted to raster files. GRID is a cell-based module of ArcInfo. It manipulates rater files in which a regular "mesh" is draped overthe landscape. The predominant phenemonon within a cell becomes the value of that cell. Morphometric measurements were performed on all of the depressions using zonal functions of GRID. Compound depressions were taken as single depressions for measurements of length, width, depth, and major axis orientation.

Nearest neighbor analysis was performed for each quadrangle. Compound depressions were divided into their components and each depression was taken into account individually. Nearest neighbor distances were calculated by using Fragstats, a powerful spatial analysis software originally created for landscape pattern analysis of digital data. Depressions were represented by their centroids. Ideally, karstic depressions are represented by their deepest points, i.e. swallow holes, for an accurate spatial description which is of paramount importance in spatial analysis. Williams (1971, 1972) was able to locate the swallow holes and drainage patterns in the polygonal karst of New Guinea. However, they are not detectable in the low-relief karst of Florida, which is covered by at least several meters of soil and thick vegetation. Therefore, in order to maintain consistency and avoid subjectivity in assessing sinkhole locations, karstic depressions were represented by their centroids that were readily and precisely determined by GRID functions in GIS.

Two GIS databases for karstic depressions were created: The compound depressions database includes morphometric parameters such as depression area, perimeter, length, width, mean diameter, length/width ratio, circularity index, major axis orientation, and approximate depth. The database for individual depressions includes centroid locations of depressions, nearest neighbor distances, and azimuth values for nearest neighbor vectors.

Among a great number of morphometric parameters proposed by various karst geomorphologists, only those that are possible to be measured or calculated by GIS based on the available data were included in this study:

-Length: length of the major axis of an ellipsoid representing the depression.

-Width: length of the minor axis of an ellipsoid representing the depression.

-Orientation: orientation of the major axis. Originally expressed by GRID as the angle from the east, counter-clockwise, it was converted to regular azimuth values.

-Area: area of each depression measured in sq.m.

-Pitting index: (Area of karst)/(Total depression area).

-Circularity index: the measure of the circularity of a depression.

Depth information was obtained by counting the number of closed contours for each depression.

Results

Depression Density

Depression densities were calculated for each topographic quad by dividing the number of depressions by area (Table 2.1). A total of 25,157 depressions were located in the 4,063.138 km^2 area examined. Mean depression density for the whole area is 6.06/ km^2. It ranges from 2.43 (Madison SE) to 15.801 (Mayo NE) with a standard deviation of 3.15.

Table 2.1. Morphometric and spatial distribution parameters of depression for topographic quadrangles.

QUADRANGLE NAME	NUMBER OF DEPRESSIONS	DEPRESSION DENSITY	TOTAL DEPRESSION AREA (sq.km)	MEAN DEPRESSION AREA (sq.km)	MEAN NEAREST NEIGHBOR DISTANCE (m)	NEAREST NEIGHBOR INDEX (R)	DISTRIBUTION PATTERN	PITTING INDEX	LENGTH/ WIDTH
WANNEE	904	5.3	10.7	0.012	186.2	0.859	Tending to cluster	15.83	1.70
FOURMILE LAKE	588	3.4	8.5	0.014	212.6	0.789	Tending to cluster	20.15	1.81
SUWANNEE RIVER	953	5.6	9.8	0.010	164.4	0.778	Tending to cluster	17.35	1.72
TRENTON	1283	7.5	20.5	0.016	174.8	0.956	Near random	8.35	1.74
MANATEE SPRINGS	953	5.6	12.4	0.013	170.8	0.809	Clustered	13.72	1.82
CHIEFLAND	1742	10.2	8.5	0.005	129.7	0.827	Tending to cluster	20.23	1.62
LEE	593	3.5	18.0	0.030	235.4	0.881	Tending to cluster	9.41	1.70
MADISON SE	405	2.4	13.0	0.032	245.4	0.765	Tending to cluster	12.84	1.99
ELLAVILLE	622	3.6	14.1	0.023	214.7	0.818	Tending to cluster	12.19	1.89
FORT UNION	482	2.9	16.6	0.034	255.5	0.864	Tending to cluster	10.20	1.80
FALLMOUTH	1002	5.8	11.4	0.011	174.9	0.843	Tending to cluster	15.06	1.80
LIVEOAK WEST	1389	8.1	19.1	0.014	161.3	0.919	Near random	8.97	1.69
HILLCOAT	444	2.6	4.2	0.009	178.8	0.578	Clustered	40.91	1.90
DAY	388	2.7	7.3	0.019	241.4	0.796	Tending to cluster	19.49	1.84
DOWLING PARK	1514	8.9	21.7	0.014	159.6	0.950	Near random	7.89	1.76
MAYO NE	2721	15.8	23.5	0.009	128.9	1.025	Near random	7.32	1.61
MAYO	1273	7.5	13.2	0.010	160.9	0.881	Tending to cluster	12.86	1.77
MAYO SE	1187	6.9	11.6	0.010	179.7	0.945	Near random	14.81	1.72
O'BRIEN	1724	10.1	16.6	0.010	160.3	1.019	Near random	10.27	1.72
O'BRIEN SE	1663	9.8	25.5	0.015	158.5	0.990	Near random	6.70	1.74
BRANFORD	766	4.5	8.4	0.011	191.0	0.814	Tending to cluster	20.15	1.81
HILDRETH	971	5.7	11.7	0.012	189.1	0.905	Near random	14.47	1.80
HATCHBEND	753	4.4	8.8	0.012	205.3	0.860	Tending to cluster	19.60	1.82
BELL	837	4.9	16.4	0.020	187.0	0.829	Tending to cluster	10.37	1.89

Distribution of depression density is also presented as a GIS layer with a spatial resolution of 10 m. It was created by calculating the number of depression centroid points in a one km^2 window moving 10 m at each step. Nearly half of the study area (~1,900 km^2) is represented by a depression density between 1 to 5 / km^2 (Figures 2.2 and 2.3).

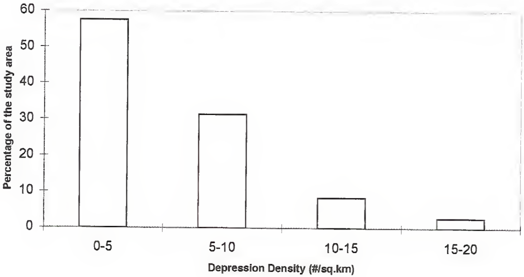

Figure 2.2. Histogram of depression density distribution.

The area of each depression was calculated by GIS functions. Based on the calculations for each quad (Table 1), total depression area varies from 4.15 km^2 (Hillcoat) to 25.4 km^2 (O'Brien SE) with a mean of 13.80 km^2 and a standard deviation of 5.38 km^2. Total depression area is 331.390 km^2, corresponding to 8.15% of the study area (4,063.14 km^2).

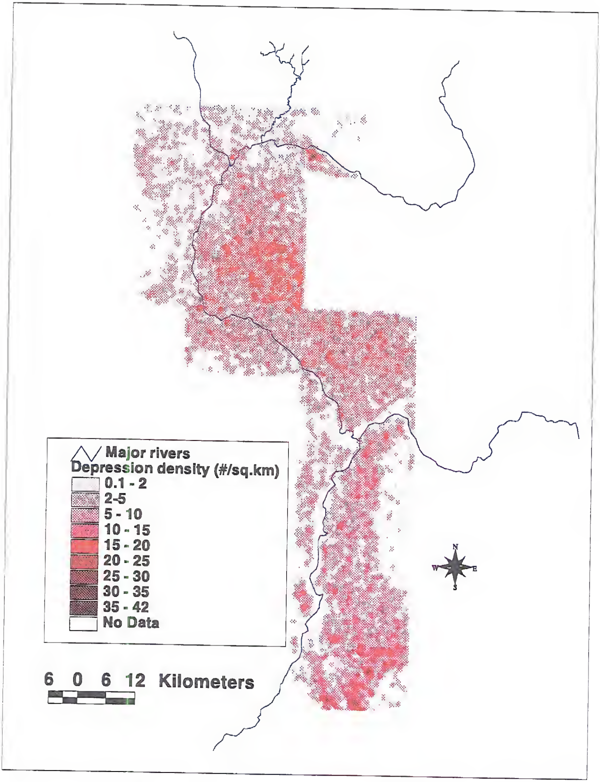

Figure 2.3. Distribution of depression density.

As a measure of surficial karst development, the pitting index (total area of karst / total depression area) provides information about the extent of karstification. For the polygonal karst landscapes covered by tightly spaced depressions, the pitting index approaches unity. Within the study area, the pitting index varies from 6.69 (O'Brien SE) to 40.91 (Day) with a mean of 14.5 and a standard deviation of 6.98 (Table 2.1).

Spatial distribution of depressions treated as points located at their centroids was analyzed using the simple nearest neighbor technique (Williams, 1972a, 1972b). The mean nearest neighbor distance (La) for karstic depressions within each quad was calculated using FRAGSTATS (Table1). It ranges from 128.95 m (Mayo NE) to 255.53 m (Fort Union) with an overall mean and standard deviation of 186.09 m and 33.3 m, respectively. The expected mean nearest neighbor distance (L_e) in an infinitely large, randomly located population with same depression density, D, is given by $L_e = 1/(2\sqrt{D})$ and ranges from 125.78 m (Mayo NE) to 320.98 m (Madison SE) for the study area.

The nearest neighbor index R, described as the ratio of L_a / L_e, was derived for corresponding quads and presented in Table 1. It ranges from 0.578 (Hillcoat) with a clustered distribution to 1.025 (Mayo NE), which represents randomly distributed depressions. Mean nearest neighbor index for the whole area is 0.854. Most of the topographic quadrangles reveal a depression distribution significantly different from random expectation (R=1) at the 0.05 level. All the depressions except those in Trenton, Live Oak West, Dowling Park, Mayo NE, Mayo SE, O'Brien, O'Brien SE and Hildreth indicate a tendency towards clustering.

Nearest neighbor analysis was also performed for the whole area by using map algebra functions of the GIS. Based on the centroid locations of depressions, layers of measured nearest neighbor distance, L_a, and expected nearest neighbor distance, L_e, were created. The distribution of nearest neighbor index (R) within the study area was obtained by the ratio of two GIS layers (L_a / L_e). A greater part of the study area is represented by a nearest neighbor index less than one (Figures 2.4 and 2.5) indicating a trend towards clustering.

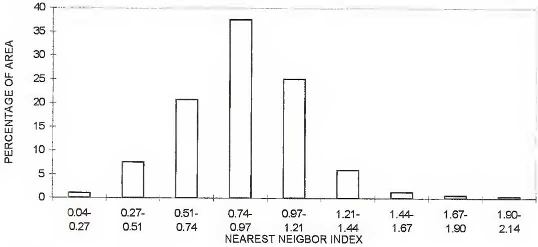

Figure 2.4. Histogram of nearest neighbor index.

Models explaining spatial evolution of sinkholes such as that proposed by Drake and Ford (1972), and Kemmerly (1986) describe a contagious evolutionary pattern in which primary or first generation sinkholes are initiated on major fractures and clustered by secondary sinkholes forming around them. The evolution of karstic depressions within the study area is discussed in Chapter 5. Only the descriptive parameters of depression morphometry and spatial distribution are addressed within the content of this chapter.

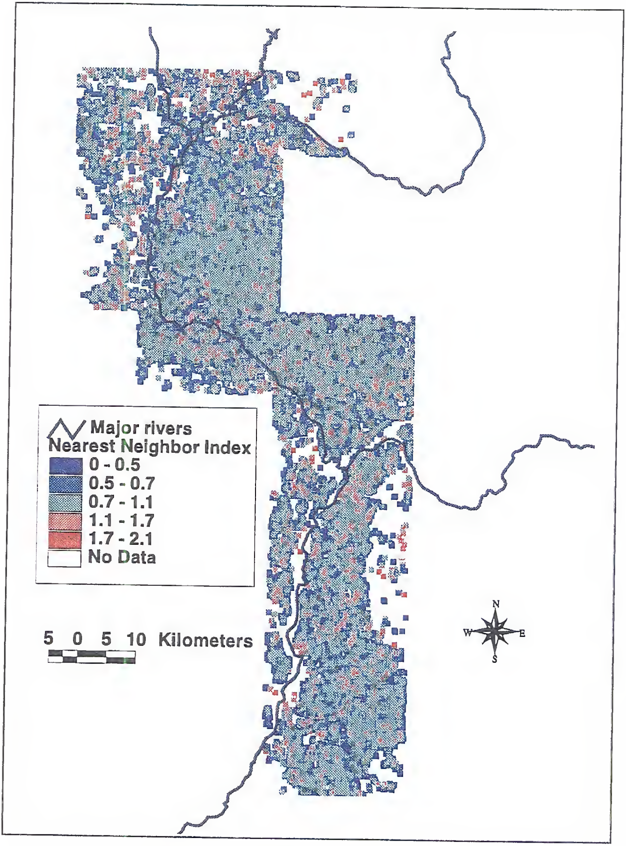

Figure 2.5. Distribution of nearest neighbor index.

A histogram of nearest neighbor distance data set for depression centroid points is shown in Figure 2.6. The mean distance to nearest neighbor is 188.097 m. The values range from 20 m to 2956.0 m with a standard deviation of 116.47 m. Cumulative percentage graph of depression nearest neighbor distance values shows that 90% of depressions are situated closer than 500 m to their nearest neighbor (Figure 2.7).

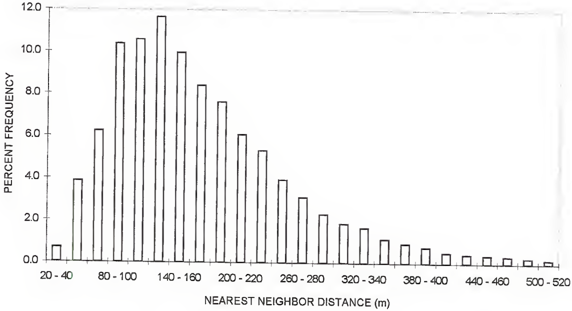

Figure 2.6. Percent frequency of nearest neighbor distance.

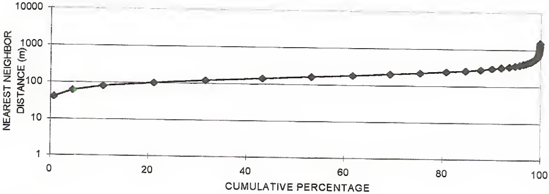

Figure 2.7. Cumulative percentage of nearest neighbor distance.

Planimetric Shape

As an index of planimetric shape, the length/width ratios and circularity index of depressions were investigated. Length and width values were taken as major and minor axis values of depressions calculated by the "zonalgeometry" function of GIS. The ratio varies between 1 for equidimensional depressions to 14.1 for extremely elongated depressions representing ancient valley floors of sinking streams. Mean L/W value and the standard deviation is 1.74 and 0.68, respectively (Figure 2.8).

Most dolines are near equidimensional in plan with a modal ratio class between 1 - 1.5. Ninety percent of the total population has a L/W ratio smaller than 2.5 (Figure 2.9). Plots of area vs. L/W for each topographic quad (Appendix A) do not show a strong tendency of elongation (high L/W) for larger sinkholes, which may be expected in time for depressions located on major fracture lines.

The relationship between length and width of depressions was analyzed for each quad. Linear plots of length vs. width are presented in Appendix B.

The planimetric shapes of depressions are also described by the circularity index, I_c, expressed as:

$$I_c = A_m/A_e$$

where A_m = measured depression area, and A_e = effective depression area.

The effective depression area is calculated by

$$A_e = \pi * r^2_e$$

The effective radius, r_e, is estimated by

$$r_e = 2(A_m /P_m)$$

where P_m is measured perimeter of the depression.

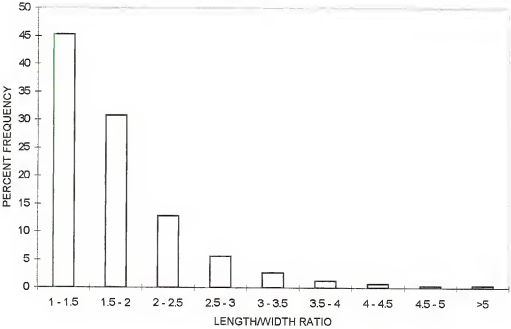

Figure 2.8. Percent frequency of L/W ratio.

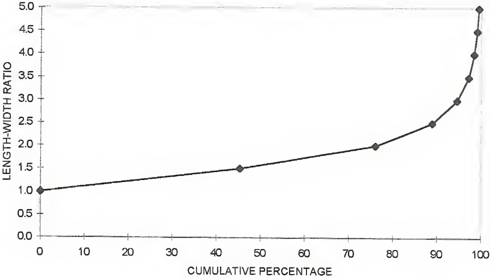

Figure 2.9. Cumulative percentage of L/W ratio.

For a perfectly circular depression, the index of circularity would be unity. The greater it departs from one, the less circular is the depression. Elongated features have values smaller than one whereas convoluted shapes present values greater than one.

Most depressions are near circular in plan with the major modal ratio class between 1-1.2 (Figure 2.10). Mean circularity index value is 1.33 with a standard deviation of 0.45. Approximately 85% of the total population have a circularity index smaller than 1.5 (Figure 2.11).

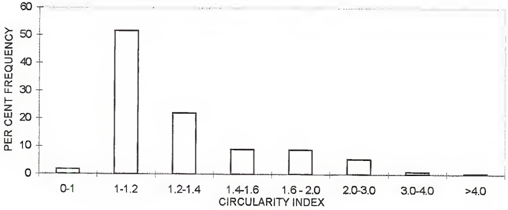

Figure 2.10. Percent frequency of circularity index.

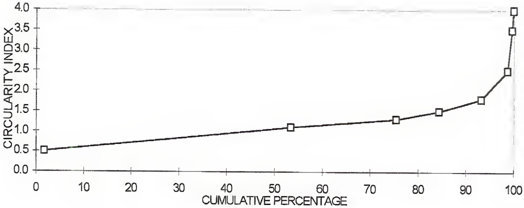

Figure 2.11. Cumulative percentage of circularity index.

Mean Diameter

Mean depression diameters were estimated by obtaining the mean of length and width for each depression. In karst morphometry, the use of mean diameter is more helpful than major and minor axes, since these measures represent maximum rather than average dimensions. Mean diameter distribution for the total population is shown in Figure 2.12. The values range from 10.1 to 2,785.9 m with a standard deviation of 106.6 and a mean of 98.6 m. The major modal class is 5 to 50 meters. Frequency distribution of mean diameter (Figure 2.13) indicates that some 95% of the total population have a mean diameter of less than 300 m.

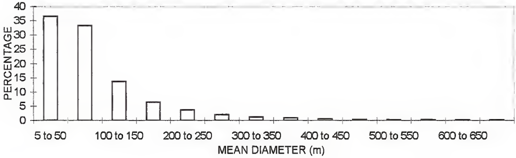

Figure 2.12. Percent frequency of mean diameter.

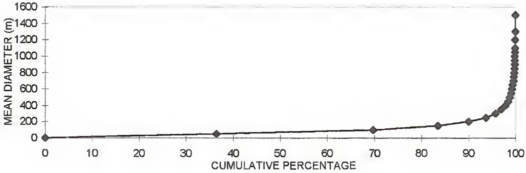

Figure 2.13. Cumulative percentage of mean diameter.

The frequency distribution of depression areas for the total measured population is given in Figure 2.14. The mean value is 14,570.31 m^2, the standard deviation 71,349.08 m^2, and the range of values from 25.0 to 5,804,750 m^2. Within the total measured population, 50% of depressions are smaller than approximately 5,000 m^2.

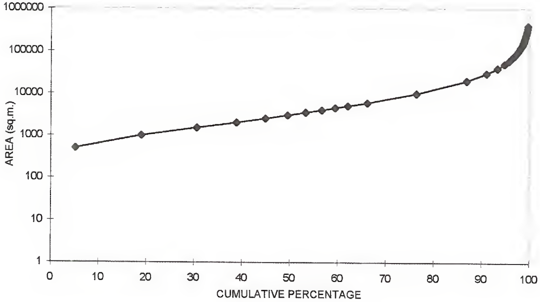

Figure 2.14. Cumulative percentage of depression area.

Depth of Karstic Depressions

Depression depth is considered as an important parameter in distinguishing landforms of temperate and tropical karst terranes. In their comparative study on various karst regions, Troester et al. (1984) concluded that depression depth distributions on temperate and tropical karst regions could be explained by an exponential equation as follows:

(number of sinkholes) = $N_o e^{-Kd}$

where N_o and K are constants, d is depth. The N_o coefficient is affected by the number of depressions, whereas the K coefficient varies within ranges corresponding to temperate and tropical karst areas. Comparing the internal relief within various karst regions, they found that the Florida karst is very flat, represented by broad, shallow depressions with a K value of 0.362 ft^{-1}.

The depth - frequency distribution for 23,031 depressions in the study area is shown in Figure 2.15. Depth values were estimated by counting the number of contours, representing the maximum depth values for depressions. The depth - frequency distribution was found to change exponentially with depth, expressed as:
number of depressions = $137292e^{0.357x}$. It should be noted that the analysis of a much larger population of depressions in this study gives a K value of 0.357 that is similar to 0.362 calculated by Troester et al. (1984) for the Florida karst.

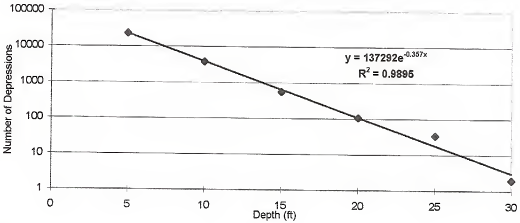

Figure 2.15. Depth-frequency distribution for the depressions.

Discussion

The landforms of the temperate Suwannee River karst area can be compared to karst areas of different morphoclimatic settings. The application of Geographic Information Systems allows the capture, storage, analysis, and presentation of morphometric and spatial distribution parameters of karstic depressions. Despite the accurate, rapid, and objective data processing of GIS, it should be kept in mind that all the analyses performed on karstic depressions are based on the resolution and precision of standard 7.5-minute USGS topographic maps with a contour interval of 5 feet. Karstic depressions in the study area may have been underrepresented because of the limited map resolution and the thick vegetation and sediment cover greatly reducing the overall relief of the terrain. Nevertheless, this study provides general information on the morphometry and spatial distribution of karst depressions on a regional scale.

Overall spatial distribution parameters of the Suwannee River basin karst area are summarized as follows:

Total area: 4063.138 sq.km.
Total depression area: 331.39 sq.km.
Number of depressions: 25157
Average depression density: 6.07 depressions/sq.km.
Average nearest neighbor distance: 186.09 m
Average nearest neighbor distance index: 0.854
Average pitting index: 12.2

A statistical summary of the morphometric parameters of karstic depressions is given in Table 2.2.

Table 2.2. Statistical summary of morphometric parameters

	Area (sq.m)	Mean Diameter (m)	L/W	Circularity Index
Mean	14571.4	98.6	1.74	1.33
Maximum	5,804,750.0	2785.9	14.1	8.86
Minimum	75.0	10.1	1.0	0.006
Standard Deviation	71355.2	106.6	0.68	0.455

Table 2.3 compares the average spatial distribution parameters obtained in this study with those of various karst regions from diverse morphoclimatic settings. This study, with the largest number of depressions examined, provides an accurate representation of the karst landforms of the subtropical Florida karst. Mean depression density is significantly lower than those calculated for other karst regions such as Papua New Guinea, New Zealand, Guatemala, Jamaica, and Puerto Rico. Despite comparable tectonic, lithologic and climatic conditions with the Yucatan karst, the Florida karst is represented by much higher depression densities. This may be resulted from the chemical aggressiveness of recharge waters enhanced by the siliciclastic overburden in Florida.

It should also be noted that the values for depression density and the nearest neighbor index calculated for the study area show great variations. Depression densities calculated for individual quadrangles range from 2.43 (Madison SE) to 15.8 (Mayo SE) overlapping with values representing both temperate and tropical karst areas. Similarly, the nearest neighbor index varying from 0.578 (Hillcoat) to 1.025 (Mayo NE) indicates a wide range of spatial distribution patterns of depressions in the study area ranging from clustered to uniform. These significant variations in spatial distribution parameters along with the morphometry of depressions in a single morphoclimatic zone implicate the existence of some other local factors (e.g. thickness of the overburden above the Floridan aquifer, potentiometric level fluctuation of the Floridan aquifer) controlling the development of karst infrastructure.

Table 2.3. Depression density and nearest neighbor statistics for various karst areas (modified after Ford and Williams, 1989).

AREA	NUMBER OF DEPRESSIONS	DENSITY	NEAREST NEIGHBOR INDEX	PATTERN
Papua New Guinea	1128	10 - 22.1	1.091 - 1.404	Near random to approaching uniform
Waitomo, New Zealand	1930	55.3	1.1236	Near random
Yucatan (Carrillo Puerto Formation)	100	3.52	1.362	Approaching uniform
Yucatan (Chicken Itza Formation)	25	3.15	0.987	Near random
Barbados	360	3.5 - 13.9	0.874	Tending to cluster
Antigua	45	0.39	0.533	Clustered
Guatemala	524	13.1	1.217	Approaching uniform
Belize	203	9.7	1.193	Approaching uniform
Guadelope	123	11.2	1.154	Near random
Jamaica (Browns Town-Waldeston Formation)	301	12.5	1.246	Approaching uniform
Jamaica (Swanswick Formation)	273	12.4	1.275	Approaching uniform
Puerto Rico (Lares Formation)	459	15.3	1.141	Near random
Puerto Rico (Aguada Formation)	122	8.7	1.124	Near random
Guangxi, China	566	1.96 - 6.51	1.60 - 1.67	Approaching uniform
Spain, Sierra de Segura	817	18 - 80	1.66 - 2.14	Near uniform
Florida, Suwannee	25,157	6.06	0.854	Tending to cluster

CHAPTER 3

FACTORS AFFECTING DEPRESSION MORPHOMETRY AND DISTRIBUTION

Prospectus

Morphometic features and spatial distribution of karstic depressions may be controlled not only by global variables such as climate, but also by local factors involved with the hydrology, hydrogeology, structural geology, and the stratigraphy of the karst terrain. These factors, brought about by the geologic setting of the area, are collectively responsible for the unique evolutionary patterns of individual karst terrains. In most cases, their influence predominates over global variables and may lead to karst landform developments distinct from those at nearby areas of the same climatic belt. Therefore, investigation of their effects on the morphometry and spatial distribution of karstic depressions is imperative in understanding karst landform development in a given area.

Ford (1964) analyzed the spatial distribution of dolines in the Mendip Hills karst area and found a relationship between the doline occurrence and topographic setting. He reported that eighty per cent of the dolines are located within narrow valley floors. He also showed that there was not a significant relationship between doline development and cave passages. La Valle (1967, 1968) related doline development in the Central Kentucky karst to geologic variables using multiple regression analysis. He found that the elongation of 25% of the dolines could be controlled by structural and topographic factors. Palmer and Palmer (1975) reported correlation between doline development and underlying cave formation in the southern Indiana karst.

Kemmerly (1976) statistically compared two random samples of dolines in Tennessee based on the agreement of their long axis orientation with systematic joint sets. He found polymodal preferred doline long-axis orientations correlating with the three systematic joint sets in the study area. In a later study on the temporal distribution of doline occurrence, Kemmerly (1980) explained a positive correlation between monthly collapse rates and deviation of rainfall from historical means.

Structural control on the orientations of dolines in the karst of West Virginia was reported by both Ogden and Reger (1977) and Wigal (1978) who also related the doline density to lithologic factors. They found the highest doline occurrence on pure, cavernous, thick-bedded limestones.

White and White (1979) used factor analysis to relate hydrologic and geologic measures to doline development in the Appalachian Highlands. They found rock type as an important factor controlling the dimensions and frequency of dolines.

Performing a regression analysis on the spatial distribution of dolines in the glacial-mantled karst of Iowa, Palmquist (1979) was able to relate doline occurrence to topographic factors such as relief, gradient and elevation; hydrologic factors such as proximity to a drainage way; and to the thickness of soil cover. He concluded that the doline initiation and enlargement in the study area were controlled by regolith thickness and by the amount of groundwater recharge and secondary porosity, respectively.

In an attempt to determine the role of material properties in the development of tropical karst landforms, Day (1982) analyzed purity, petrographic character, and hardness of rocks representing 13 areas of tropical karst in the Caribbean and Central America. He reported a negative correlation between limestone purity and rock hardness determined by in situ measurements of compressive strength using a Schmidt Test Hammer. In their study on the collapse sinkholes in Puerto Rico, Soto and Morales (1984) noted a possible structural control on the development of sinkholes whose long axis orientations showed a significant concentration in northeast direction.

Karstic depressions on the flat-lying dolomitic rocks of the southeastern Minnesota was systematically mapped and analyzed by Dalgleish and Alexander (1984). They found the bedrock stratigraphy to be the primary control on the distribution of sinkholes. Among the secondary controls were slope of the land surface, and composition of surficial materials.

Based on an inventory of modern sinkhole occurrences in west central Florida, Littlefield et al. (1984) reported that sinkhole development commonly occurred along linear patterns especially along the largest photolinear features. In a similar study by Beggs and Ruth (1984), modern sinkhole occurrences documented by the Florida Department of Transportation were correlated with actual rainfall data and geologic controls in the study area. They found no relationship between the rainfall data and sinkhole occurrences that seemed to be controlled by the depth to limerock and phreatic surface.

The spatial distribution of modern sinkholes in west central Florida was statistically compared by Upchurch and Littlefield (1987) with that of ancient karstic depressions identified on topographic maps and aerial photographs. They concluded that the distribution of ancient karstic depressions in areas of uncovered karst significantly predicted the locations of modern sinkholes.

Schmidt and Scott (1984) indicated the importance of structural features such as the Ocala Uplift and Sanford High on the spatial distribution and morphometric features of karstic depressions in Florida. In a detailed study based on the reported sinkhole inventory of the former Florida Sinkhole Research Institute, Wilson and Beck (1992) attempted to relate new sinkhole occurrence in Orlando area to a variety of hydrologic and geologic data. They reported new sinkholes occurring in high recharge areas because the potentiometric level of the Floridan aquifer decreased below its mode value. No relationship existed between photolinears and spatial distribution of sinkholes, mainly because the thick mantle deposits prevented most of the fractures from being detected as photolinears.

This chapter explains and discusses the procedure and the results of an attempt to investigate the effect of hydrogeologic factors on the karst geomorphology of the Suwannee River basin. Since the entire analysis was performed in a GIS environment, the selection of factors addressed in this discussion is constrained by the availability of data in digital format. Yet, the digital data layers utilized in this study cover a variety of hydrologic and geologic factors that may have played significant roles in the regional karst landform evolution. It should be noted, however, the precision of GIS analysis performed here depends upon the accuracy of the digital data layers, which is a direct function of their spatial resolution.

Factors considered in this regional analysis include; thickness of the overburden material above the karstic limestones of the Floridan aquifer, depth to water table, soil type, potentiometric level fluctuation, lithology of the vadose zone, and fracture traces. Spatial and morphometric parameters of depressions include depression density, length, width, length-width ratio, average diameter, area and perimeter.

Methodology

The procedure followed in this analysis consists of a series of GIS operations on the karstic depressions database and the depression density layer described in Chapter 2. These two GIS layers were compared with rasterized data layers representing the geologic and hydrologic controls within the study area. The morphometric data summarized within various categories of control layers were transferred to spreadsheet format in which statistical summaries of morphometric parameters were obtained. Data on the spatial distribution of depressions were utilized by summarizing the depression density layer (Figure 2.3) within various categories of controlling raster layers. Statistical summaries of the depression density layer were expressed by the histograms prepared within the Spatial Analyst extension of the ArcView 3.0 software.

The thickness of the overburden layer was created by applying map algebra functions of GRID, a module of ARC/INFO for the analysis of rasterized data. Depth to bedrock (limestone) layer was subtracted from the topographic elevation layer in order to obtain the thickness values of the overburden material covering the karstic limestone surface within the study area. The resultant layer has a spatial resolution of 62.8 m (side length of the square-shaped cells of GRID layers).

The fluctuation of the Floridan aquifer potentiometric level is represented by a GRID layer created from a digitized contour map prepared by the Suwannee River Water Management District. It represents the total fluctuation between the maximum and minimum levels of the Floridan aquifer potentiometric level as of 12/1988. The layer has a cell size of 200 m.

The rest of the GRID layers representing the depth to water table, soil types, and the vadose zone lithology were converted from the vector layers created by the Suwannee River Water Management District as sublayers of the DRASTIC system. DRASTIC is a standardized system for evaluating ground water pollution potential using hydrogeologic settings (EPA, 1985). The word "DRASTIC" is an acronym representing the most important mappable factors that control the ground water pollution potential; Depth to water, net Recharge, Aquifer media, Soil media, Topography (slope), Impact of the vadose zone, Conductivity (hydraulic) of the aquifer. Among these factors only the depth to water, impact of the vadose zone, and the soil media sublayers show significant variation in the study area so as to affect the distribution of morphometry and density of karstic depressions. These layers were converted to GRIDS with 50 m cell size and their relationships with spatial and morphometric distribution of karstic depressions was analyzed by using the Spatial Analyst extension of the ArcView 3.0 program.

Tectonic control on the development of karst landforms was investigated comparing fracture traces with the major axis orientations and nearest neighbor vectors of karstic depressions compiled in two different GIS databases presented in Chapter 2.

In addition to the karstic depressions depicted on the 1/24,000 scale topographic quads, reported sinkholes compiled in the sinkhole database of the Florida Geological Survey were also analyzed in this study. Despite its bias towards the inhabited areas, the reported sinkhole database provides insight to the current karst development within the study area. Their distribution with regard to the above mentioned geologic controls was also analyzed within the GIS environment.

Results

Lithology of the Vadose Zone

With a cell size of 50 m, the layer representing the vadose zone lithology displays the distribution of silt/clay, shale, sand and gravel, and karstic limestone as the lithologies comprising the vadose zone in the study area (Figure 3.1). The predominant vadose zone lithology within the Suwannee River basin is comprised of silt/clay as indicated by the DRASTIC GIS layer. However, most of the karstic depressions selected for this study are underlain by sand and gravel. The distribution of depression density within vadose zone lithologies is given in Figure 3.2. Percentages of areas corresponding to depression density ranges are in Table 3.1.

Table 3.1. Percentages of areas corresponding to depression density ranges for the vadose zone lithologies.

Depression Density (#/sq.km)	Silt/Clay (1)	Shale (4)	Sand and gravel with significant silt and clay (5&6)	Sand and gravel (8)	Karstic limestone (9)
0-5	73.2%	20.8%	44.5%	33.1%	19.2%
5-10	24.4%	41.6%	44.5%	37.3%	57.7%
10-15	2.4%	37.5%	11%	20.8%	19.2%
15-20	-	-	-	7.4%	3.8%
20-25	-		-	1.4%	-

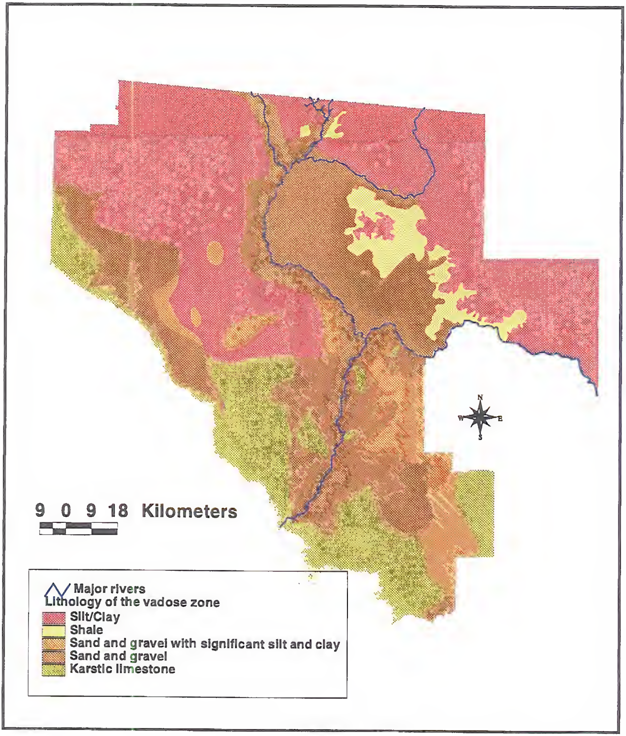

Figure 3.1. Distribution of vadose zone lithology within the study area.

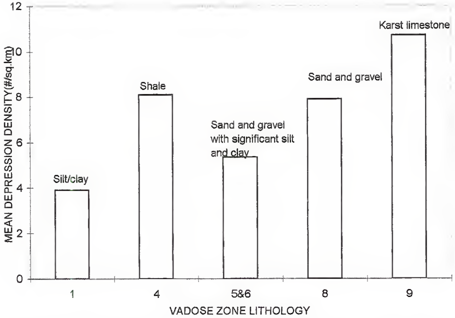

Figure 3.2. Distribution of depression density within the vadose zone lithologies

Thickness of the Overburden Material

Thickness of the overburden material ranges from zero within the Gulf Coastal Lowlands to 156.48 m at the Northern Highlands where thick deposits of the Hawthorn Group overlie the Floridan aquifer (Figure 3.3). It tends to increase with the topographic elevation. Mean thickness value is 19.32 m, with a standard deviation of 21.5.

A greater part of the study area is overlain by a thin soil layer of 0-6 m in thickness. In this area, the Floridan aquifer is unconfined and receives significant recharge through diffuse infiltration of the surface runoff. Semiconfined hydrogeologic conditions occur where the overlying material gets thicker and contains clay layers of the Hawthorn Group. These local semiconfined conditions are mostly encountered close to the Cody Scarp, where impermeable layers within the outliers of the retreating Hawthorn

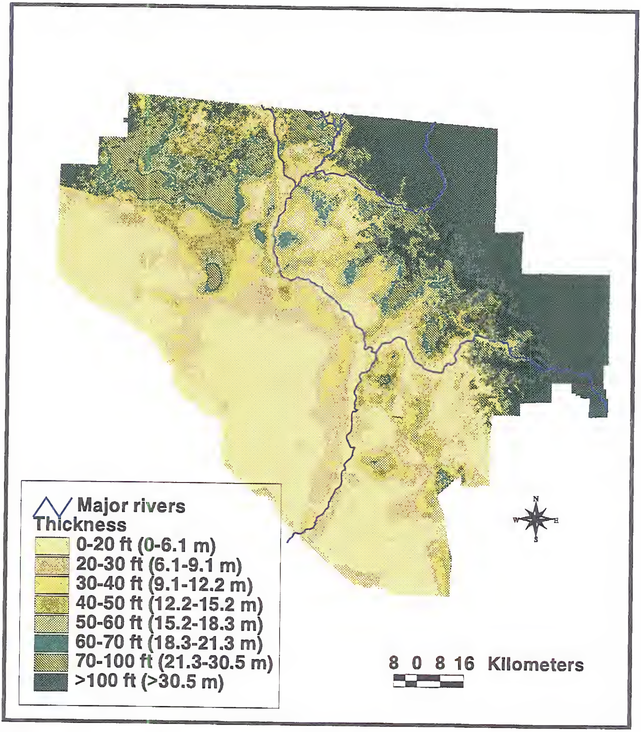

Figure 3.3. Distribution of overburden thickness within the study area.

Group sediments cover the Floridan aquifer. At the Northern Highlands physiographic region, thickness of the overburden material increases significantly to the northeast from 30 m to approximately 155 m.

The spatial distribution of karstic depressions within the zones of overburden thickness is given in Figure 3.4. Depression density tends to remain between 7 to 8 depressions per sq. km. within the 0-24.4m (0-80 ft) overburden thickness range. A significant decrease in the number of depressions is observed for greater thickness values of the overburden material. Mean depression density drastically goes down to 2.3 depressions per sq.km where thickness of the overlying material is greater than approximately 35 m (120 ft). This results from the confined conditions brought about by the increased silt/clay content of the overburden material.

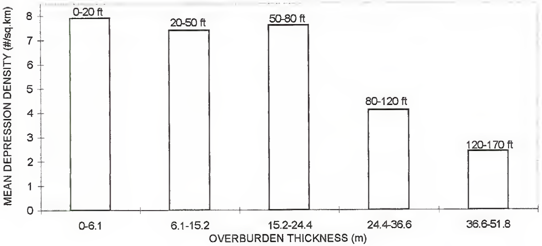

Figure 3.4. Changes in depression density within the zones of the overburden thickness.

The distribution of depression density within the zones of the overburden thickness values is also expressed as percentages of areas corresponding to depression density intervals in Table 3.2.

Table 3.2. Percentages of areas corresponding to depression density ranges for the zones of the overburden thickness.

Depression Density (#/sq.km)	Overburden Thickness 0 - 6.1 m (0-20 ft)	Overburden Thickness 6.1 - 15.2 m (20-50 ft)	Overburden Thickness 15.2 – 24.4 m (50-80 ft)	Overburden Thickness 24.4 - 36.5 m (80-120 ft)
0-5	36.5%	36.7%	37.2%	75.5%
5-10	36.5%	38.3%	33.3%	18.9%
10-15	18.2%	18.2%	24.4%	5.6%
15-20	7.3%	5.8%	5.1%	-
20-25	1.5%	1.0%	-	-

Distribution of morphometric parameters of karstic depressions can not be explained solely by the variation of the overburden thickness. A collective interpretation of the overburden thickness variation together with the type of vadose zone lithology provides a better understanding of the morphometric distribution of depressions. Figure 3.5 summarizes the lithological variation within the zones of the overburden thickness. Mean depression area varies only between 13179.9 to 15763.9 sq.m. for the values of overburden thickness up to 21 m (Figure 3.6). With further increase in overburden thickness, depression area is controlled by the lithologic properties of the overlying unit. Mean depression area reaches a maximum of approximately 23,500 sq.m., for the overburden thickness zone of 21 to 30 m corresponding to the outliers of the semipermeable Hawthorn Group within the Marginal Zone. It then significantly decreases for thickness values greater than 30 m owing to the elevated silt and clay contents of the overlying unit.

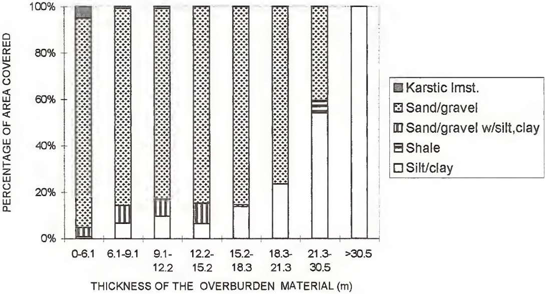

Figure 3.5. Changes in vadose zone lithology with the thickness of the overburden.

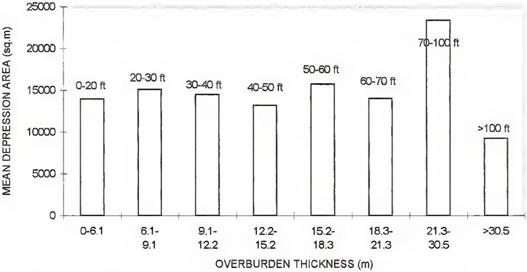

Figure 3.6. Changes in mean depression area with the overburden thickness.

Mean values of depression diameter and length/width ratio show even less variation within the zones of overburden thickness (Figures 3.7 & 3.8). Smaller length/width ratios observed for thickness values grater than 30 m indicate a tendency for elongation of depressions as the thickness and cohesiveness of the overburden material increase.

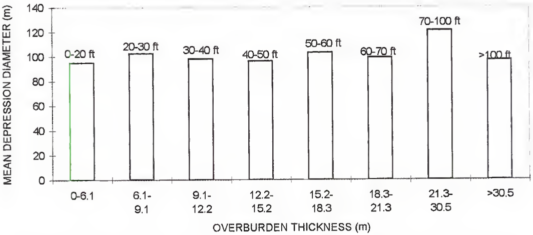

Figure 3.7. Changes in mean depression diameter with the overburden thickness.

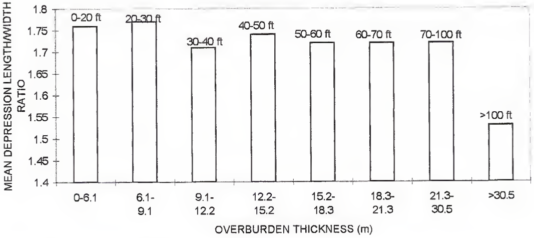

Figure 3.8. Changes in mean length/width ratio with the overburden thickness.

Floridan Aquifer Potentiometric Level Fluctuation

Potentiometric level fluctuation values of the Floridan aquifer range from 1.25 m at the western part of the study area to 11.77 m at north, with a mean value of 3.65 m. The standard deviation is 2.08 (Figure 3.9). A complicated surface water - ground water interaction through karstic conduits explained in Chapter 1 is also revealed by the high potentiometric level fluctuation along the Suwannee River. Regions of minimum potentiometric level fluctuations west of the Suwannee River correspond to the discharge area of the Floridan aquifer.

The spatial distribution of karstic depressions within the zones of potentiometric level fluctuation approaches a normal distribution curve (Figure 3.10). Depression density values generally increasing with the potentiometric level fluctuation reach their maximum value for the fluctuation interval of 4.3 - 5.2 m (14-17 ft) and gradually declines for greater fluctuation rates.

The distribution of depression density ranges within the zones of the potentiometric level fluctuation is expressed as percentages in Table 3.3.

Table 3.3. Percentages of areas corresponding to depression density ranges for the zones of Floridan aquifer potentiometric level fluctuations.

Depression Density (#/sq.km)	Fluc. 1.2-2.1 m (4 –7 ft)	Fluc. 2.1-3.0 m (7-10 ft)	Fluc. 3.0-4.3 m (10-14 ft)	Fluc. 4.3-5.2 m (14-17 ft)	Fluc. 5.2-6.4 m (17-21 ft)	Fluc. 6.4-7.3 m (21-24 ft)	Fluc. 7.3-8.5 m (24-28 ft)	Fluc. 8.5-9.4m (28-31 ft)	Fluc. 9.4-10.6 m (31-35 ft)
0-5	64.3%	33.4%	30.5%	21.5%	31.5%	64.8%	71.2%	100%	81.6%
5-10	33.3%	35.5%	38.2%	39.3%	44.3%	32.4%	25.4%	-	18.4%
10-15	2.4%	20.7%	22.0%	27.7%	10.8%	2.7%	2.8%	-	-
15-20	-	7.4%	8.2%	9.1%	3.3%	-	0.7%	-	-
20-25	-	2.1%	1.1%	2.5%	-	-	-	-	-
25-30	-	0.5%	-	-	-	-	-	-	-
30-35	-	0.3%	-	-	-	-	-	-	-

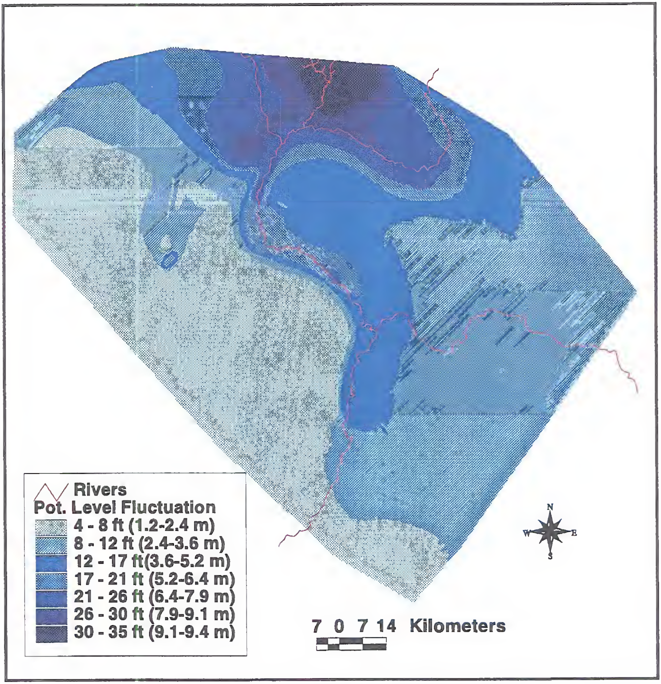

3.9. Potentiometric level fluctuation of the Floridan aquifer.

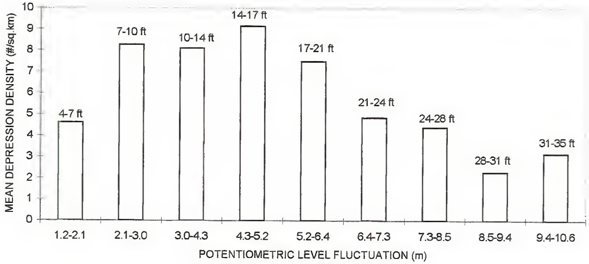

Figure 3.10. Changes in mean depression density with the potentiometric fluctuation.

Distribution of mean depression area within the zones of potentiometric level fluctuation shows a unimodal pattern with a major mode for potentiometric level fluctuations between 6.4 to 9.1 m (Figure 3.11). For fluctuations greater than 9.1 m, mean depression area decreases significantly because of the confined hydrogeologic conditions. Mean depression diameter reaches its maximum of 127.9 m within the fluctuation interval of 7.9 - 9.1 m (Figure 3.12). Variation of mean length/width ratio indicates an increase in elongation of depressions with increasing fluctuation values (Figure 3.13). It tends to decrease for fluctuation values greater than 7.9 m.

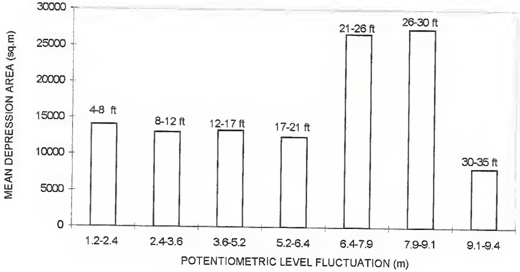

Figure 3.11. Changes in mean depression area with potentiometric fluctation.

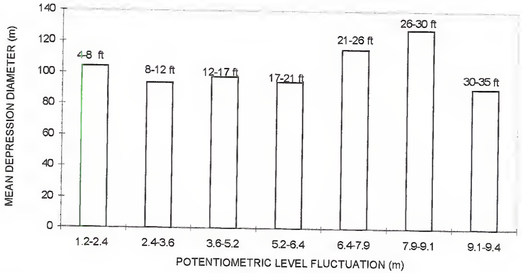

Figure 3.12. Changes in mean depression diameter with potentiometric fluctation.

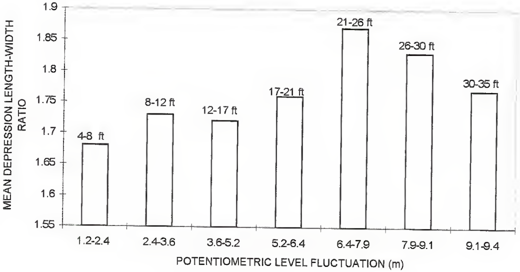

Figure 3.13. Changes in mean length/width ratio with potentiometric fluctation.

Soil Type

The soil media layer with a cell size of 50 m displays the distribution of a variety of soil types such as nonshrinking and/or nonaggregated clay, peat, muck, (soil type = 1); sandy loam (soil type = 6); shrinking and/or aggregated clay (soil type = 7); and, sand (soil type = 9)(Figure 3.14). Greater part of the Suwannee River basin is covered by "nonshrinking and nonaggregated clay, peat, and muck". However, within the study area, "sand" and "shrinking and/or aggregated clay" categories occur as dominant soil types.

Values of depression density are summarized within the zones of soil media in Figure 3.15. In soil type 7 depicted as "shrinking and/or aggregated clay", mean karstic depression density peaks at 8.6 depressions per sq.km.. The "sand" category is also represented by a high density of depressions (~7.5 dep./sq.km.).

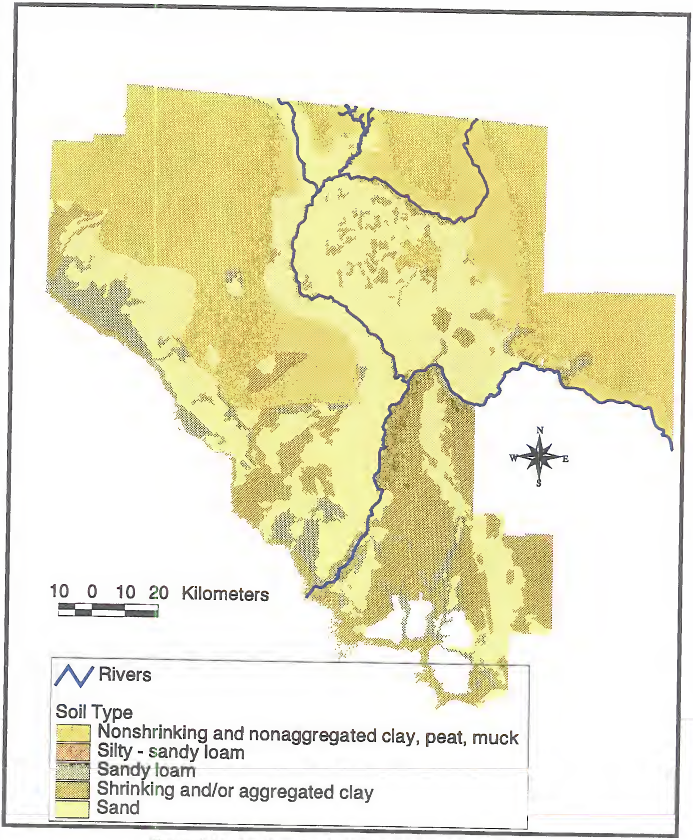
10 0 10 20 Kilometers
N
W
E
S
Rivers
Soil Type
Nonshrinking and nonaggregated clay, peat, muck
Silty - sandy loam
Sandy loam
Shrinking and/or aggregated clay
Sand

Figure 3.14. Distribution of soil types within the study area.

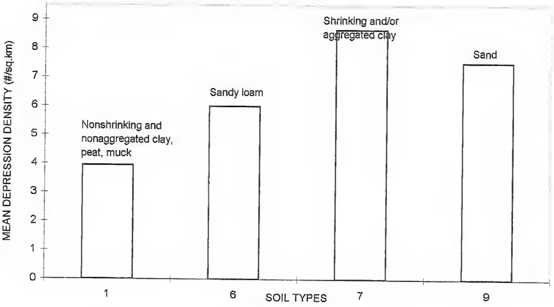

Figure 3.15. Changes in mean depression density with soil types.

The distribution of depression density categories within the zones of soil types is summarized by the percentage of corresponding area in Table 3.4.

Table 3.4. Percentages of areas corresponding to depression density ranges for the soil types.

Depression Density (#/sq.km)	Soil type: 1	Soil type: 6	Soil type: 7	Soil type: 9
0-5	75.0%	69.0%	25.7%	37.1%
5-10	23.1%	31.0%	42.6%	35.8%
10-15	1.9%	-	22.3%	20%
15-20	-	-	8.1%	6.1%
20-25	-	-	1.3%	1.0%

Evaluation of morphometric features of karstic depressions for each soil category reveals that the depression area and mean depression diameter are greatest for the soil type 1 (nonshrinking and nonaggregated clay, peat, muck) (Figures 3.16, 3.17 & 3.18).

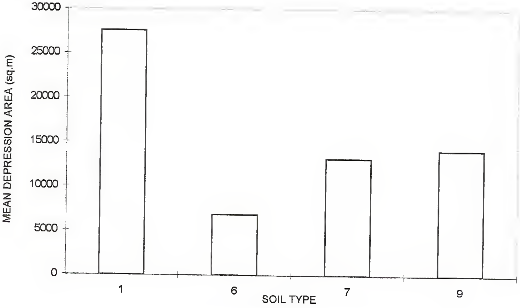

Figure 3.16. Changes in mean depression area with soil types.

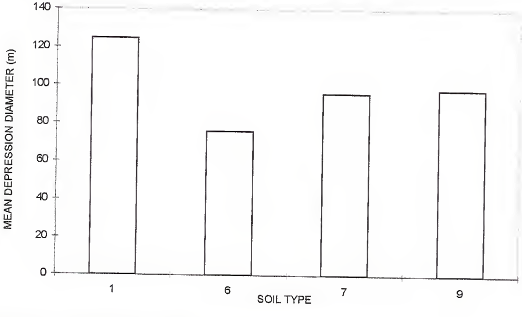

Figure 3.17. Changes in mean depression diameter with soil types.

Areas with soil types 9 and 7 (sand, and shrinking and/or aggregated clay) have the most irregular depression shapes, with the length/width ratios getting as high as 1.75.

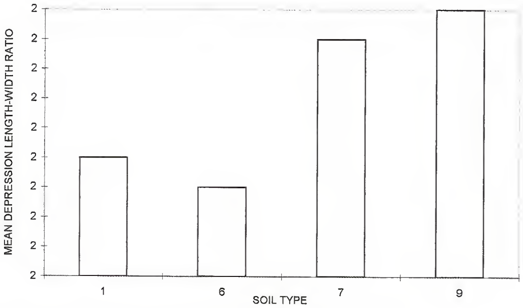

Figure 3.18. Changes in mean length/width ratio with soil types.

Depth to Water Table

The GRID layer of "depth to water table" has a cell size of 50 m as well. Ranges of depth displayed in the map include; 0-4.5m (0-15 ft), 4.5-9.1 m (15-30 ft), 9.1-15.2 m (30-50 ft), 15.2-22.9 m (50-75 ft), 2.9-30.5 m (75-100 ft) and >30.5m (Figure 3.19). Depth to water table within the Suwannee River basin varies between 0 to 4.5 m along the coastal zone and the Suwannee River, and increases with the topographic elevation of the area. The Northern Highlands physiographic province is represented by the deepest water table conditions.

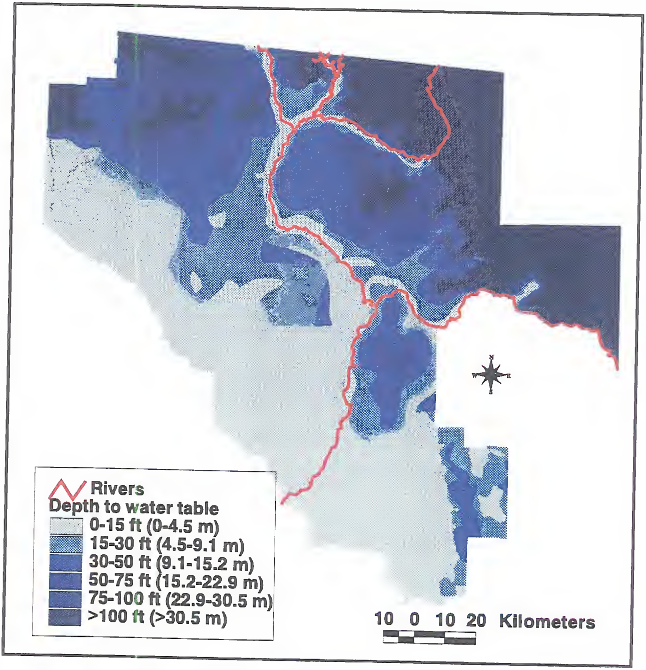

Figure 3.19. Distribution of depth to water table within the study area.

Depressions are most densely located where depth to water table is between 9.1 to 15 m. (Figure 3.20). Depression density gradually decreases from around 9 to less than 3 depressions per sq.km for water table configurations deeper than 15 m. This trend is correlated with the increase in silt/clay content of the vadose zone above the water table (Figure 3.21). Low densities for water depth values greater than 20 m roughly correspond to semiconfined and confined conditions of the Floridan aquifer where interstratal dissolution and collapse sinkholes predominate over solution sinkholes.

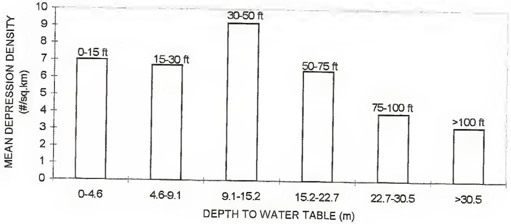

Figure 3.20. Changes in mean depression density with depth to water table.

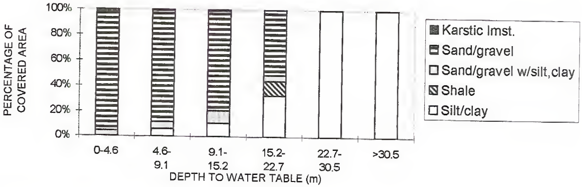

Figure 3.21. Changes in vadose zone lithology with depth to water table.

Table 3.5 shows the percent distribution of areas corresponding to depression density intervals within the zones of the depth to water table.

Table 3.5. Percentages of areas corresponding to depression density ranges for the zones of the depth to water table.

Depression Density (#/sq.km)	Depth to water: 0-4.6 m (0-15 ft)	Depth to water: 4.6-9.1 m (15-30 ft)	Depth to water: 9.1-15.2 m (30-50 ft)	Depth to water: 15.2-22.8 m (50-75 ft)	Depth to water: 22.8-30.5 m (75-100 ft)	Depth to water: >30.5 m (>100 ft)
0-5	43.0	40.0	24.4	44.3	87.5	80
5-10	39.3	40.2	35.1	36.1	12.5	20
10-15	14.2	16.8	26.9	19.4	-	-
15-20	4.9	2.9	11.1	3.3	-	-
20-25	1.12	0.4	2.6	-	-	-
25-30	0.4	-	-	-	-	-
30-35	0.2	-	-	-	-	-

In areas where water table is less than 30.4 m deep, mean depression area increases with depth to water table (Figure 3.22). The decrease in mean depression area observed for deeper water table depths is caused by the thick and cohesive overburden layer within the Northern Highlands physiographic region. The variation of mean depression diameter within the zones of depth to water table tends to increase with depth (Figure 3.23), whereas mean length/width ratio of depressions approaches unity as the depth to water table increases (Figure 3.24). In other words, depressions become more equidimensional as the water table gets deeper.

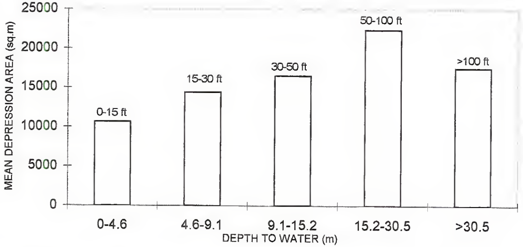

Figure 3.22. Changes in mean depression area with depth to water table.

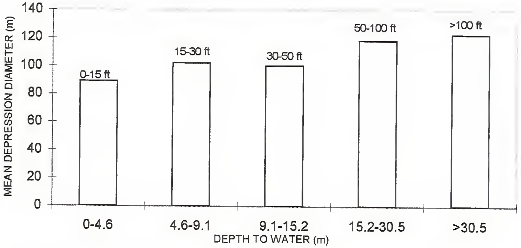

Figure 3.23. Changes in mean depression diameter with depth to water table.

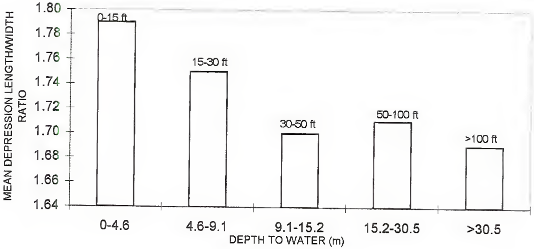

Figure 3.24. Changes in mean depression length/width ratio with depth to water table.

Photolineaments and Orientation of Depressions

The influence of fractures on karstic depression development was investigated by overlaying the map of fracture traces detected as photolinears on the layer of depression density (Figure 3.25). The digitized map of fracture traces compiled by the Florida Geological Survey shows regional photolineaments with preferred orientations in NE-SW and NW-SE directions.

Orientation of depressions was analyzed in two phases. The long axis orientations of 24,757 depressions were measured in GIS and classified into eighteen 10° classes. Alignment of depressions with regards to each other (nearest neighbor direction vector) was investigated using Euclidian distance functions of GIS based on the centroid locations of depressions.

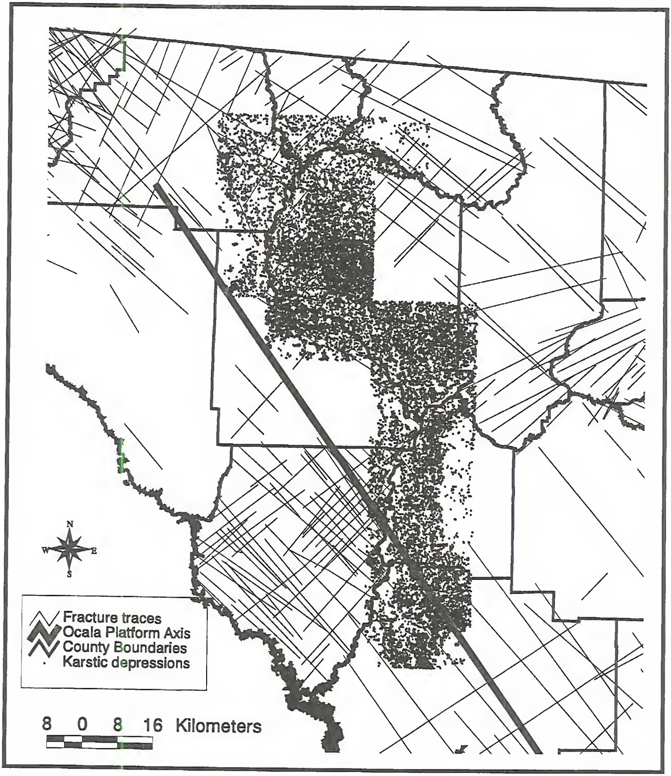

Figure 3.25. Map of photolinears and depression density within the study area.

The distribution of long axis orientations of depressions does not indicate a preferred direction (Figure 3.26). No attempts were made to statistically infer a difference of one subclass of azimuths from others because of the apparent homogenous distribution of their percent frequencies. The lack of dominant long axis orientation may be related to the absence of controlling regional structural trends.

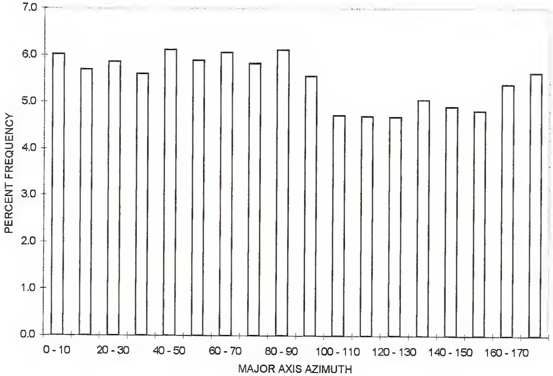

Figure 3.26. Histogram of depression major axis orientations.

The distribution of nearest neighbor direction vectors, however, indicates a preponderance of orientation for the azimuth range between 80 -100° (Figure 3.27). Approximately 18% of all depressions have a nearest neighbor vector between 80 -100°. The second most common nearest neighbor vector azimuth range occurs between 160 - 180° with a percentage of about 15%.

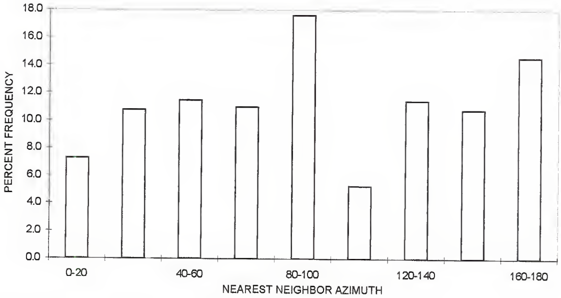

Figure 3.27. Histogram of nearest neighbor directions.

Collective interpretation and comparison of major axis and nearest neighbor vector orientations with regional photolineaments do not reveal an apparent pattern of preferred orientation common to both data sets. However, the implications of dominant nearest neighbor vector orientations can be explained by considering the aspect of topographic slope within the study area.

Topographic Slope

A majority of karstic depressions analyzed in this study occur at the relatively flat-lying karst terranes of the Gulf Coastal Lowlands physiographic province (Figure 1.2). However, most karstic activity takes place within the Marginal Zone along the Cody escarpment in which topographic relief is much more pronounced (Figure 3.28). The importance of this area in current karst landform development can be explained by addressing the chemical aggressiveness of allogenic surface waters originating from the Northern Highlands. It should also be noted that increased topographic relief has been

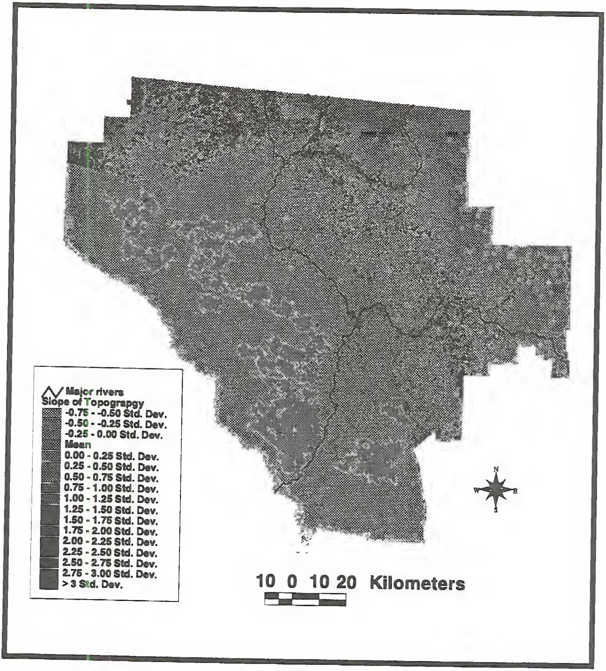

Figure 3.28. Map of topographic slope within the study area.

instrumental in sustaining surface runoff essential for the formation and development of solution sinkholes.

The preferred orientation of nearest neighbor vectors in an azimuth interval of 80-100 degrees does not correspond to the regional fracture pattern. However, its close agreement with the predominant E-W aspect of topographic slope might indicate that the alignment of karstic depressions is controlled by the relief of local topography (Figure 3.29).

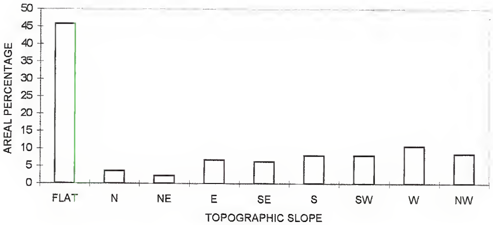

Figure 3.29. Histogram of topographic slope direction distribution within the study area.

Reported Sinkholes

Based on the database compiled by the Florida Geological Survey, the distribution of sinkholes reported in the study area between 1948 and 1992 is given in Figure 3.30. Approximately 95% of all reported sinkholes located in the study area occur where the Floridan aquifer is unconfined or semiconfined. However, since a great number of new sinkholes may have been unnoticed or unreported especially at the rural parts of the study

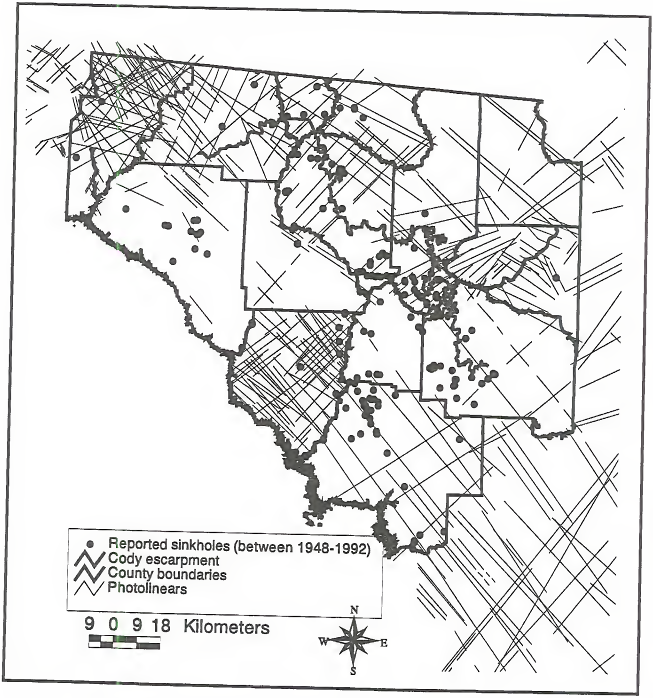

Figure 3.30. Distribution of reported sinkholes within the study area.

area, actual population of new sinkholes can be much higher than is suggested by the database. In order to eliminate the problem of under-reporting, Wilson (1995), based on the types of land-use, recommends various adjustment factors for reported sinkhole frequencies.

In this study, an overall morphometric analysis of reported sinkholes is attempted as they are described in the database. Because of the problem of under-reporting, frequency and density distribution of new sinkhole formation is not addressed. From the morphometric standpoint, new sinkholes are strikingly different from closed depressions depicted in topographic maps. They tend to be much smaller and circular in shape than those karstic depressions whose dimensions are constrained by the map scale and changed over time due to erosion and coalescing sinkholes. Structural control on new sinkhole development is clearly seen especially at the south and southeast of the area where sinkholes are aligned along NW-SE photolineaments (Figure 3.30). The influence of E-W topographic slope is also suggested especially close to high relief areas.

Distribution of reported sinkholes with regards to the vadose zone reveals that almost 80% of the 163 sinkholes occur within sand and gravel (Figure 3.31). Despite its most wide-spread coverage within the study area, the silt/clay vadose zone lithology hosts only 6.1% of the total reported sinkholes. The mean diameter shows a relatively homogenous distribution except for the shale lithology in which the mean diameter is close to 10 meters within a population of only three sinkholes (Figure 3.32) Sinkholes occurring within karstic limestone, i.e. with a little or no overburden, have the smallest mean diameter.

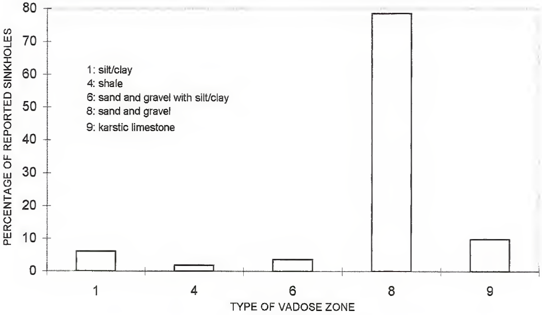

Figure 3.31. Changes in reported sinkhole frequency with vadose zone lithology.

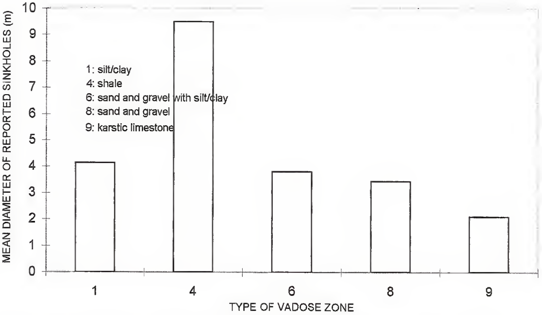

Figure 3.32. Changes in mean diameter with vadose zone lithology for reported sinkholes.

Similarly, sinkhole length/width ratio approaches the unity for karstic limestones and increases with the sand and gravel content of the vadose zone material (Figure 3.33). Mean depth values for different vadose zone types range from 1.88 to 6.79 (Figure 3.34).

Approximately 51% of the reported sinkholes occur within the 3.0-4.2 m fluctuation range of the Floridan aquifer potentiometric level (Figure 3.35). The mean diameter shows a little variation around 4 meters and reaches 11 meters for the 7.6-8.5 m fluctuation range (Figure 3.36). The length/width ratio of reported sinkholes is normally distributed within the zones of the potentiometric level fluctuation (Figure 3.37). Sinkholes occurring within the 6.7-7.6 m fluctuation interval represent the maximum length/width ratio in the study area. The ratio approaches unity for higher values of fluctuation. Similarly, mean depth values slightly varying around 3 meters reach a maximum of 7.7 for the 6.7-7.6 m fluctuation interval (Figure 3.38).

The distribution of reported sinkholes with regard to the depth to water table is given in Figure 3.39. More than half of the sinkholes occur within the water table depth range of 4.5 to 9.1 m. Areas with a depth to water table more than 30.4 meters have the largest sinkholes (Figure 3.40), whereas water table depth range of 4.5 to 9.1 m represents the deepest sinkholes (Figure 3.41). Length/width ratio within the zones of the depth to water table does not show significant variation (Figure 3.42). Sinkholes with a water table depth of 4.5 to 15.24 m are relatively irregular.

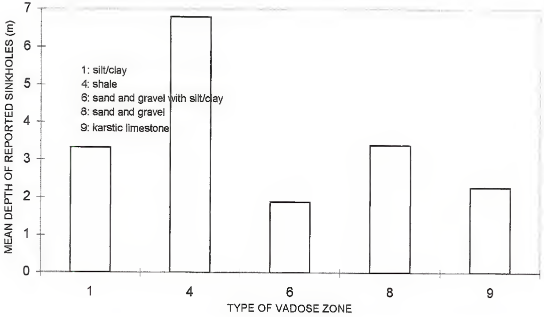

Figure 3.33. Changes in mean depth with vadose zone lithology for reported sinkholes.

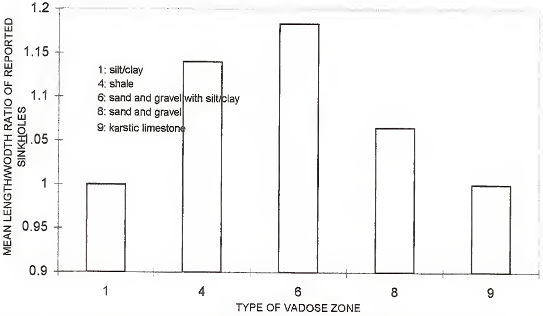

Figure 3.34. Changes in mean length/width ratio with vadose zone lithology for reported sinkholes.

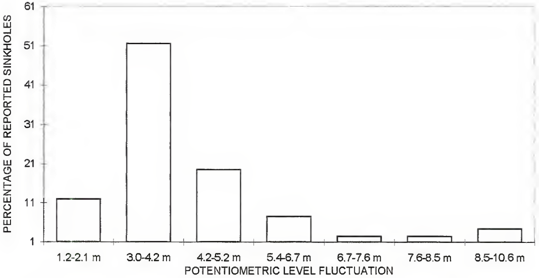

Figure 3.35. Changes in reported sinkhole frequency with potentiomeric level fluctuation of the Floridan aquifer.

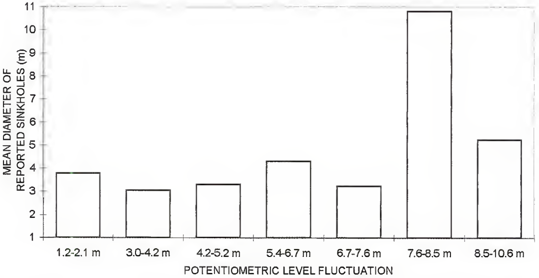

Figure 3.36. Changes in mean diameter with potentiomeric level fluctuation of the Floridan aquifer for reported sinkholes.

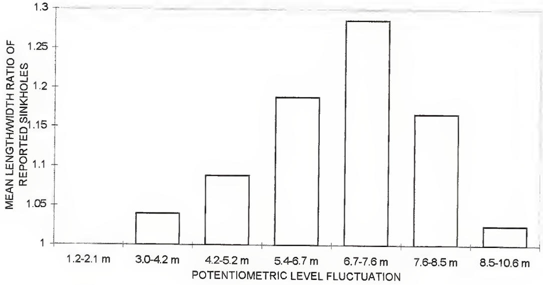

Figure 3.37. Changes in mean length/width ratio with potentiometric level fluctuation of the Floridan aquifer for reported sinkholes.

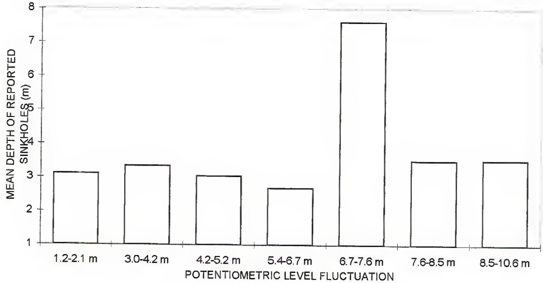

Figure 3.38. Changes in mean depth with potentiometric level fluctuation of the Floridan aquifer for reported sinkholes.

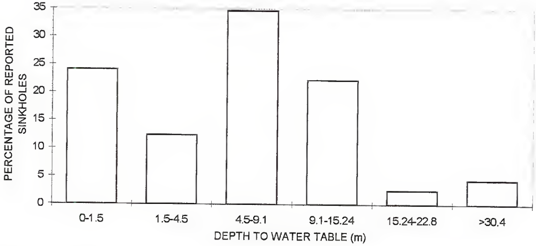

Figure 3.39. Changes in reported sinkhole frequency with depth to water table.

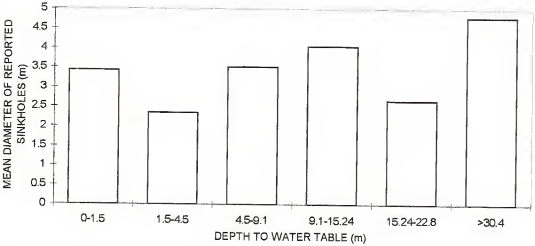

Figure 3.40. Changes in mean diameter with depth to water table for reported sinkholes.

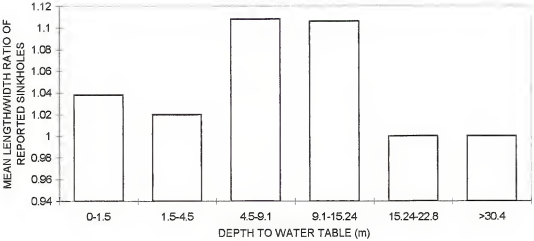

Figure 3.41. Changes in mean length/width ratio with depth to water table for reported sinkholes.

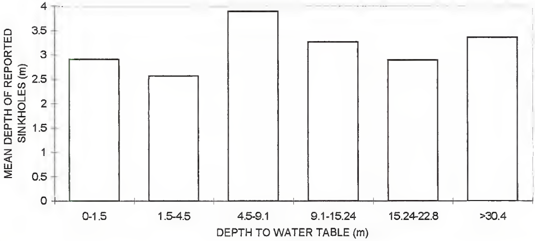

Figure 3.42. Changes in mean depth with depth to water table for reported sinkholes.

Most of the reported sinkholes are located in areas with an overburden thickness less than 6.9 m (Figure 3.43). Mean sinkhole depth within the zones of the overburden thickness show an irregular variation suggesting that the thickness of the overlying material is not a direct controlling factor on the morphology of new sinkholes (Figure 3.44). Mean diameter and L/W ratios are greatest in areas where overburden thickness varies between 15.2 to 18.3 m (Figures 3.45 and 3.46).

Some 55% of the total reported sinkholes are covered by sand (Figure 3.47), in which the highest L/W ratio and diameter values are attained (Figures 3.48 and 3.49). Sinkholes within the soil type "shrinking and/or aggregated clay" have the highest depth value of 12 m (Figure 3.50).

Discussion

The application of GIS has made possible the comparison of large data sets containing detailed spatial and thematic information on a variety of geologic controls with two comprehensive data layers of depression morphometry and density. It also provided a consistent level of accuracy, objectivity and speed into a technique that conventionally consisted of extremely time consuming, labor intensive and user-biased processes. Therefore, this study successfully demonstrates that the GIS can be applied to investigate geomorphologic characteristics of karst terrains and provide intensive analyses of spatially defined data sets.

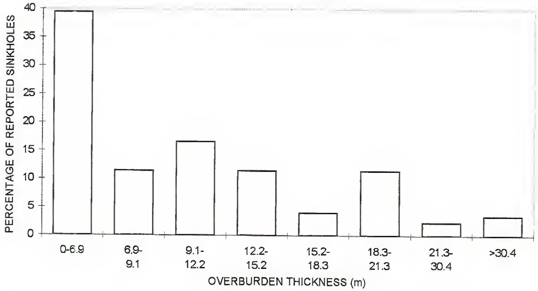

Figure 3.43. Changes in reported sinkhole frequency with the thickness of the overburden material.

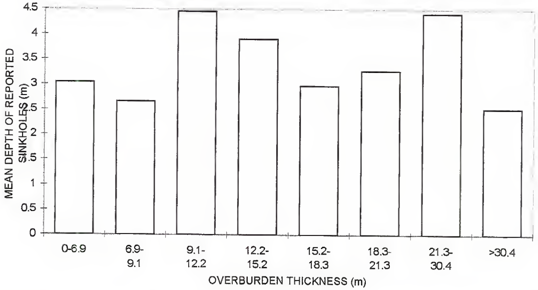

Figure 3.44. Changes in mean depth with the thickness of the overburden material for reported sinkholes.

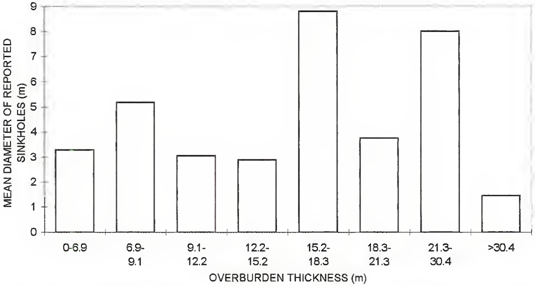

Figure 3.45. Changes in mean diameter with the thickness of the overburden material for reported sinkholes.

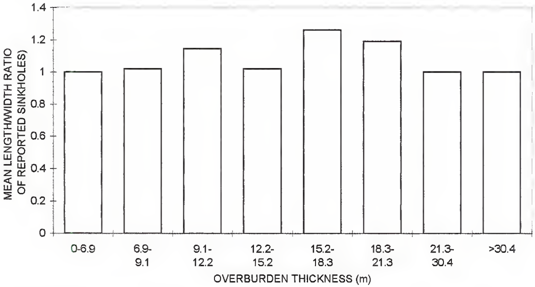

Figure 3.46. Changes in mean length/width ratio with the thickness of the overburden material for reported sinkholes.

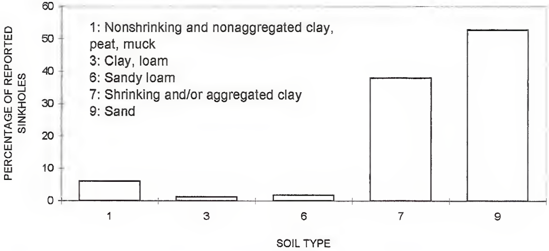

Figure 3.47. Changes in reported sinkhole frequency with the soil type.

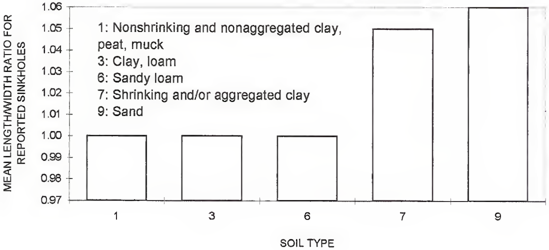

Figure 3.48. Changes in mean length/width ratio with the soil type.

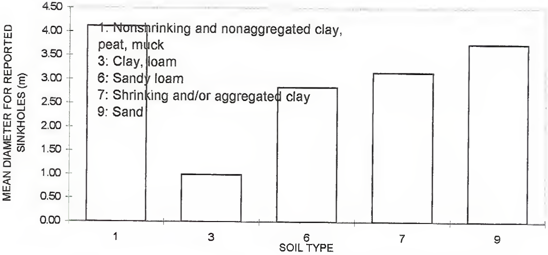

Figure 3.49. Changes in mean diameter with the soil type for reported sinkholes.

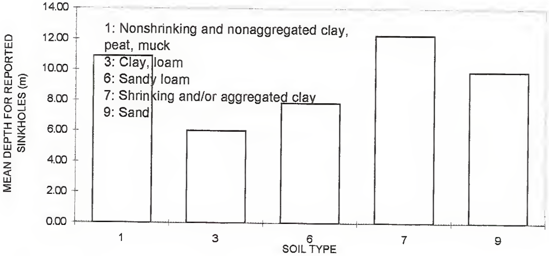

Figure 3.50. Changes in mean area with the soil type for reported sinkholes.

Despite the precision and the significant amount of information provided by the GIS analysis, a satisfactory answer to the question of controlling factors on the geomorphologic evolution of the Suwannee River area karst terrane has not been achieved. None of the geologic and hydrologic controls can be singled out as the most influential factor on the morphometry and frequency of karstic depressions. In order to gain a better understanding of controlling mechanisms of karstic depression development all the factors described above must be taken into consideration in an holistic approach. For example, the influence of the overburden thickness above the Floridan aquifer can only be comprehended by considering the type of overburden material, i.e. type of vadose zone. The mean morphometric parameters and percentages of clay contents within the zones of the overburden thickness are summarized in Table 3.6.

Table 3.6. Summary of the mean morphometric parameters and the clay content within the zones of the overburden thickness.

OVERBURDEN THICKNESS	AREA (sq.m)	MEAN DIAMETER (m)	L/W	PERCENT OF AREA WITH CLAY
0-6.1 m (0-20 ft)	13,969.9	94.7	1.76	0.82
6.1-9.1 m (20-30 ft)	15,115.8	102.4	1.76	6.61
9.1-12.2 m (30-40 ft)	14,495.6	98.0	1.71	10.43
12.2-15.2 m (40-50 ft)	13,179.9	96.1	1.74	6.40
15.2-18.3 m (50-60 ft)	15,763.9	102.9	1.72	12.32
18.3-21.3 m (60-70 ft)	14,005.2	98.6	1.72	33.33
21.3-30.5 m (70-100 ft)	23,365.8	120.6	1.72	58.41
>30.5 m (>100 ft)	9,263.5	96.5	1.53	100

The influence of the type of vadose zone lithology becomes important especially for the overburden thickness greater than 30.5 m (100 ft). Significant decreases in all of the morphometric parameters indicate smaller and less elongated depressions for areas where the Floridan aquifer is covered with thick impermeable material. Largest dimensions of depression morphometry occur within the overburden thickness zone of 21.3-30.5 m (70-100 ft) where lateral dissolution occurs within the semipermeable horizons of the overburden material especially within the Marginal Zone.

Among the layers addressed in this analysis, depth to water table and fluctuation of the potentiometric level represent modern hydrogeologic conditions. We have no knowledge of their configurations during the initiation and early development of "ancient" karstic depressions depicted on topographic maps. These layers, along with the overburden thickness, soil and vadose types play a much more important role in modern sinkhole development. Unfortunately, the population of reported sinkholes is far from being adequate to draw statistically meaningful results as to the controlling factors on the "modern" sinkhole development within the Suwannee River basin.

Nevertheless, the variation of depression morphometry with depth to water table can be interpreted by considering the lithology of the material above the water table (lithology of the vadose zone). Table 3.7 displays the variations of morphometric parameters along with the clay contents within the zones of the depth to water table. The gradual increase in depression area observed for depth to water values less than 30.5 m (100 ft) can be explained by the greater area of influence caused by a deeper water table. Regions of deep water table represent recharge areas to the unconfined Floridan aquifer. Rapid and focused infiltration of surface runoff into the karst aquifer reactivates the paleo depressions and conduit systems by removing the infilling material. This very common process in the multicyclic karst network of Florida results in gradual growth of depressions. Smaller morphometric dimensions for water table depths greater than 30.4 m correspond to the confined hydrogeologic conditions caused by the elevated clay contents of the vadose zone.

Table 3.7. Summary of the mean morphometric parameters and the clay contents within the zones of the depth to water table.

DEPTH TO WATER TABLE	AREA (sq.m)	MEAN DIAMETER (m)	L/W	PERCENTAGE OF AREA WITH CLAY
0-4.6m (0-15 ft)	10,650	89.1	1.79	0
4.6-9.1 m (15-30 ft)	14,410	101.9	1.75	4.95
9.1-15.2 m (30-50 ft)	16,493	100.1	1.70	10.6
15.2-30.5 m (50-100 ft)	22,332	118.2	1.71	65.0
>30.5 m (>100 ft)	17,488	122.4	1.69	100

Surprisingly, the influence of fracture traces on sinkhole morphology and alignment is not obvious. This may be explained by the changes in the planimetric shapes of depressions because of erosional processes and depression growth and coalescence In a regional perspective, karstic depressions tend to align and have their major axes oriented in almost every directions regardless of the dominant regional fracture pattern. More detailed, finer resolution of fracture tracing by using SPOT images was attempted in this study, but not discussed here because of the inevitable subjectivity of the procedure in detecting extremely fuzzy and thus controversial fracture tracings obscured by the soil cover.

In conclusion, the “ancient” karstic depressions analyzed in this study have been influenced by all of the factors to various degrees as discussed in this Chapter. However, the most important controlling factor still to be addressed (Chapter 5) is “time”. It is responsible for the evolution of karst landforms in which deformation and coalescing of depressions through either competitive or contagious processes have resulted in significantly different depression morphometry and density patterns.

CHAPTER 4
KARSTIC EROSION RATE CALCULATIONS

Prospectus

In an attempt to explain the observed differences in karst landform evolution with climatic differences, studies were directed to investigate whether or not the variations in karst terrains are caused by variations in processes, i.e. dissolution of carbonate rocks. After Corbel's (1957) highly controversial interpretation of available data on dissolution rates collected from different climatic belts of the world, karstic erosion rates have been reported from a variety of regions in Tropical, Temperate, and Arctic/Alpine morphoclimatic zones, representing a variety of karst terranes. However, their accuracy may show great variations mainly because of the poor quality of hardness or runoff data and the use of a variety of techniques based on unrealistic assumptions in calculating erosion rates (Smith and Atkinson, 1976).

Several studies on the karstic erosion rates in Florida have provided contrasting values resulting from differences in calculation methods and lack of reliable data at the time of measurements (Corbel, 1959; Runnels, 1971; Brooks, 1967). These studies are based on the oversimplistic assumption that some estimation of the mean hardness can represent entire regions without taking into consideration the significant seasonal variability of chemical hardness. A more accurate calculation of karstic erosion rate for the Florida karst can be achieved by applying a basin-wide hydrochemical budget method. In this method, the accuracy of karstic denudation rate calculations is considerably increased by applying mass flux rating curves to flow duration curves obtained from stream or spring discharge hydrographs. Chemical and hydrologic monitoring of spring or stream waters provides instantaneous determinations of solute concentration for corresponding instantaneous discharge. Summation of these instantaneous values results in an accurate estimation of solute discharge rate in which changes in solute concentration with discharge are taken into account. Gunn's (1981) application of this technique to limestone solution rate calculations yielded values 4% lower than those computed by using mean hardness values for the entire basin in Waitomo, New Zealand.

Background

The effect of climate on karstic dissolution rate is maintained by the collective control of climatic factors such as temperature, biologic activity, and the amount and seasonality of runoff (precipitation – evapotranspiration) on karst processes. Therefore, there have been many efforts to describe well-defined climatic models of karst development in which characteristic landforms of various climatic belts could be explained by the variation of karstic dissolution rates. Based on the increased solubility of carbon dioxide at lower temperatures, Corbel (1957, 1959) argued that the greatest erosion rates should occur in the Arctic and high Alpine regions. However, this view has proven to be oversimplistic since it did not consider the well-developed soil zones and highly elevated carbon dioxide contents of the soil gasses created by the increased biogenic activity in warmer climates (Lehman, 1964; Sweeting, 1964; Jakucs, 1973). The importance of soil cover in controlling karstic dissolution rates was tested and illustrated by Bauer (1964), who reported erosion rates of 9.0 and 28.0 m^3/km^2/year for the bare and soil-covered limestones, respectively, in the Austrian Alps. In addition to the thick and biologically active soil covers in temperate and tropical climates, large values of annual runoff especially in humid tropics were considered to be responsible for the elevated rates of karstic erosion (Balazs, 1971).

In an attempt to resolve the conflict brought about by opposing views on the effect of climate in controlling karstic processes, Smith and Atkinson (1976) compiled and classified numerous measurements of hardness and erosion rates representing a variety of climatic conditions. Surprisingly, the samples collected from temperate climates showed the greatest values and variability of hardness (mean = 211 mg/L $CaCO_3$, standard deviation = 86.5 mg/L $CaCO_3$). They concluded that the observed variations in hardness values are not directly controlled by the climate, but by other factors such as type of vegetation, soil type and texture, organic activity and seasonal changes in soil moisture that play important roles in supplying carbon dioxide. Along with the geologic and hydrogeologic characteristics of the karst terrane, these factors may exert as great an influence as macroclimate and account for wide variations of average hardness within a single area.

Analyzing the data on erosion rates representing different climatic settings, Smith and Atkinson (1976) concluded that the rate of dissolution was largely controlled by runoff. The effect of latitudinal climatic belts on erosion rates is relatively minor. Runoff and erosion rates are similar in tropical and temperate areas. Because of the decreased values of evapotranspiration, Arctic/Alpine areas show a greater range of runoff and higher erosion rates than the Temperate and Tropical zones. Therefore, high erosion rates calculated for Arctic/Alpine areas do not result from particularly aggressive waters of low temperatures (Ford, 1971) but are likely to be caused by greater runoff values induced by less evapotranspiration.

Reliable estimates of karstic erosion rates require flow duration curves of lengthy flow records (30 -50 years). The relationship between discharge and solution load (mass flux curve/ instantaneous rate of removal) is used to find mass flux values for corresponding discharge readings from the flow duration curve. They are then weighted by the proportion of time for which discharge occurs.

The instantaneous removal rate of dissolved material is calculated by the product of total hardness and stream (or spring) discharge at any one time. Since the hardness values often fluctuate because of the changes in discharge, it is recommended that samples represent various discharge conditions (Smith and Atkinson, 1976). Calculations based on mass flux and flow duration curves accurately represent variations in total solute load due to stream flow fluctuations.

Methodology

In calculating the dissolutional erosion rate within the Lower Suwannee River basin (Suwannee River basin below Withlacoochee), data collection stations were selected at locations so as to consider the mass flux input to and output from the area (Figure 4.1). Input to the area is calculated by the discharge measurements at Ellaville and Santa Fe – Fort White, which are represented by total alkalinity readings at stations numbered SUW100, and SFR070. Stream flow output from the system was based on data collected at Wilcox, the most downstream gauging station on the Suwannee River. Total alkalinity

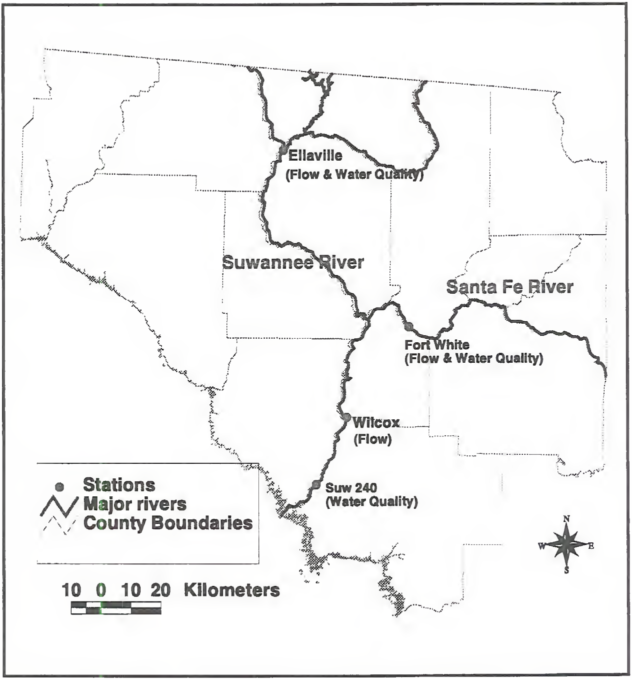

Figure 4.1. Location map of flow and water quality stations.

values representing the output from the system was collected at SUW240, some 25 km downstream of Wilcox. Discharge measurements used in preparing flow duration curves consist of daily readings from 1960 through 1996. However, records of water quality cover a much shorter time period between 1989 and 1996. Monthly readings are available for every month especially after 1989. Despite a long historical data on stream discharge, estimation of dissolutional rate was constrained by the relatively shorter records of water quality measurements.

Most of the alkalinity in the surface waters of the study area results from bicarbonates dissolved from limestone and dolomitic bedrock. It is reported in units of miligrams per liter as calcium carbonate (Fellers, 1993).

The methodology followed is as outlined in Smith and Atkinson (1976):

1. Plots of water alkalinity against discharge for input and output stations were prepared (Figures 4.2, 4.3, 4.4).
2. By multiplying discharge and alkalinity values, plots of dissolved load (mass flux) vs. discharge were prepared (Figures 4.5, 4.6, 4.7).
3. Flow duration curves for all stations were produced (Appendix C).
4. By using the regression equations obtained at step 2, dissolved loads corresponding to each flow duration curve ranges were found, multiplied by the discharge value representing the range, and weighted by the proportion of time for which each discharge occurs.
5. All the product values obtained in step 4 were added to calculate overall annual dissolutional erosion from the Lower Suwannee River basin.

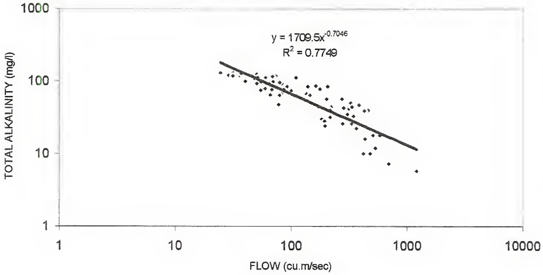

Figure 4.2. Discharge – total alkalinity relationship for the Upper Suwannee River basin.

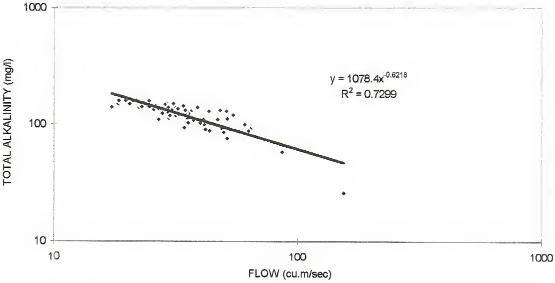

Figure 4.3. Discharge – total alkalinity relationship for the Santa Fe River basin.

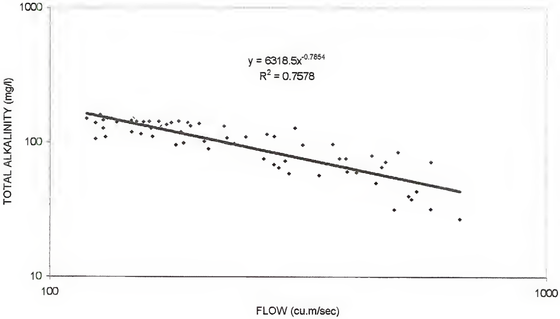

Figure 4.4. Discharge – total alkalinity relationship for the Lower Suwannee River basin.

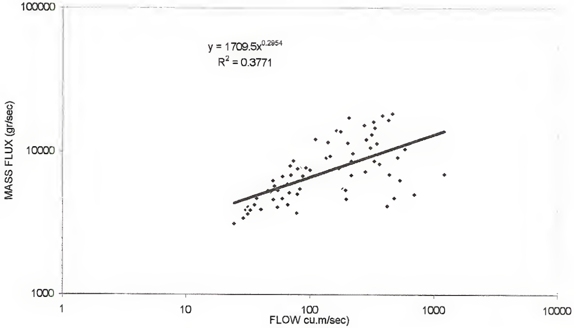

Figure 4.5. Discharge – mass flux relationship for the Upper Suwannee River basin.

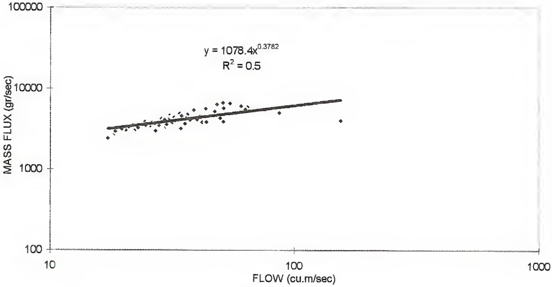

Figure 4.6. Discharge – mass flux relationship for the Santa Fe River basin.

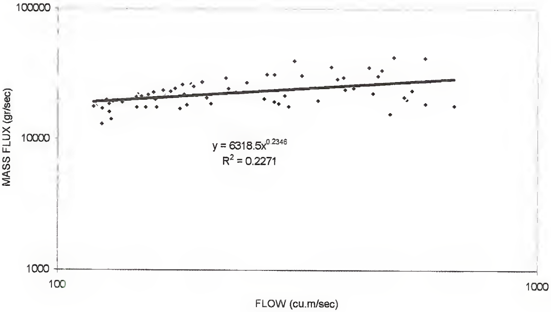

Figure 4.7. Discharge – mass flux relationship for the Lower Suwannee River basin.

Results

Results of dissolutional erosion rate calculation are given in mass units as follows:

Input to the system:

Ellaville: 239,954.5 ton/year. Fort White: 139,852.5 ton/year

Output from the system:

Wilcox: 740,454.6 ton/year

Output - input = 365,647.6 ton/year of mass is removed from the Lower Suwannee River basin.

The net rate of limestone dissolution in any given time interval can be estimated from

$$S = M/(a.d.10^3)$$

where

S = net solutional erosion rate (m^3/km^2)

M = mass of limestone eroded (kg)

a = drainage basin area (km^2)

d = density of the limestone (g/cm^3)

Substituting 365,6647,600 kg for the mass of limestone eroded in one year, 4144 km^2 for the drainage area of the Lower Suwannee River basin, and 2.2 g/cm^3 for the density of limestone in this formula yields a net solutional erosion rate of 40.1 m^3/km^2/year for the Lower Suwannee River basin. This is equal to an average lowering rate of 40.1 mm/1000 years.

The magnitude and frequency of solute discharge events were examined by calculating percentages of annual dissolved load removal corresponding to flow intervals (Figures 4.8, 4.9, 4.10). In all basins (Upper Suwannee, Santa Fe, and Lower Suwannee) only a small fraction of the annual dissolved load (between 5 to 7 %) is removed by low frequency-high magnitude flows which occur only 5 per cent of the time. Mean to low flows that occur approximately 60 per cent of the time for the Upper and Lower Suwannee River basins transport 58 and 60 per cent of the annual dissolved load, respectively. As for the Santa Fe River basin, mean and low flows prevailing 45 per cent of the time account for the removal of 35 per cent of the annual dissolved load. The statistical summaries of water hardness, mass flux, and runoff values calculated for each basin are given in Tables 4.1, 4.2 and 4.3.

Table 4.1.Statistical summary of hydrologic and chemical parameters for the Santa Fe river basin.

Santa Fe River	Flow (m^3/s)	Total Alkalinity(mg/L)	Mass Flux (gr/sec)
Mean	35.57	126.21	4121.70
Median	30.72	132.00	3985.33
Standard Deviation	17.00	25.27	843.70
Minimum	17.25	26.00	2414.56
Maximum	154.34	160.00	6626.88

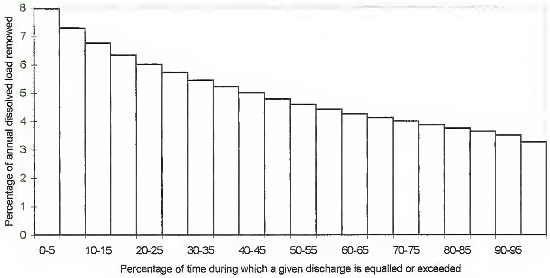

Figure 4.8. Annual dissolved load carried by different flows in the Upper Suwannee River basin.

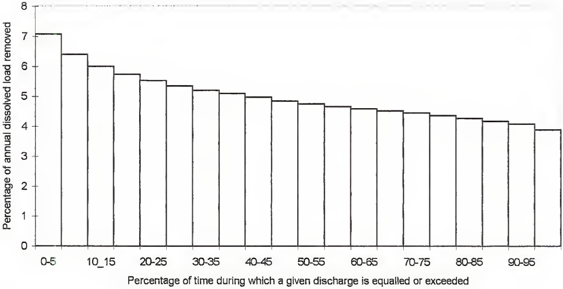

Figure 4.9. Annual dissolved load carried by different flows in the Santa Fe River basin.

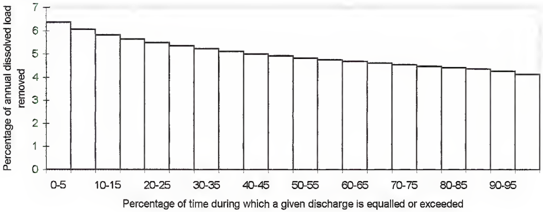

Figure 4.10. Annual dissolved load carried by different flows in the Lower Suwannee River basin.

Table 4.2. Statistical summary of hydrologic and chemical parameters for the Upper Suwannee River basin.

Upper Suwannee	Flow (m^3/s)	Total Alkalinity(mg/L)	Mass Flux (gr/sec)
Mean	203.47	71.18	7866.88
Median	108.89	75.00	6882.89
Standard Deviation	212.52	37.55	3869.66
Minimum	24.41	5.80	3173.54
Maximum	1209.26	130.00	18464.64

Table 4.3.Statistical summary of hydrologic and chemical parameters for the Lower Suwannee River basin.

Lower Suwannee	Flow (m^3/s)	Total Alkalinity(mg/L)	Mass Flux (gr/sec)
Mean	293.00	107.31	23291.64
Median	225.71	115.00	21916.85
Standard Deviation	177.90	36.96	6228.24
Minimum	118.66	27.00	13088.37
Maximum	1090.32	160.00	42607.44

Seasonal changes of the mass flux and stream discharge are shown in Figures 4.11, 4.12 and 4.13. Removal of dissolved limestone from each basin shows pronounced seasonal variations. Rainy seasons correlate with greater amounts of solutional loads whereas mass flux tends to decline with decreasing flow rates. Mass flux from the system is increased by prolonged durations of high flows and seems to be not affected by extreme flood events.

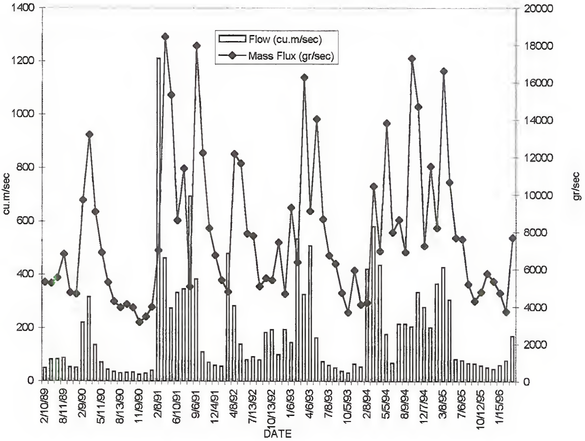

Figure 4.11. Seasonal changes of the flow and mass flux for the Upper Suwannee River basin.

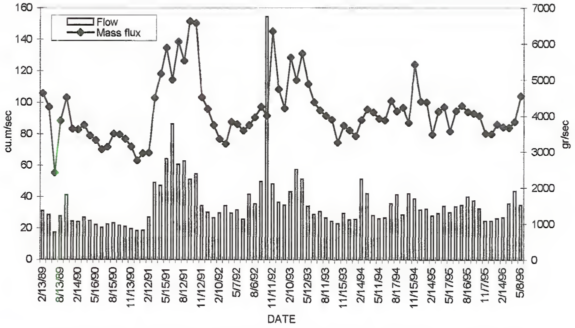

Figure 4.12. Seasonal changes of the flow and mass flux for the Santa Fe River basin.

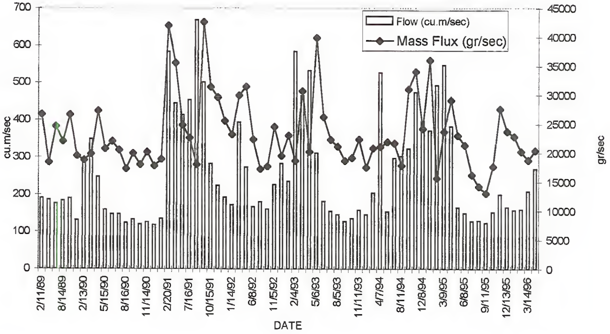

Figure 4.13. Seasonal changes of the flow and mass flux for the Lower Suwannee River basin.

Discussion

The karst of Florida has developed under thick soil covers and been subject to high runoff conditions of a subtropical climatic setting. Based on the available data, the best estimate of the net karstic dissolution rate in the Lower Suwannee River basin is 40.1 m^3/km^2/year. This is equal to a denudation rate of 40.1 mm/1000 years. Despite the reliability of mass balance approach over conventional techniques, qualitative assessment of potential errors indicates that this value should be considered as the minimum erosion rate for the study area. Because of the lack of surface water runoff data at the outlet of the Lower Suwannee River basin, data collected at the Wilcox station which is some 25 km upstream of the water quality measurement site had to be utilized (Figure 4.1). The effect of this operation can be readily observed by the low degree of correlation between the runoff and mass flux values calculated for the Lower Suwannee River basin (Figure 4.7). The actual discharge value from the system to the Gulf of Mexico may be significantly higher than that measured at Wilcox. Consequently higher discharge values should correspond to total alkalinity measurements and result in greater values of karstic dissolution rates. In addition to that, removal of dissolved carbonate through nonpoint subsurface seepage and submarine springs to the Gulf of Mexico is not considered in this study.

In the application of mass flux technique to karstic erosion rate calculations at least 30 to 50 water samples are recommended to be taken over the whole range of discharge conditions and seasons (Smith and Atkinson, 1976; Ford and Williams, 1989). Total alkalinity data record obtained in this study cover a wide range of hydrologic conditions between February 1989 and May 1996 and. Therefore, despite its relatively short duration, water quality data are a reasonable representation of hydrologic variation in the Lower Suwannee River basin.

The denudation value of 40.1 mm/1000 years is comparable with previous estimates of erosion rates in Florida. Brooks (1967) reports 1.5 inches/1000 year (38.1 mm/1000 year) for the Suwannee River basin. Based on the hardness values of the springs in North peninsular Florida, Opdyke et al. (1984) calculated a denudation rate of 1 m per 38,000 years (26.3 mm/1000 years). Runnels (1971) reports an erosion rate of 35 m^3/km^2/year for Florida. Some published examples of erosion rates throughout the world are given in Table 4.4.

Table 4.4. Published erosion rates of different geographic locations (modified after Smith & Atkinson, 1976).

Locality	Erosion rates (m^3/km^2/year)
TEMPERATE ZONE	
Derbyshire,UK	115; 136; 42; 128; 73; 98 Pitty, 1968
Mendip Hills, UK	81 Atkinson, unpublished
Yugoslavia	109; 66; 93; 66; 55; 58; 66; 48; 90; 28; 14 Corbel, 1965
Dinaric karst	43; 43; 63; 55; 64; 19; 56 Gams, 1969
Joux Valley, Swiss Jura Mountains	98 Aubert, 1967, 1969
Krakow Plateau	20 Corbel, 1965
Poland	19; 16; 32; 21; 17; 10; 24 Pulina, 1971
R. San Antonio, Texas	4 Corbel, 1971

Table 4.4. (continued)

Locality	Erosion rates ($m^3/km^2/year$)
Somerset Island, Canada	2 Smith, 1972a
Yugoslavia	47; 83; 82; 60; 90; 79; 93; 77; 83; 104; 104 Gams, 1969, 1972
E. Siberia	32; 6; 1; 4 Pulina, 1968
Cookeman Plain, Australia	24 Jennings, 1972a,b
TROPICAL ZONE	
Indonesia	63; 99; 86; 63 Balazs, 1971
Florida	35 Runnels, 1971
Florida	5; 8 Corbel 1959
Jamaica; West Indies	69;39;86;96 Smith, 1969, 1970
Puerto Rico	42 Corbel, 1971
Yucatan, Mexico	30; 16 Corbel, 1959b
Waitomo, New Zealand	69 Gunn, 1981
ARCTIC/ALPINE ZONE	
Alaska	530; 40; 8 Corbel, 1959a, b

Based on the worldwide database of karstic erosion rates and runoff values, Smith and Atkinson (1976) provided regression equations of erosion rate upon runoff for different climatic belts. Substituting a runoff value of 418 mm estimated by water budget calculations for the Lower Suwannee River basin provides erosion rates of 32.04 and 30.8 $m^3/km^2/year$ for the Tropical and Temperate regression equations, respectively. The Temperate regression equation calculated by taking into account the proportion of limestone areas within the watershed gives a karstic erosion rate of 44.8 $m^3/km^2/year$ for the Lower Suwannee River basin.

CHAPTER 5
EVOLUTION OF KARST IN THE SUWANNEE RIVER AREA

Prospectus

Extensive dissolution of the Florida carbonate platform through numerous sea level changes has resulted in a multisequential and complicated karst pattern at various horizons within the carbonate rocks of the Floridan aquifer. Dissolution has taken place along the saltwater/freshwater mixing zones of ancient coastlines, at paleo-water tables of the Floridan aquifer, and at depths of the carbonate platform where mixing-corrosion and possibly hypogenic cave formation occur. Therefore, Florida presents an excellent example of a multisequential karst network formed by the superposition of extensively dissolved horizons within thick carbonate rocks. The sequences of karst progression were controlled by a variety of factors such as phreatic-vadose zone fluctuations induced by sea level changes, structural movements, paleokarst templates, deposition and erosion of siliciclastic material, and the formation of a fluvial system. The importance of these factors varied in each sequence of karst development.

The last episode of the karst development within the Suwannee River basin involves glacio-eustatic changes and the resultant marine terraces formed during the Pleistocene. Most sand ridges identified at various elevations in peninsular Florida are considered to be the remnants of constructional features formed along ancient shorelines (White 1958; Pirkle et al., 1970). Despite a considerable disagreement on the number and distribution of marine terraces, Cooke's (1945) widely accepted idea suggests a chronological sequence of terrace formation in which each successively lower terrace is younger than those above it. Consequently, higher elevation terraces are older.

The idea of chronological formation of marine terraces has important implications regarding the post-Miocene karstic evolution of the area (Vernon, 1951; White, 1958). As the Pleistocene sea retreated, total period of subaerial exposure diminished towards the sea, and consequently less time was available for karstification to occur. In other words, within the area covered by the Pleistocene marine terraces, karst should be most mature at the highest elevations.

This study tests the hypothesis that the age of karst decreases from higher to lower elevations, i.e., from older to younger marine terraces, within the area where the Floridan aquifer is unconfined or semiconfined. It is also hypothesized that the post-Miocene evolution of karst landforms in the Suwannee River basin has been controlled by the retreat of Pleistocene sea-level highstands and is reflected by the morphometric and spatial distribution characteristics of karstic depressions.

Background

A period of drastically declined sea levels that occurred at the end of the Oligocene and especially during the Messinian is considered to represent extensive karst formation in Florida (Randazzo, 1997). Subaerial exposure of the thick sequence of carbonate rocks has resulted in the formation of extensive cave systems and surficial depressions that were later overlain by the Miocene siliciclastic deposition. In the Suwannee River basin of the northwest Florida, karstification has resumed upon the erosion of the Hawthorn Group and followed the template of pre-Miocene surficial karst (Randazzo, 1997).

Despite a generally accepted perspective of the Miocene and Pliocene sea-level fluctuations and accompanying subaerial exposures of the Florida Platform, much confusion exists on the number, identification, and even the existence of Pleistocene marine terraces. After Cooke's (1945) first description of seven shoreline terraces associated with the interglacial episodes, various interpretations of marine terraces were made by MacNeil (1949), Vernon (1951), and Alt and Brooks (1965). Scott (1997) opposes the use of "terrace formations" as stratigraphic units indicating that they were abandoned by most stratigraphers. He also refutes Puri and Vernon's (1964) view that the Pleistocene sea levels were some 70-m higher than the present sea level and marine terraces were correlated with each stillstand. He maintains that the maximum Pleistocene sea level high stand was not more than 20 m above the present sea level.

The structural and stratigraphic framework of Florida has been an integral part of studies on the karst landform development. Schmidt & Scott (1984) noted the importance of the Chattahoochee "anticline" in the panhandle and the Sanford High and the Ocala Platform in the peninsula in controlling the distribution of karst features. They claim that karst features are most abundant near the crests of these structures where the carbonates are overlain by thin permeable sediments. They also relate sinkhole morphology to the lithologies of these overlying sediments.

One of the important topographic features of the Suwannee River basin is the Cody Escarpment. The influence of this retreating karstic escarpment on the ground water chemistry and consequently on the evolution of karst was addressed by Upchurch and Lawrence (1984). They described three hydrochemical domains associated with the confined uplands, escarpment zone, and unconfined lowlands below the escarpment. As a result of the chemically aggressive localized recharge from the uplands, the escarpment area is "...a zone of vertical karst development with initiation of new conduits and reactivation of old ones" (Upchurch and Lawrence, 1984, p. 23).

In his study on the morphometric analysis of sinkholes in the Suwannee River area, Beck (1985) stated that while depression density increased towards the escarpment, average depression size decreased. He proposed that the decrease in the depression density in areas away from the escarpment was brought about by the merging and infilling of sinkholes.

In an attempt to investigate factors controlling karst progression in the Suwannee River basin, Price (1984) compared two areas with different karstification rates, and drew attention to the importance of fracture zones in sinkhole initiation. He concluded that the vigorous karstic dissolution took place within the transition zone near the Cody Escarpment where fluctuation of ground water is greatest.

Methodology

The methodology employed here to explain the surficial karst evolution invokes substitution of space for time. As a well-known strategy in evolutionary geomorphology, substitution of space for time assumes that the variations of morhometric and spatial distribution parameters between depressions on increasingly older terranes reflect development through time, provided that all the other variables are constant. It has been successfully applied to karst geomorphology by various karst geomorphologists (Williams, 1971; Fermor, 1972; Feeney, 1977; Day, 1983). Day's (1983) study on the doline development in Barbados involves the application of space – time substitution for conditions very similar to those in the Suwannee River karst area. Investigating the morphological and spatial variations of dolines developed on an uplifted series of reef terraces, Day (1983) reported a sequential development of karstic depressions. Doline densities were found to be increasing with the age of the terraces, i.e. with increased elevation. Expansion, interference, coalescence, and subdivision of dolines have all played partial roles in the development of karstic depressions.

In a similar study, Bahtijarevic (1996) compared morphometric parameters of depressions sampled on various elevations within the Suwannee River area. Despite the limited areal coverage and poor correlation between the topographic elevation and morphometric parameters such as area, mean depression diameter, she concluded that the depressions have evolved from higher to lower elevations as controlled by the sequential order of the marine terraces.

In this study, substitution of space for time was performed by analyzing the variation of the morphometric and spatial distribution of depressions within the GIS layers of elevation and marine terraces. The GIS layers of karstic depressions include information on the morphometric parameters such as length, width, area, length/width ratio, mean diameter, and circularity ratio, as well as information on the spatial distribution of karstic depressions such as depression density, nearest neighbor distance, and the pitting index. The Suwannee River Water Management District provided the GIS layers of topography and marine terraces. The analysis was performed by using the GIS software ArcView 3.0 and its Spatial Analyst extension.

Results

In an attempt to observe the reflections of the karst landform evolution on the morphometry of karstic depressions, the changes in morphometric and spatial distribution parameters with elevation and marine terraces were examined. All the arguments made here are based on the mean values of the total depression population occurring in 24 topographic quadrangles in the Lower Suwannee River basin. Since the depressions considered in these arguments constitute the whole population, no attempts were made to statistically test the difference between mean values of morphometric parameters representing the ranges of elevation and marine terraces.

Morphometric Evolution of Karstic Depressions

The study area consists of low-lying, flat areas of karst plains bounded to the east by the Cody Escarpment and the higher elevations of the Northern Highlands. Elevations within the study area range from sea level to 75 m with vast areas within the range of 0-25 m (Figure 5.1). In this study, the Cody Escarpment was defined by the 100-ft (30.48 m) topographic contour above which collapse sinkholes predominate because of the thickening of the overburden material above the Floridan aquifer.

Of the eight marine terraces included in the GIS layer, only five contain the karstic depressions delineated for this study (Figure 5.2). These terraces and their corresponding elevations are as follows (after Cooke, 1945): Pamlico,7.62 m (25 ft); Talbot, 12.80 m (42 ft); Penholoway, 21.33 m (70 ft); Wicomico, 30.48 m (100 ft); Sunderland, 51.81 m (170 ft).

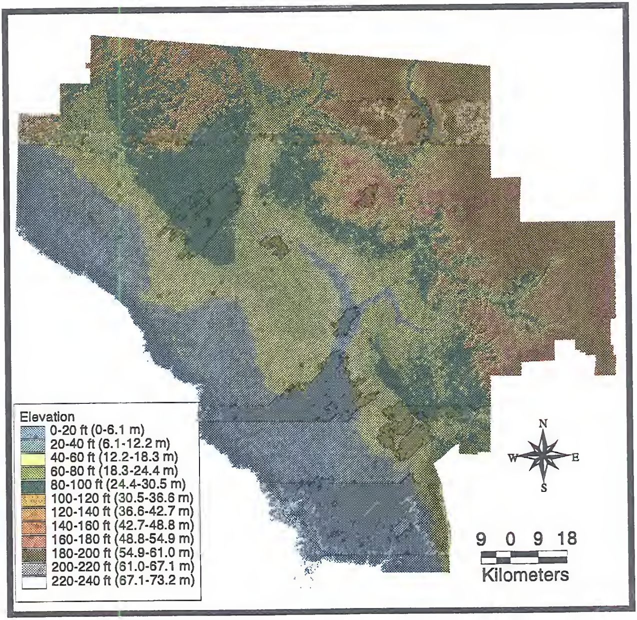

Figure 5.1. Map of elevation.

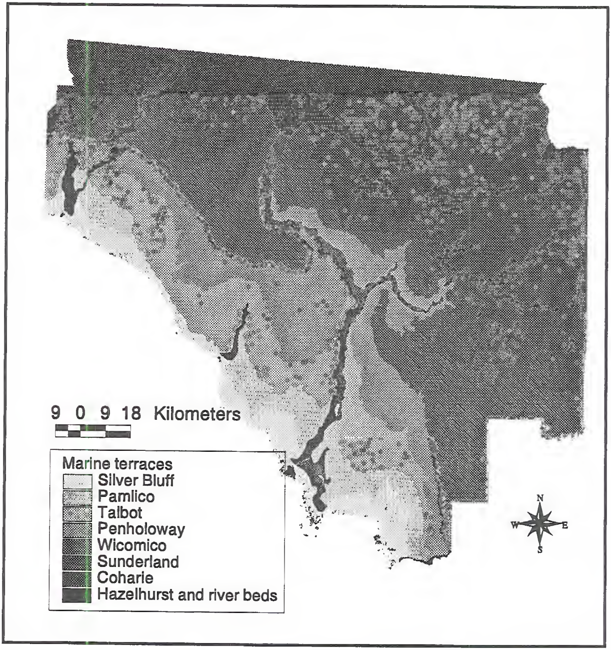

Figure 5.2. Map of the marine terraces within the study area.

Most karstic activity takes place within the area covered by the Penholoway and Wicomico terraces between 12.80 m (42 ft) to 30.48 m (100 ft). Karstic depressions located within the Sunderland marine terrace deposits above 30.48 m (100 ft) are mostly collapse depressions formed in areas with considerable overburden material. Discussions on the substitution of space for time to resolve the karstic evolution of the Suwannee River basin apply to the area west of the Cody Escarpment, i.e., lower than 100 ft (30.48 m) where the Floridan aquifer is unconfined or semiconfined.

Depression area

The changes in mean area of depression population with the selected elevation classes are given in Figure 5.3 and Table 5.1. The mean depression area shows a polymodal distribution with a major mode value for the elevation range between 18.3-24.4 m (60-80 ft). The slight dip of mean depression area within the major mode corresponds to the marginal zone of significant modern karst activity and local semiconfined conditions of the Floridan aquifer. The mean depression area continues to decrease for elevations higher than 30.48 m (100 ft) within the Northern Highlands physiographic region in which depression morphometry is controlled by the thickness and the lithologic characteristics of the overburden material, as explained in Chapter 3.

With the exception of depressions at very low elevations, karstic evolution within the study area seems to correlate somewhat with the sequential subaerial exposures of the Floridan aquifer controlled by the glacio-eustatic sea level changes in the Pleistocene. The apparent increase in the mean depression area correlates with higher altitude especially for the region between the Suwannee River and the Cody Escarpment. This indicates the growth of depressions by coalescence and expansion through time.

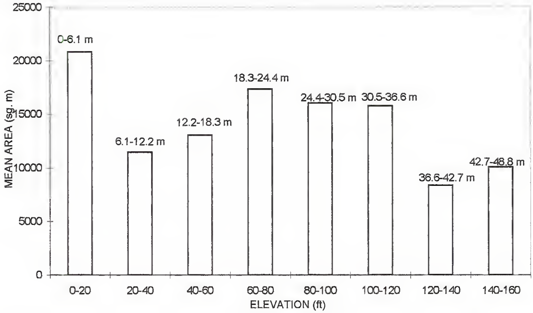

Figure 5.3. Changes in the mean area of the depression population with elevation.

Table 5.1. Statistical summary of depression area (m^2) within the ranges of elevation.

ELEVATION Meters (feet)	MEAN	MEDIAN	STANDARD DEVIATION	MINIMUM	MAXIMUM	COUNT
0-6.1 (0-20)	20821	5400	54224	250	550700	328
6.1-12.2 (20-40)	11459	2925	41302	125	1213750	4626
12.1–18.3 (40-60)	13042	3175	45265	25	1324425	6645
18.3–24.4 (60-80)	17326	3600	63761	175	2713350	5508
24.4-30.5 (80-100)	15988	2600	109202	100	5804750	5462
30.5-36.6 (100-120)	15730	1850	148915	225	2621850	322
36.6-42.7 (120-140)	8333	4350	12419	250	69350	90
42.7-48.8 (140-160)	10054	7262	9158	575	48700	42

The changes in mean area of depression population with marine terraces are given in Figure 5.4 and Table 5.2. Despite rather high values of mean depression area for the Pamlico terrace which represents the lowest and therefore the youngest karstic depressions, the general trend of depression growth follows a sequential order. Mean areas of depressions increase with the age of marine terraces supporting the hypothesis of depression growth with time.

Table 5.2. Statistical summary of the depression area (m^2) within the marine terraces.

TERRACES	MEAN	MEDIAN	STANDARD DEVIATION	MINIMUM	MAXIMUM	COUNT
PAMLICO	17087	5325	43915	700	307200	61
TALBOT	10492	2675	40823	175	1213750	3559
PENHOLOWAY	13024	3325	44704	75	1324425	7368
WICOMICO	16129	3075	84507	100	5804750	8171
SUNDERLAND	22800	3075	130353	125	3418550	1609

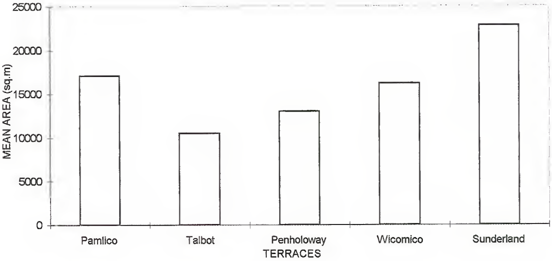

Figure 5.4. Changes in the mean area of the depression population with marine terraces.

Mean depression diameter

The variation of mean diameter mimics that of depression area within the elevation intervals (Figure 5.5 and Table 5.3). Similarly, the mean diameter of depressions shows a trimodal distribution with the major modal elevation range of 18.3-24.4 m (60-80 ft).

Table 5.3. Statistical summary of mean depression diameter (m) within the ranges of elevation.

ELEVATION Meters (feet)	**MEAN**	**MEDIAN**	**STANDARD DEVIATION**	**MINIMUM**	**MAXIMUM**	**COUNT**
0-6.1 (0-20)	128	86.4	120	18	854	328
6.1-12.2 (20-40)	92	64.2	92	13	1293	4629
12.1–18.3 (40-60)	97	66.1	97	5	1335	6645
18.3–24.4 (60-80)	109	70.5	114	14	1867	5508
24.4-30.5 (80-100)	94	59	117	11	2785	5462
30.5-36.6 (100-120)	75	50	125	17	1867	322
36.6-42.7 (120-140)	89	74	60	17	306	90
42.7-48.8 (140-160)	105	97	52	27	278	42

As for the marine terraces, the mean diameter of depressions shows a similar distribution as the mean depression area. Figure 5.6 and Table 5.4 reveal that the mean depression diameter increases with the age of the marine terraces except for the depressions located at the lowest marine terrace, namely Pamlico.

Table 5.4. Statistical summary of the mean diameter (m) within the marine terraces.

TERRACES	**MEAN**	**MEDIAN**	**STANDARD DEVIATION**	**MINIMUM**	**MAXIMUM**	**COUNT**
PAMLICO	119	85	109	30	727	61
TALBOT	86	60	88	14	1293	3559
PENHOLOWAY	97	67	96	10	1335	7368
WICOMICO	101	64	113	11	2785	8171
SUNDERLAND	109	64	142	13	2251	1609

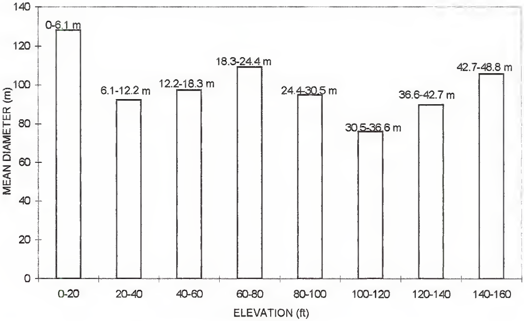

Figure 5.5. Changes in the mean diameter of the depression population with elevation.

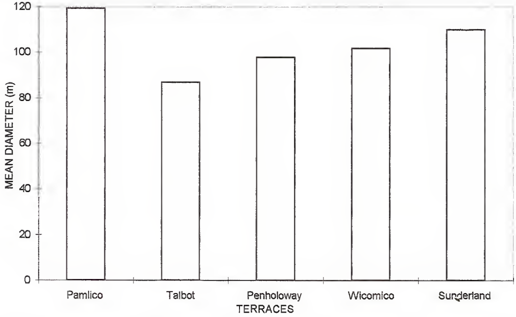

Figure 5.6. Changes in the mean diameter of the depression population with marine terraces.

Planimetric shapes and allometry of depressions

The correlation between the altitude and depression morphometry is further supported by the observed variations with elevation in the planimetric shapes of depressions. The circularity index as described in Chapter 2, is a measure of the circularity of a depression. It approaches unity as depressions become circular.

Data displayed in Tables 5.5 & 5.6 and Figures 5.7 & 5.8 suggest that external asymmetry observed in the younger depressions of lower elevations gradually disappears. Depressions at higher elevations have had longer subaerial exposure time and grown to be more circular through coalescence and surficial erosion.

Table 5.5. Statistical summary of the length/width ratio within the ranges of elevation.

ELEVATION Meters (feet)	**MEAN**	**MEDIAN**	**STANDARD DEVIATION**	**MINIMUM**	**MAXIMUM**	**COUNT**
0-6.1 (0-20)	1.90	1.67	0.74	1.03	5.76	328
6.1-12.2 (20-40)	1.79	1.57	0.77	1.00	14.11	4626
12.1–18.3 (40-60)	1.77	1.57	0.70	1.00	10.60	6645
18.3–24.4 (60-80)	1.74	1.54	0.67	1.00	8.30	5508
24.4-30.5 (80-100)	1.68	1.53	0.57	1.00	6.25	5462
30.5-36.6 (100-120)	1.54	1.40	0.57	1.00	7.03	322
36.6-42.7 (120-140)	1.64	1.42	0.64	1.03	4.71	90
42.7-48.8 (140-160)	1.46	1.31	0.40	1.04	2.61	42

Table 5.6 Statistical summary of the circularity index within the ranges of elevation.

ELEVATION Meters (feet)	**MEAN**	**MEDIAN**	**STANDARD DEVIATION**	**MINIMUM**	**MAXIMUM**	**COUNT**
0-6.1 (0-20)	1.45	1.26	0.54	1.02	4.40	315
6.1-12.2 (20-40)	1.32	1.19	0.43	0.02	6.64	4475
12.1–18.3 (40-60)	1.37	1.21	0.49	0.01	8.86	6336
18.3–24.4 (60-80)	1.33	1.18	0.22	0.06	5.24	5227
24.4-30.5 (80-100)	1.29	1.16	0.40	0.01	5.29	5246
30.5-36.6 (100-120)	1.18	1.11	0.28	0.05	3.34	317
36.6-42.7 (120-140)	1.20	1.11	0.25	0.10	2.32	89
42.7-48.8 (140-160)	1.17	1.07	0.25	1.01	2.47	41

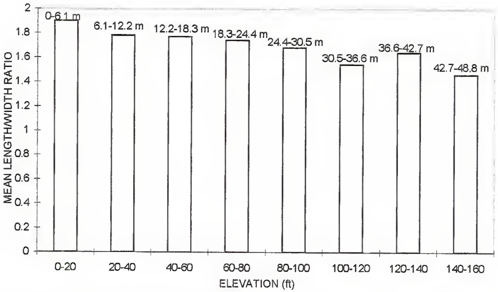

Figure 5.7. Changes in the mean length/width ratio of the depression population with elevation.

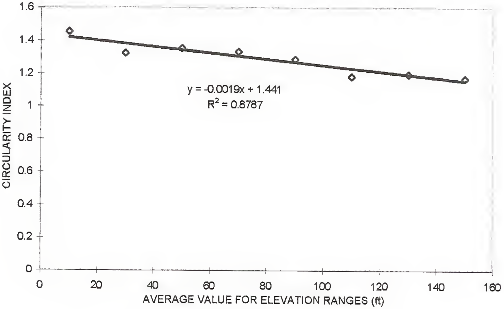

Figure 5.8. Changes in the mean circularity index for the depression population with elevation.

The changes in length/width ratio and circularity index of the depression population with marine terraces are given in Figures 5.9 & 5.10. The general trend of planimetric shape variation with terraces indicates a decrease in elongation and an increase in circularity as terraces get older. The statistical summary of the mean length/width ratio shows a drop from 1.89 for the Pamlico terrace to 1.66 for older depressions located at the Sunderland terrace (Table 5.6).

Table 5.6. Statistical summary of the length/width ratio within the marine terraces.

TERRACES	MEAN	MEDIAN	STANDARD DEVIATION	MINIMUM	MAXIMUM	COUNT
PAMLICO	1.89	1.70	0.72	1.06	4.27	61
TALBOT	1.73	1.55	0.65	1.00	8.05	3559
PENHOLOWAY	1.74	1.56	0.66	1.00	7.26	7368
WICOMICO	1.71	1.53	0.62	1.00	8.30	8171
SUNDERLAND	1.66	1.50	0.59	1.00	7.03	1609

The decrease of the mean circularity index from 1.43 to 1.29 indicates a considerable increase in circularity as depressions grow older (Table 5.7).

Table 5.7. Statistical summary of the circularity index within the marine terraces.

TERRACES	MEAN	MEDIAN	STANDARD DEVIATION	MINIMUM	MAXIMUM	COUNT
PAMLICO	1.43	1.24	0.50	1.01	3.82	60
TALBOT	1.31	1.17	0.42	0.05	6.64	3461
PENHOLOWAY	1.34	1.20	0.46	0.01	8.70	7056
WICOMICO	1.31	1.17	0.44	0.01	5.29	7799
SUNDERLAND	1.29	1.15	0.41	0.03	5.04	1530

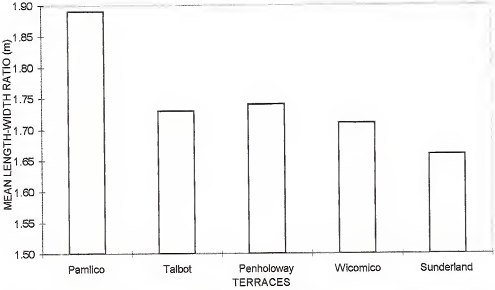

Figure 5.9. Changes in the mean length/width ratio of the depression population with marine terraces.

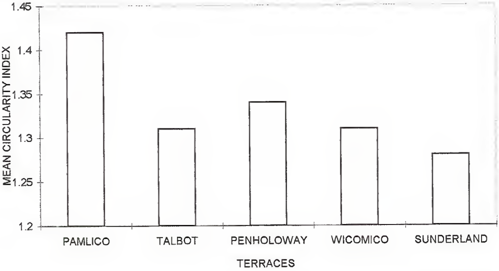

Figure 5.10. Changes in the mean circularity index of the depression population with marine terraces.

Allometry is described as the study of the relative rates of change observed in two variables of a system (Bull, 1975). In landform studies, a power function in the form of $y=bx^a$ was widely used for correlating changes in variables of a geomorphologic system (Bull, 1975; Kemmerly, 1976; Palmquist, 1979). Bull (1975) provides a thorough discussion on the theoretical background of the concept of allometry accompanied by a variety of examples on its application to geomorphologic systems.

Based on the time-dependency of variables, allometry is regarded as static or dynamic. A static allometry refers to measurements of the variables of a geomorphologic system at one time in its history. A dynamic allometry implies a time-dependent relationship between variables based on the measurements of a landform or a process performed at different times. Data required for describing dynamic allometry can be obtained either by temporal measurements of system's variables or by substitution of space data for time data when applicable (Abrahams, 1972; Faulkner, 1974; Welch, 1970).

Application of the allometric power function to doline morphometry yields a length-width relationship as $L= bW^a$, where L and W represent length and width of depressions, respectively. The exponent "a" is described as the growth ratio (Imbrie, 1956; Kemmerly, 1976), and reflects the ratio of the rates of change of the variables L and W. The coefficient "b" is defined as the initial growth index (Kemmerly, 1976). If length changes more rapidly than width, positive allometry exists ($a>1$); if width changes more rapidly than length, negative allometry exists ($a<1$). Allometry is replaced by isometric conditions when the rates of growth for length and width are the same ($a=1$) (Bull, 1975).

The length of the depression major and minor axes in the study area were examined to determine if there is a mathematical relationship between the two variables and to compare depression populations representing different elevation ranges. The power functions describing the relationships between the depression length and width for elevation ranges are given in Appendix D and summarized in Table 5.8.

Table 5.8. Allometric relationships in elevation ranges.

ELEVATION Meters (feet)	b	a	R^2	n
0-6.1 (0-20)	1.4806	1.0446	0.83	327
6.1-12.2 (20-40)	1.2584	1.0728	0.81	4627
12.1–18.3 (40-60)	1.4305	1.0382	0.82	6444
18.3–24.4 (60-80)	1.3256	1.0532	0.84	5509
24.4-30.5 (80-100)	1.4246	1.0305	0.86	5465
30.5-36.6 (100-120)	1.462	1.0027	0.83	322
36.6-42.7 (120-140)	1.7743	0.9667	0.80	91
42.7-48.8 (140-160)	1.3383	1.0123	0.82	42

Regression analyses of relationships between depression length and width for various elevation ranges were performed to test the validity of the null hypothesis that isometry exists in the depression population ($a=1$ in $L= bW^a$). Except for the elevation intervals between 6.1 to 30.5 m (20 to 100 ft) in which allometric changes of length and width are strongly supported at the 5 percent level, the null hypothesis is not rejected. The exponent in the power function between length and width is significantly different from the isometric value at the 10 percent level for the depressions within the elevation range between 0-6.1 m (0-20 ft), and suggests a tendency towards isometry at the 5 percent level. There is strong support for the null hypothesis at the elevation ranges above 30.38 m (100 ft), indicating isometric conditions in which the rate of changes of length and width are similar.

A plot of the growth ratio (exponent "a") against average values of topographic intervals suggests that the rate of changes observed for the depression length and width decreases with elevation (Figure 5.11). The relationship between the growth ratio and elevation is expressed as "growth ratio = -0.0005*elevation + 1.0698" and explains approximately sixty percent of the variation. The decrease of the growth ratio with elevation especially for the elevation range between 6.1 - 30.5 m (20 - 100 ft) can be explained by the older depressions approaching steady state in the area between the Suwannee River and the Cody Escarpment.

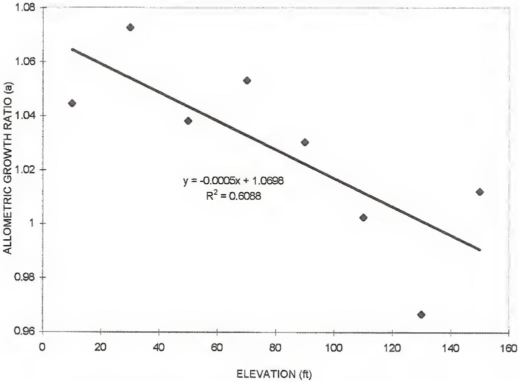

Figure 5.11. Changes in the allometric growth rate (a) of the depression population with elevation.

Despite a slightly higher rate of change of length indicated by the positive allometry for most of the elevation ranges, there is no evidence for a preferred depression growth along major axis. Variation of length/width ratio with mean depression area plotted for various elevation intervals does not suggest a significant preferential growth along length or width (Appendix E).

Depression length – width relationships for the marine terraces were also expressed by a set of power functions (Table 5.9 and Appendix D). Allometry prevails for all but the lowest terrace. Regression of length over width indicates that the null hypothesis (a=1) can not be rejected for the Pamlico terrace at five percent significance level. However, positive allometry exists for Talbot, Penholoway, Wicomico, and Sunderland.

Table 5.9. Allometric relationships within marine terraces.

TERRACES	**b**	**a**	**R^2**	**COUNT**
PAMLICO	1.7121	1.0097	0.75	61
TALBOT	1.2563	1.0683	0.83	3559
PENHOLOWAY	1.1360	1.0480	0.80	7368
WICOMICO	1.3498	1.0459	0.85	8171
SUNDERLAND	1.376	1.0352	0.88	1609

Changes in the allometric growth ratio with terraces are shown in Figure 5.12. Excluding the isometric value for the Pamlico terrace, there is a strong tendency for the allometric growth ratio to decrease with the terrace age. This supports the interpretation made for the growth ratio changes observed to correlate with the elevation. The lower values of the allometric growth ratio for higher terraces clearly indicate that the rate at which depression morphometry changes is much less for older depressions.

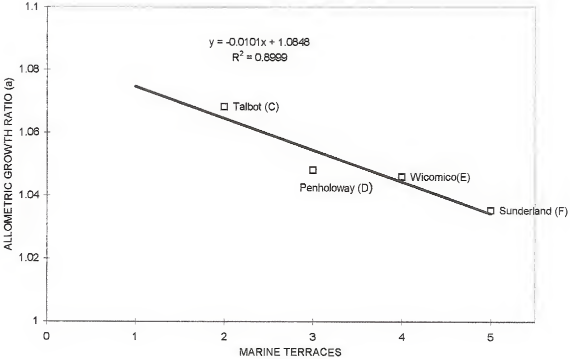

Figure 5.12. Changes in the allometric growth ratio (a) of the depression population with marine terraces.

Evolution of the Spatial Distribution of Depressions

The spatial organization of depressions was examined by using two GIS layers containing information on the depression density and mean nearest neighbor distance. Spatial distribution of depressions provides important evidence supporting the idea that the karstic evolution of the Suwannee River area has been strongly controlled by the sequential recessions of the Pleistocene seas.

The area between the Suwannee River and the Cody Escarpment (elevation range of 6.1-30.5 m, 20-100 ft), is represented by a major modal distribution of depressions (Figure 5.13). The depression density shows a unimodal distribution and varies only from 7.5 to 8.1 (Table 5.10). A slight decrease in depression density within the altitude range of 18.3-24.4 m (60-80 ft) is caused by the lack of karstic activity on the hills of the Bell ridge southeast of the confluence between the Suwannee and Santa Fe rivers. The modal range of elevation between 24.4-30.5 m (80-100 ft) corresponds to the significant karstic activity within the Marginal Zone. Depression density drastically decreases for elevations higher than 30.5 m (100 ft) representing the confined hydrogeologic conditions of the Northern Highlands physiographic province.

Table 5.10. Statistical summary of depression density within elevation ranges.

ELEVATION Meters (feet)	**Mean**	**Maximum**	**Minimum**	**Standard Deviation**
0-6.1 (0-20)	3.7	19.7	0.25	2.9
6.1-12.2 (20-40)	7.5	40.4	0.25	5.4
12.1–18.3 (40-60)	7.6	39.5	0.25	3.9
18.3–24.4 (60-80)	7.5	41.7	0.25	4.8
24.4-30.5 (80-100)	8.1	42.0	0.24	5.5
30.5-36.6 (100-120)	5.8	26.9	0.30	4.6
36.6-42.7 (120-140)	2.9	15.6	0.24	2.2
42.7-48.8 (140-160)	2.1	8.10	0.27	1.2
48.8-54.8 (160-180)	2.4	5.68	0.43	1.1
54.8 – 61.0 (180-200)	1.3	2.08	0.69	0.4

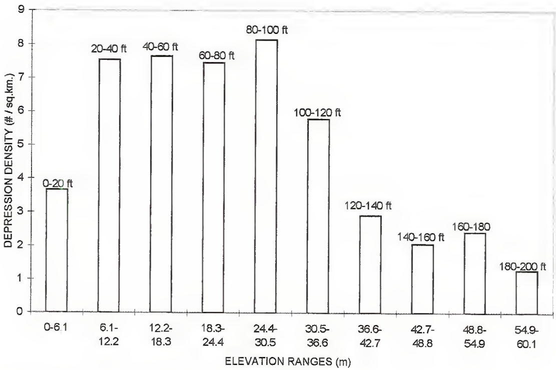

Figure 5.13. Changes in the density of the depression population with elevation.

Similarly, spatial distribution of depressions between marine terraces shows a unimodal pattern (Figure 5.14). Depression density essentially remains constant around 8.0 within the Talbot, Penholoway, and Wicomico terraces. It drops to 5.9 for the heavily confined karst terranes of the Sunderland terrace (Table 5.11).

Table 5.11. Statistical summary of depression density within marine terraces.

TERRACES	**Mean**	**Maximum**	**Minimum**	**Standard Deviation**
PAMLICO	2.8	10.3	0.2	1.9
TALBOT	8.2	40.4	0.2	5.6
PENHOLOWAY	8.0	30.4	0.2	4.0
WICOMICO	8.4	31.5	0.2	5.3
SUNDERLAND	5.9	26.3	0.2	4.9

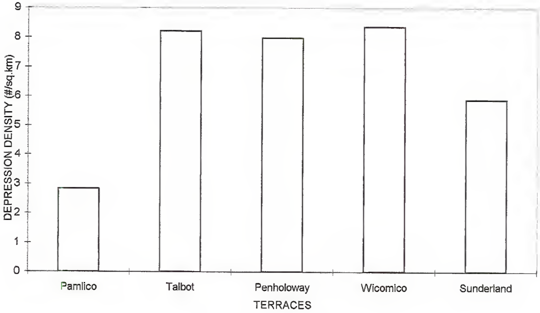

Figure 5.14. Changes in the density of the depression population with marine terraces.

Mean nearest neighbor distance of the total depression population for elevation ranges shows a generally decreasing trend with altitude up to the approximate elevation of the Cody Escarpment (30.48 m) (Figure 5.15). The nearest neighbor distance values gradually drop from 222.18 to 180.12 meters and show a significant and steady increase for areas higher than 30.48 m (100 ft). (Table 5.12).

Table 5.12. Statistical summary of mean nearest neighbor distance (m) within the elevation ranges.

ELEVATION Meters (feet)	**Mean**	**Maximum**	**Minimum**	**Standard Deviation**
0-6.1 (0-20)	222.2	1401.8	32.4	169.7
6.1-12.2 (20-40)	171.7	1424.0	20.0	105.1
12.1–18.3 (40-60)	180.6	1180.5	20.0	92.6
18.3–24.4 (60-80)	180.1	2056.0	20.0	113.5
24.4-30.5 (80-100)	169.8	1982.0	20.0	112.6
30.5-36.6 (100-120)	198.7	957.0	32.4	127.9
36.6-42.7 (120-140)	299.0	1790.2	60.0	282.4
42.7-48.8 (140-160)	405.7	1386.1	130.0	320.3

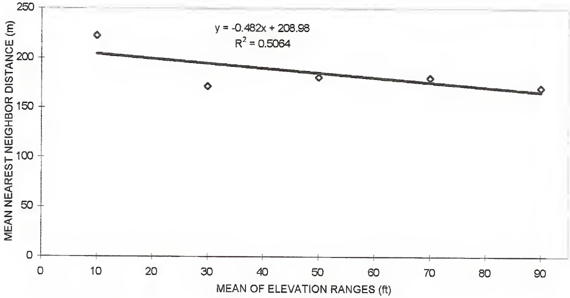

Figure 5.15. Changes in the mean nearest neighbor distance of the depression population with elevation.

Unlike the generally decreasing trend of nearest neighbor distance for higher altitudes, older marine terraces do not show a closer packing arrangement of depressions (Figure 5.16). After a significant drop between the Pamlico and Penholoway terraces, the mean nearest neighbor distance values fluctuate approximately between 164 and 171 meters and rise to 190 meters for the area between the Wicomico and Sunderland terraces (Table 5.13).

Table 5.13. Statistical summary of nearest neighbor distance (m) within marine terraces.

TERRACES	Mean	Maximum	Minimum	Standard Deviation
PAMLICO	264.0	777.9	50.0	159.7
TALBOT	163.8	1330.0	20.0	96.5
PENHOLOWAY	180.6	2056.0	20.0	95.2
WICOMICO	171.2	1982.0	20.0	109.4
SUNDERLAND	191.1	1790.2	32.4	139.9

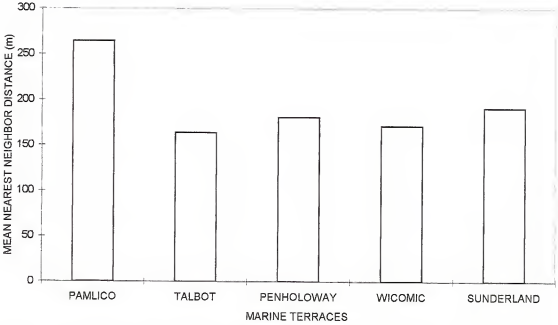

Figure 5.16. Changes in the mean nearest neighbor distance of the depression population with marine terraces.

One of the useful parameters describing the extent of surficial karst development involves the area of internal runoff, which increases as depressions form and grow larger. The area of internal runoff can be used directly or after normalized by the total karst area as in the pitting index proposed by Williams (1971). As a direct measure of the surficial karst development, pitting index is calculated by dividing total karst area to the total depression area (area of internal runoff). It decreases as the percentage of area occupied by depressions grows, and becomes unity in highly karstified areas where all drainage is internal.

In accordance with the general trend of spatial and morphometric parameters discussed above, the variation of pitting index indicates that the extent of surficial karst increases within the marginal zone between the Suwannee River and the Northern

Highlands physiographic province. A linear equation obtained by plotting pitting index as a function of distance from the Cody Escarpment explains approximately sixty percent of the variation (Figures 5.17 & 5.18). A pitting index value of 5.71 for the 1 km wide zone along the approximate location of the Cody Escarpment (100 ft contour line) suggests a well developed karst closer to the escarpment. It gradually rises to 11.03 for areas located 5 to 6 km away from the scarp where karst is not as developed because of the relatively shorter time of subaerial exposure.

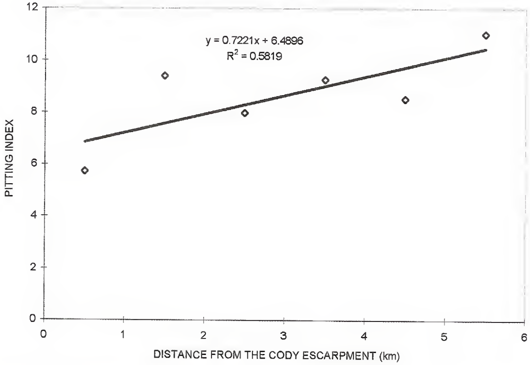

Figure 5.17. Changes in the pitting index with distance from the Cody Escarpment.

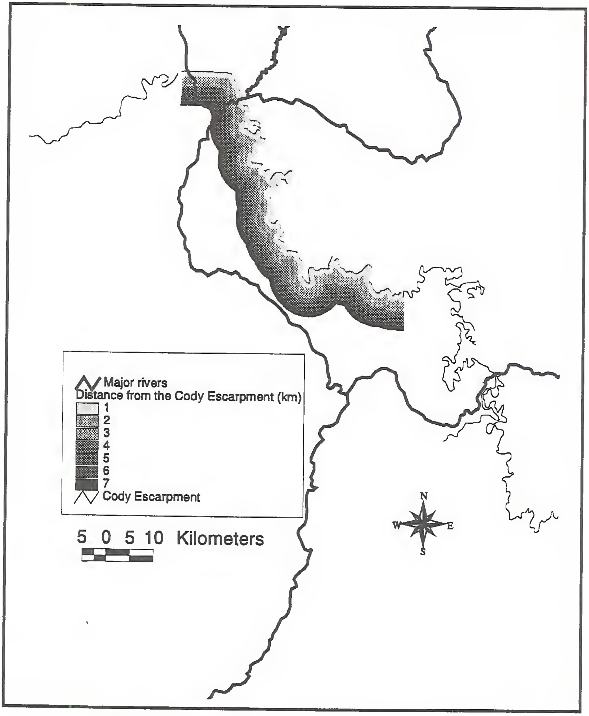

Figure 5.18. Zones of equal distance from the Cody Escarpment.

Discussion

Following a major sea level drop in the Oligocene, the geologic history of the northwest peninsular Florida includes extensive siliciclastic deposition accompanied by regional structural movements, numerous sea level changes during the Neogene and Quaternary, resulting in the exposure of the carbonate platform to repeated freshwater phreatic and vadose conditions.

Early Miocene time witnessed the continuation of the structural movements associated with the formation of the Ocala Platform (uplift) (Vernon, 1951). It is widely believed that most of the karstic and fluvial activity was significantly affected by regional fracturing (Vernon, 1951; Ceryak et al., 1983). However, the Miocene was not only a period of crustal adjustment but also of significant marine and nonmarine siliciclastic deposition. Sea level reached a Miocene maximum during the middle part of this epoch and covered the Florida Platform (Scott, 1997). Sediments of the Hawthorn Group extended across the Ocala Platform (Brooks, 1966; Scott, 1997). Deposition of clayey sediments on the carbonates of the Ocala Platform hampered the infiltration of surface runoff and thus limited the development of karst. Further dissolution of karstic conduits did not commence until the overburden was eroded from the higher parts of the Ocala Platform following a dramatic sea-level drop during the Late Miocene (Scott, 1997).

The partial erosion of the Miocene siliciclastics and the exposure of underlying carbonates to karstic processes accompanied by the continuous retreat of the Cody Escarpment because of the headward erosion by surface runoff from the highlands. Earlier karst phases and the resultant template of karst development induced by the Oligocene sea level drop may have played an important role in the development of preferential dissolution, resulting in a multisequential karst infrastructure. However, it is very likely that early karst development was mainly controlled by the fracture and joint patterns caused by the development of the Ocala Platform.

Regional fracture and joint patterns are also believed to be important in early development of surficial drainage patterns on the exposed karst terrains of the Ocala Platform. Based on his observations on the physiography and geomorphology of northern Florida, Brooks (1966) proposes that the ancestral Suwannee River was an east flowing river whose path to the Atlantic ocean was obstructed by the formation of the Trail Ridge. He states that early in the Pleistocene, it was captured by another stream eroding from the Gulf of Mexico eastward. The river's current path, mostly parallel to the axis of the Ocala Platform, is believed to be controlled by the fracture patterns and the stratigraphy of the area (Ceryak et al., 1983). As suggested by its relatively smaller delta, it is a geologically young river extending into the Gulf with a few large distributary channels (Davis, 1997).

Formation of the Suwannee River has had profound effects on the development of karst in the area. Creating a local base level, the river has increased the hydraulic gradient and controlled the groundwater flow pattern. Extensive dissolution of the carbonate rocks during that period has caused well-developed karst landforms only to be repeatedly covered and exhumed by the post–Miocene sea level fluctuations. Consequently, the karst landscape in the study area consists of both young depressions that have been developing since the last subaerial exposure of the carbonate rocks and of the older depressions subjected to multisequential karst processes. It is further complicated by the interactions between these depressions of different generations.

Despite the complicated development of karst landforms in the study area, substitution of space for time has proven to be useful in unraveling the evolutionary pattern of karstic depressions within the Suwannee River basin. Information obtained by examining the variation of spatial and morphometric parameters is critical in explaining the temporal changes in the depression morphometry and distribution.

The substitution of space for time was applied to test a rather simple working hypothesis that the karstification within the study area has evolved from higher to lower altitudes. This trend of karst evolution, then, should be observed in the morphometric and spatial distribution patterns of depression with different geomorphologic age. Because of their longer period of subaerial exposure, higher areas are expected to possess more frequent and/or larger and more complex depressions than lower, i.e., geomorphologically younger terrains. The results of this study as summarized in Tables 5.14 & 5.15, support the working hypothesis especially for depressions located between the Suwannee River and the Cody Escarpment, where the Floridan aquifer is unconfined or locally semiconfined. Higher mean values of morphometric parameters observed for the lowest elevation ranges and terraces may not be representative because of the relatively smaller populations of depressions in these areas. Those anomalies may also be caused by dry valleys formed by the sinking of stream systems into the karst aquifer. Notwithstanding the relatively great variance values within ranges, the trends indicated by the mean values of morphometric parameters can be considered reliable since they do not represent random samples but the population.

Despite relatively constant values of depression density, decreasing pitting index values at higher elevations indicates the existence of more developed karst landscapes due to longer subaerial exposure periods at geomorphologically older terrains. A closer packing arrangement for these depressions is indicated by decreased nearest neighbor distance values (Table 5.14).

Table 5.14. Summary of mean spatial parameters.

ELEVATION **Meters (feet)**	**DEPRESSION DENSITY**	**NEAREST NEIGHBOR DISTANCE (m)**
0-6.1 (0-20)	3.6	222.2
6.1-12.2 (20-40)	7.5	171.7
12.1–18.3 (40-60)	7.6	180.6
18.3–24.4 (60-80)	7.4	180.1
24.4-30.5 (80-100)	8.1	169.8
30.5-36.6 (100-120)	5.8	198.7
36.6-42.7 (120-140)	2.9	229.0
42.7-48.8 (140-160)	2.0	405.7

Despite some exceptions at very low elevations and near the Cody Escarpment, the generally increasing trends of mean depression area and mean diameter with elevation suggest that depressions in geomorphologically older terrains in the Gulf Coastal Lowlands physiographic province, where the Floridan aquifer is unconfined or semiconfined, grow larger by coalescence and expansion. Their planimetric shapes, although influenced by the thickness and the lithology of the overburden, as explained in Chapter 3, tend to be more circular as indicated by a general decrease in the length/width ratio and by circularity ratios approaching unity with for higher elevations (Table 5.15). Therefore, any evidence for structural control on the initiation and development of depressions has been greatly obscured by the coalescence of depressions and the effects of surficial erosion.

Table 5.15. Summary of mean morphometric parameters.

ELEVATION Meters (feet)	AREA (m^2)	LENGTH (m)	WIDTH (m)	L/W	MEAN DIAMETER (m)	CIRCULARITY INDEX
0-6.1 (0-20)	20821.0	168.4	87.7	1.90	128.1	1.45
6.1-12.2 (20-40)	11459.3	119.6	64.8	1.78	92.2	1.32
12.1–18.3 (40-60)	13042.2	124.8	69.6	1.77	97.2	1.36
18.3–24.4 (60-80)	17326.7	139.8	78.4	1.74	109.1	1.33
24.4-30.5 (80-100)	15988.4	119.7	69.7	1.68	94.7	1.29
30.5-36.6 (100-120)	15731.4	94.5	58.8	1.67	76.6	1.18
36.6-42.7 (120-140)	8333.6	110.5	68.7	1.64	89.6	1.20
42.7-48.8 (140-160)	10054.2	125.7	85.1	1.46	105.4	1.17

Depression growth by coalescence is actively taking place as indicated both by allometric and isometric relationships between the length and width of depressions. However, it should be noted that the rate of changes decreases with the age of the karst terrane. Older karst terranes with greater depression density and larger total depression area are closer to a dynamic equilibrium than younger depressions occurring at lower elevations. Therefore, the rate of change in their planimetric dimensions is slower.

Conceptual Model of Karst Evolution

Based on the above discussions, a conceptual model depicted in Figure 5.19 attempts to describe the sequential development of karst from late Oligocene to recent and explains the relative importance of a variety of parameters in controlling the karstic evolution of the Suwannee river area.

One of the early karstification sequences in the area started with the subaerial exposure of the thick carbonate platform in response to a major sea level drop during the late Oligocene. Surficial and underground dissolution was controlled by joint systems and bedding planes. Diffuse autogenic recharge caused extensive dissolution at shallow depths within the epikarstic zone (Figure 5.19-a).

Early Miocene witnessed the deposition of siliciclastic sediments and crustal adjustments associated with the development of the Ocala Platform. These structural and stratigraphic changes have drastically affected the pattern of karst evolution in the area. Fracture systems formed during this period have become instrumental in later karst development. Karstification was interrupted by the deposition of the impermeable material onto the paleokarst surface (Figure 5.19-b).

Surficial erosion of the impermeable cover started in response to the increasing fluvial activity in the Pleistocene (Figure 5.19-c). Particularly, formation of the Suwannee River created a local base level and increased the intensity of both surficial and subsurface erosional activity. Removal of the impermeable cover along the retreating Cody Escarpment exposed the carbonate rocks and initiated a new sequence of karstification. Diffuse autogenic recharge through soil layers caused extensive dissolution within the epikarst mainly because of the increased chemical aggressivity induced by the soil gasses. On the other hand, allogenic recharge originating from the nonkarstic regions caused focused corrosion along the retreating Cody Escarpment. The karstification pattern was controlled by the fracture systems and the Oligocene karst template.

Figure 5.19 (a-f). Evolution of karst in the Lower Suwannee River area, Late Oligocene to recent.

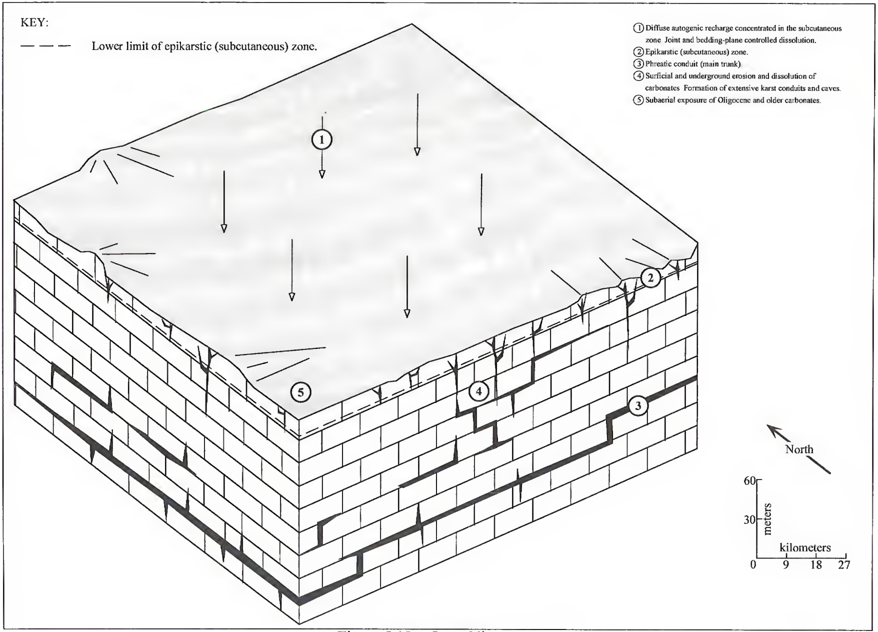
KEY:
— — — Lower limit of epikarstic (subcutaneous) zone.
① Diffuse autogenic recharge concentrated in the subcutaneous zone Joint and bedding-plane controlled dissolution.
② Epikarstic (subcutaneous) zone.
③ Phreatic conduit (main trunk)
④ Surficial and underground erosion and dissolution of carbonates Formation of extensive karst conduits and caves.
⑤ Subaerial exposure of Oligocene and older carbonates.
①
②
③
④
⑤
North
60
30
meters
kilometers
0
9
18
27

Figure 5.19-a Late Oligocene.

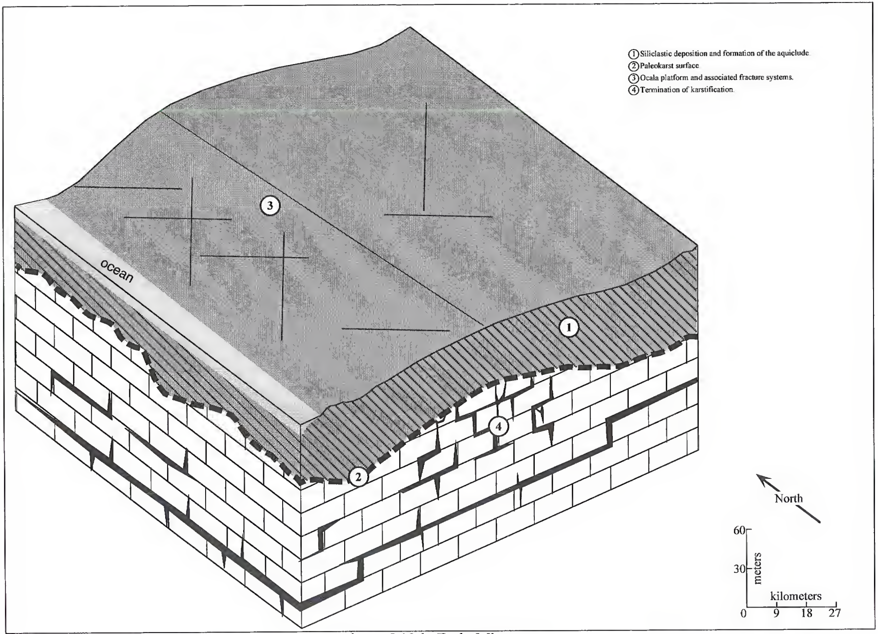
①Siliclastic deposition and formation of the aquiclude
②Paleokarst surface
③Ocala platform and associated fracture systems.
④Termination of karstification
ocean
①
②
③
④
North
60
30
meters
kilometers
0
9
18
27

Figure 5.19-b Early Miocene.

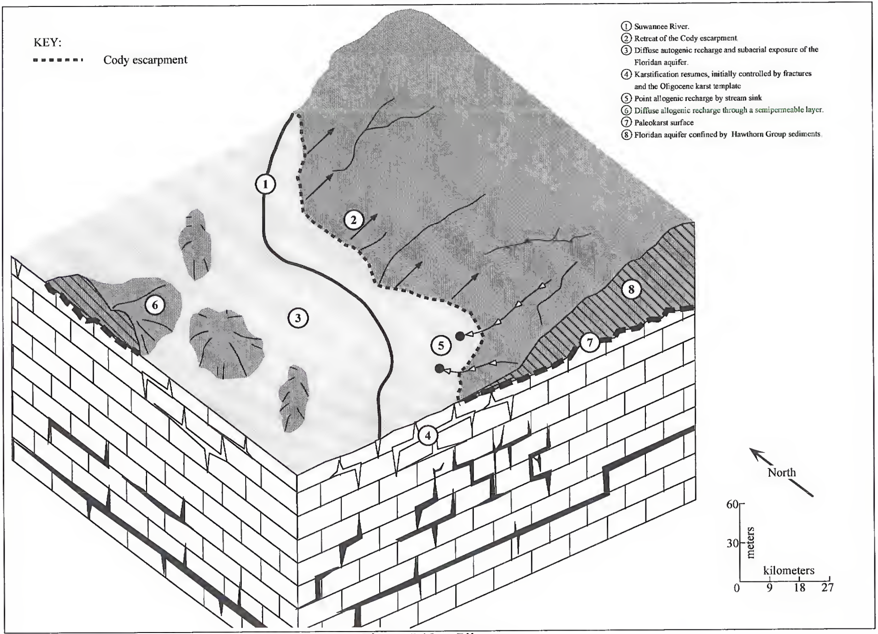
KEY:
Cody escarpment
① Suwannee River.
② Retreat of the Cody escarpment
③ Diffuse autogenic recharge and subaerial exposure of the Floridan aquifer.
④ Karstification resumes, initially controlled by fractures and the Oligocene karst template
⑤ Point allogenic recharge by stream sink
⑥ Diffuse allogenic recharge through a semipermeable layer.
⑦ Paleokarst surface
⑧ Floridan aquifer confined by Hawthorn Group sediments
1
2
3
4
5
6
7
8
North
60
30
meters
kilometers
0
9
18
27

Figure 5.19-c Pliocene.

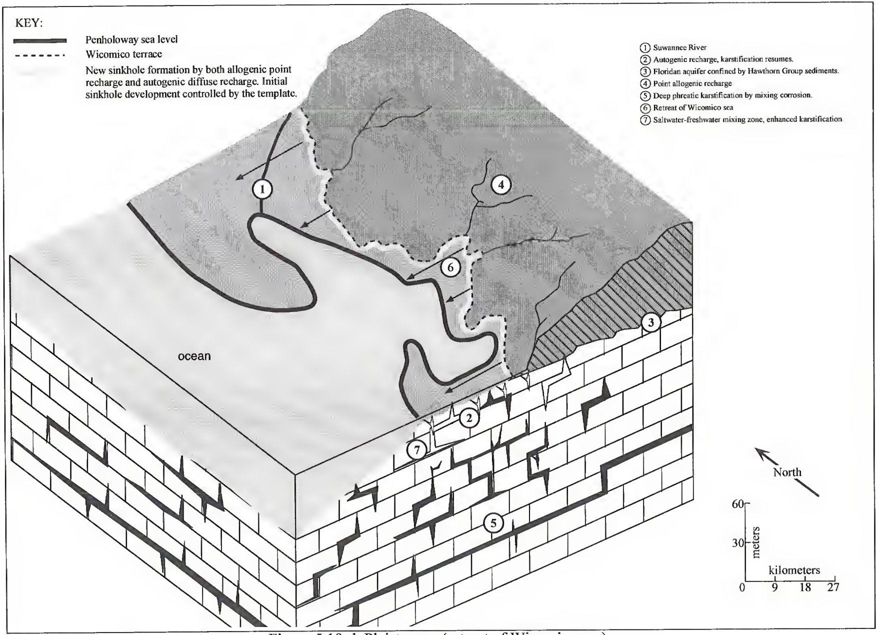
KEY:
Penholoway sea level
Wicomico terrace
New sinkhole formation by both allogenic point recharge and autogenic diffuse recharge. Initial sinkhole development controlled by the template.
① Suwannee River
② Autogenic recharge, karstification resumes.
③ Floridan aquifer confined by Hawthorn Group sediments.
④ Point allogenic recharge
⑤ Deep phreatic karstification by mixing corrosion.
⑥ Retreat of Wicomico sea
⑦ Saltwater-freshwater mixing zone, enhanced karstification
①
④
⑥
③
②
⑦
⑤
ocean
North
60
30
meters
kilometers
0
9
18
27

Figure 5.19-d Pleistocene (retreat of Wicomico sea).

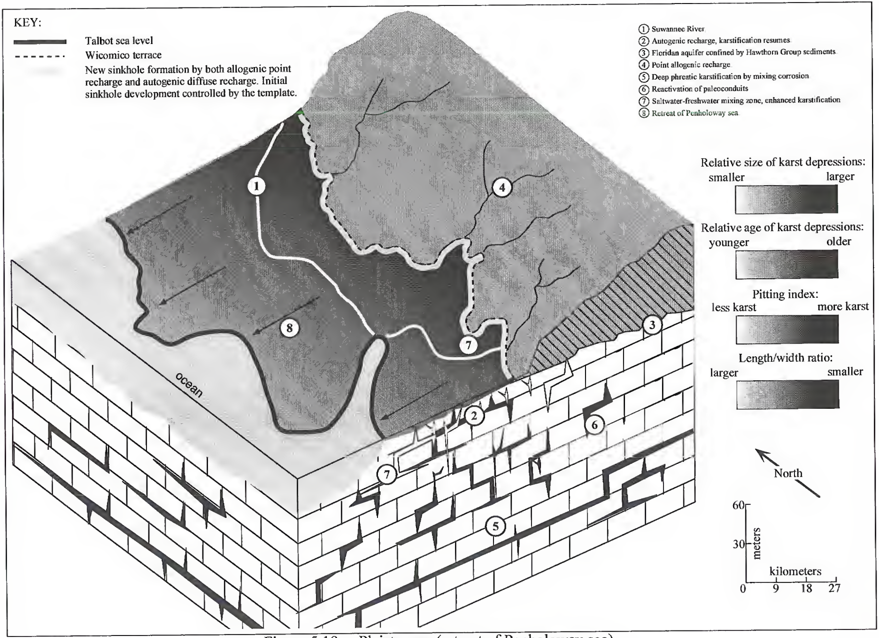
KEY:
Talbot sea level
Wicomico terrace
New sinkhole formation by both allogenic point recharge and autogenic diffuse recharge. Initial sinkhole development controlled by the template.
① Suwannee River
② Autogenic recharge, karstification resumes
③ Floridan aquifer confined by Hawthorn Group sediments
④ Point allogenic recharge
⑤ Deep phreatic karstification by mixing corrosion
⑥ Reactivation of paleoconduits
⑦ Saltwater-freshwater mixing zone, enhanced karstification
⑧ Retreat of Penholoway sea
Relative size of karst depressions:
smaller
larger
Relative age of karst depressions:
younger
older
Pitting index:
less karst
more karst
Length/width ratio:
larger
smaller
ocean
1
2
3
4
5
6
7
7
8
North
60
30
meters
kilometers
0
9
18
27

Figure 5.19-e Pleistocene (retreat of Penholoway sea).

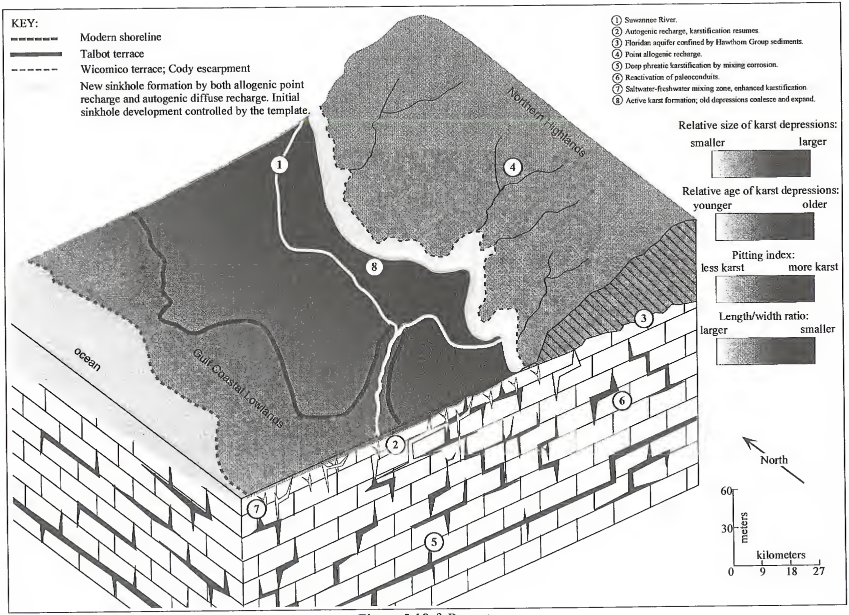
KEY:
Modern shoreline
Talbot terrace
Wicomico terrace; Cody escarpment
New sinkhole formation by both allogenic point recharge and autogenic diffuse recharge. Initial sinkhole development controlled by the template.
① Suwannee River.
② Autogenic recharge, karstification resumes.
③ Floridan aquifer confined by Hawthorn Group sediments.
④ Point allogenic recharge.
⑤ Deep phreatic karstification by mixing corrosion.
⑥ Reactivation of paleoconduits.
⑦ Saltwater-freshwater mixing zone, enhanced karstification
⑧ Active karst formation; old depressions coalesce and expand.
Relative size of karst depressions:
smaller
larger
Relative age of karst depressions:
younger
older
Pitting index:
less karst
more karst
Length/width ratio:
larger
smaller
Northern Highlands
Gulf Coastal Lowlands
ocean
1
2
3
4
5
6
7
8
North
60
30
meters
kilometers
0
9
18
27

Figure 5.19-f Recent.

The final sequence of karst development in the Suwannee River area involved the gradual subaerial exposure of the carbonate platform in response to the progressive regression of interglacial seas. New areas of carbonate platform were exposed to karst activitiy as the Pleistocene seas retreated (Figures 5.19-d-e-f). This sequential pattern of subaerial exposure controlled the age of karstication. Older depressions at higher elevations coalesced and expanded resulting in more circular and larger depressions. The rate of change in their planimetric dimensions decreased as they approached the steady state conditions. Both diffuse autogenic recharge in the karst plain and focused allogenic recharge originating from the impermeable highlands resulted in extensive karstification and activation of paleokarst conduits. Areas of enhanced dissolution within the saltwater-fresh water mixing zone migrated as the Pleistocene coastlines retreated. Deep phreatic conduits were formed by the mixing-corrosion.

CHAPTER 6
SUMMARY AND CONCLUSIONS

Analysis of the morphometric and spatial distribution parameters (depression area, depression diameter, depression length-width ratio, circularity index, depression density, pitting index, nearest neighbor distance) of the karstic depressions within the Lower Suwannee River basin reveals that the Florida karst is represented by broad, shallow depressions with an average density of 6.07 and an average pitting index of 14.5. Morphometric and spatial distribution parameters of karstic depressions show a great variation within the Lower Suwannee River area and thus, preclude a simple morphoclimatic classification of karst landforms.

Despite a well representation of temperate karst landforms such as dolines and dry valleys, the subtropical Lower Suwannee River area does not exhibit tropical landforms of cockpit and tower karst. This may be explained by a muted surficial expression of a much more developed karst landform covered by at least several meters of soil material. In addition, relatively stable tectonics and lack of significant uplift that have been effective over the Florida platform may also account for the low-relief karst landform pattern. From the lithological point of view, numerous studies have shown that the tropical landforms of cockpit and tower karst tend to form within massive, jointed limestones with very low primary porosity (Smith and Atkinson, 1976; Ford and Williams, 1989). The Tertiary carbonates of the Floridan aquifer with relatively less joint frequency and significant primary porosity are not conducive to the extreme karst landforms observed in the massive limestones of the tropics. Groundwater flow and storage within the Floridan aquifer takes place both within the intergranular and diagenetic (karstic) porosity, confirming both the Darcian and turbulent flow models.

The depression morphometry and distribution are not controlled by a single geologic or hydrogeologic factor examined in this study. Comparison of morphometric and spatial distribution parameters with geologic and hydrogeologic factors such as thickness of the overburden above the Floridan aquifer, potentiometric level fluctuation of the Floridan aquifer, depth to water table, soil type, and the lithology of vadose zone suggests that all of the factors examined collectively affect the morphometry and distribution of karstic depressions. The influence of thickness of the overburden material, or depth to the water table depends strongly upon the lithology of the vadose zone. Similarly, fluctuation of the Floridan aquifer potentiometric level does not impose any control on the morphometry and distribution of karstic depressions in areas where confining conditions occur.

The major axes of karstic depressions do not show a preferred orientation or conformity to the prevailing directions of structural features. However, the alignment of depressions evaluated by the frequency of nearest neighbor direction vectors does indicate a tendency of depressions to align in approximately east-west direction. This preferred orientation of depression alignment does not conform the prevailing regional fracture traces. Its close agreement with the predominant east-west aspect of topographic slope might indicate that the alignment of karstic depressions is controlled by the relief of local topography.

Application of the mass flux technique to available data indicates that the best estimate of the net karstic dissolution rate in the Lower Suwannee River basin is 40.1 m^3/km^2/year. This is equal to a denudation rate of 40.1 mm/1000 years. Mass flux from the system is increased by prolonged durations of high flows and does not seem to be affected by extreme flood events. Only 5 to 7 % of the annual dissolved load is removed by low frequency flood flows. Temporal distribution of dissolved load shows seasonal variations. Rainy seasons correlate with greater amounts of solutional loads whereas mass flux tends to decline with decreasing flow rates.

The post-Miocene geologic history of the Lower Suwannee River area represents a transition from confined hydrogeologic conditions to water table conditions caused by the retreat of the confining layer along the Cody Escarpment. Fracture systems formed by the initiation and development of the Ocala Platform throughout the Miocene Epoch have been instrumental in the evolution of karst landforms. Cave systems and surficial depressions initially formed by concentrated autogenic recharge through the confining layer were further modified by allogenic recharge originating from the retreating highlands of insoluble rocks. As the escarpment has retreated, autogenic diffuse recharge has been predominant in previously confined zones and further modified the karst terrane.

The course of karstic evolution in Florida was also strongly influenced by inherited templates resulting from the repeated subaerial exposures of the previously karstified surface. In each exposure, induced by glacio-eustatic sea level changes, the drained conduits of the previous karst phases provided an instant vadose zone with already established input to output connections. This inherited template of karst was instrumental in guiding runoff underground and focusing solution within the epikarst. Karst features developed in vadose and phreatic zones during low sea levels were reactivated and re-submerged several times. However, these various karst phases were not identical processes controlled by the same parameters. Rather, they were individual sequences of karstification with different hydrologic, geologic, and structural conditions. In that sense, the karst in the Lower Suwannee River area is not multicyclic, but multisequential.

Morphometric and spatial distribution characteristics of karstic depressions suggest that the last phase of the post-Miocene karstic evolution within the Lower Suwannee River basin has been controlled by the retreat of the Pleistocene sea level stands. During the Pleistocene, as interglacial seas retreated, marine terraces were formed by sequential sea level lowstands and the total period of subaerial exposure diminished towards the sea. Consequently, geomorphologically younger karst landforms formed as the elevation of marine terraces decreased. This evolutionary pattern of karst landforms resulted in the development of more frequent and/or larger and more complex depressions at higher elevations.

The population of karstic depressions examined in this study is derived from 1:24,000 scale topographic maps with a 5 ft contour interval and does not include sinkholes that are too small to be depicted in topographic maps. Therefore, care should be taken in comparing the morphometric and spatial distribution parameters obtained in this study with those of other karst areas cited in a large number of publications. Similarly, the accuracies of ancillary data layers utilized to infer the factors effecting karst development and evolution are constrained by their spatial resolution. By and large, this study is based on a regional approach and attempts to gather general information on the karst landforms of the Lower Suwannee River basin. In comparison with similar studies of equivalent resolution, examination of some twenty-five thousands depressions in an area of 4,063 km^2 in this study represents the most comprehensive morphometric analysis of karstic depressions of its kind. The accuracy of this technique can be enhanced by focusing in a smaller area and utilizing finer resolution data collected by means of aerial photographs or higher technology processes (e.g. airborne laser swath mapping system) and field studies.

This study represents a successful application of Geographic Information Systems to karst landform analysis in a regional scale. Aside from the morphometric characterization and the evolutionary analysis of the surficial karst landforms, this study provides two comprehensive databases in ArcView format. The databases contain information on the morphometric and spatial distribution parameters of the entire depression population within the study area. Utilization of these comprehensive databases illustrates the evolutionary history of karst in one of the best-developed areas in the world and provides insight concerning the interactive parameters which form present and future karst landscape.

APPENDIX A

DEPRESSION AREA AND LENGTH-WIDTH RATIO RELATIONSHIPS FOR TOPOGRAPHIC QUADRANGLES

WANNEE (112A)

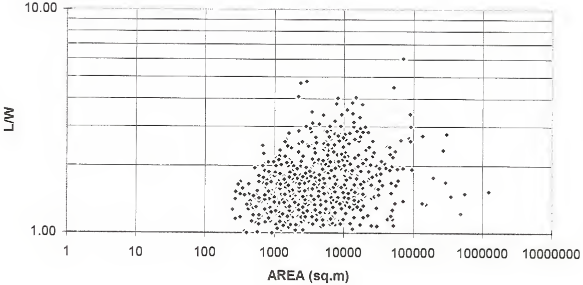

FOURMILE LAKE (112B)

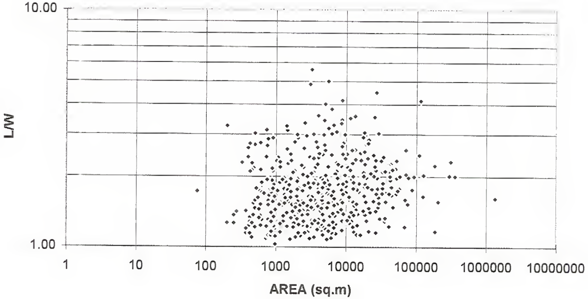

SUWANNEE RIVER (112C)

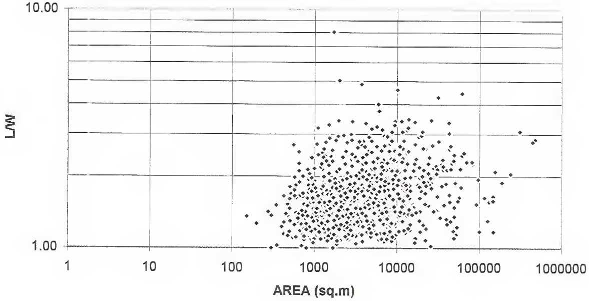

TRENTON (112D)

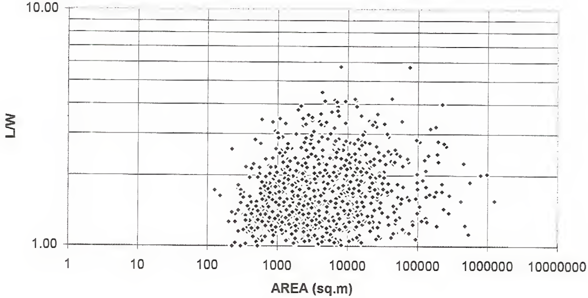

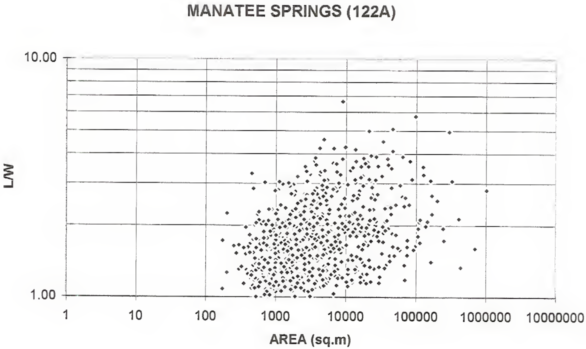
MANATEE SPRINGS (122A)
L/W
10.00
1.00
1
10
100
1000
10000
100000
1000000
10000000
AREA (sq.m)

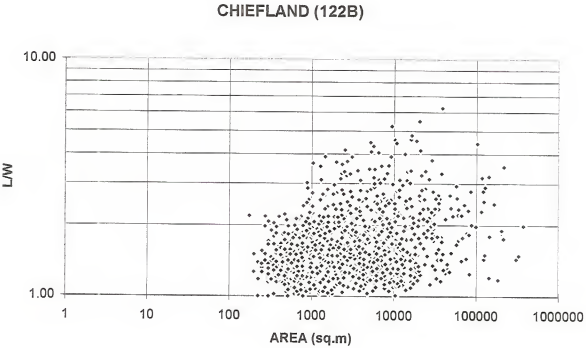
CHIEFLAND (122B)
L/W
10.00
1.00
1
10
100
1000
10000
100000
1000000
AREA (sq.m)

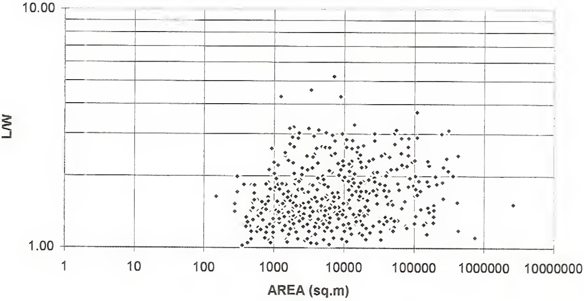

LEE (59B)

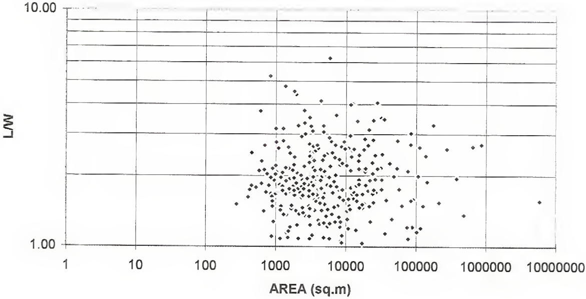

MADISON SOUTH (59D)

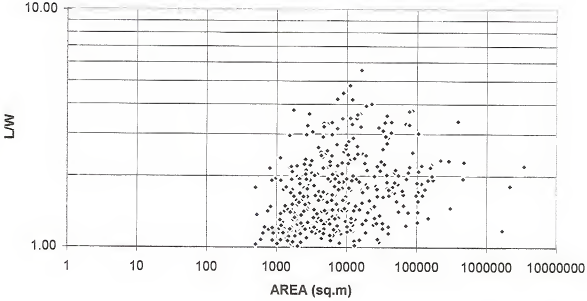

FORT UNION (60B)

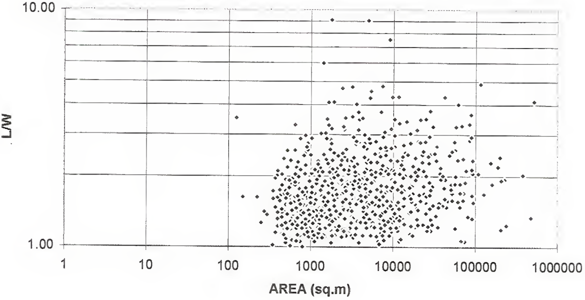

FALLMOUTH (60C)

LIVE OAK WEST (60D)

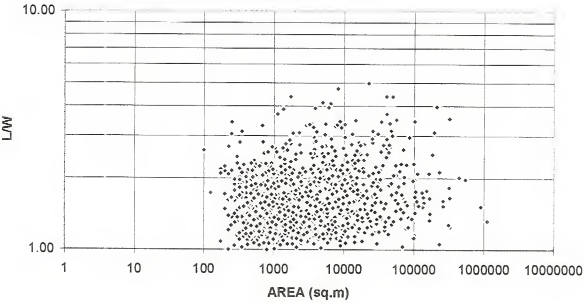

HILLCOAT (61A)

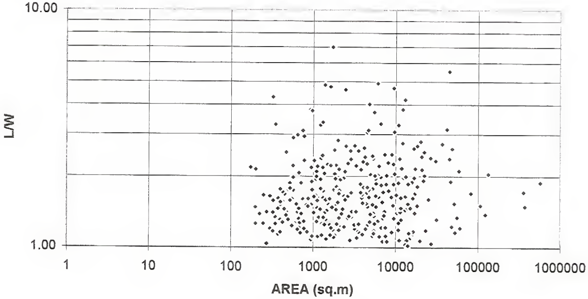

DAY (78B)

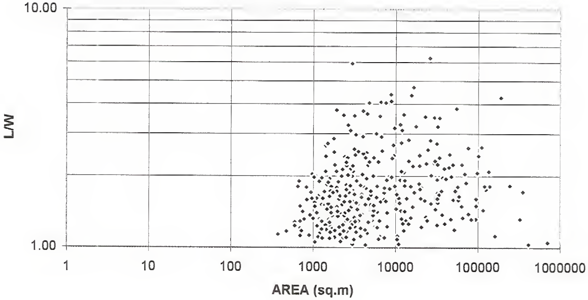

DOWLING PARK (79A)

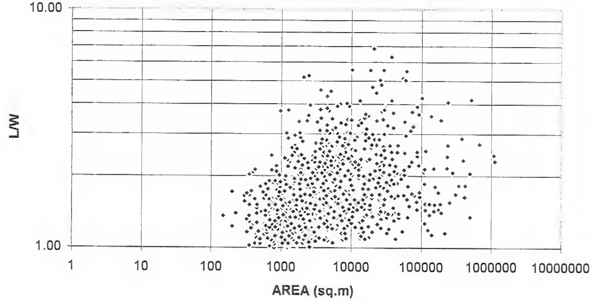

MAYO NE (79B)

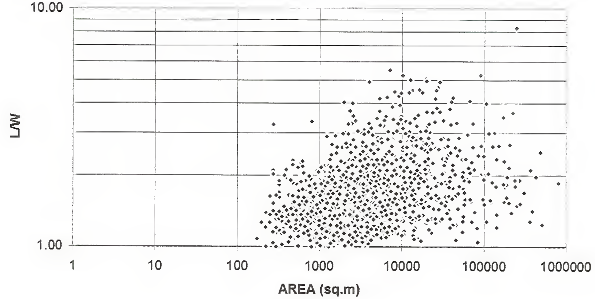

MAYO (79C)

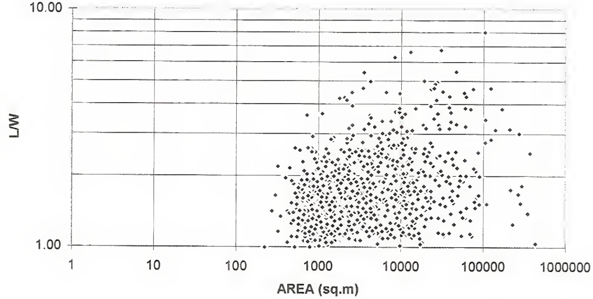

MAYO SE (79D)

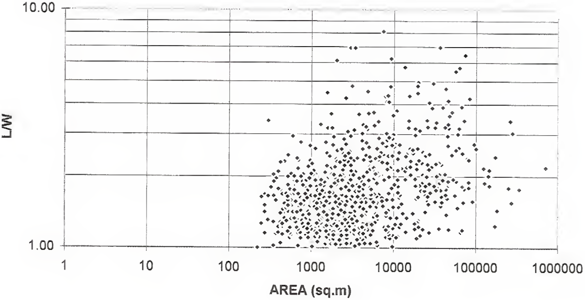

O'BRIEN (80C)

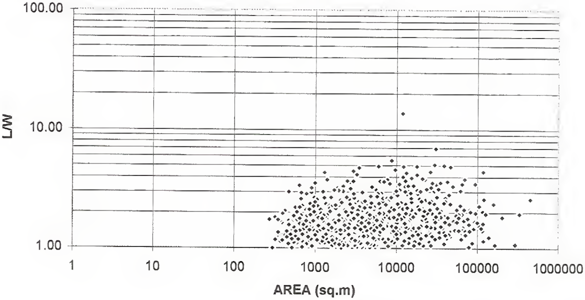

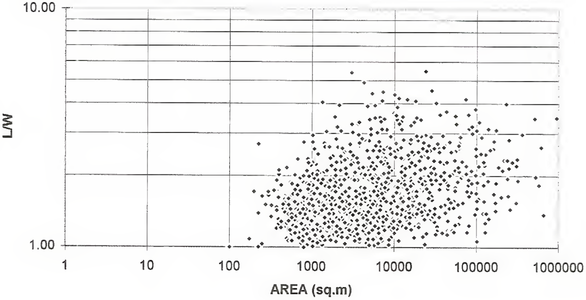

O'BRIEN SE (80D)

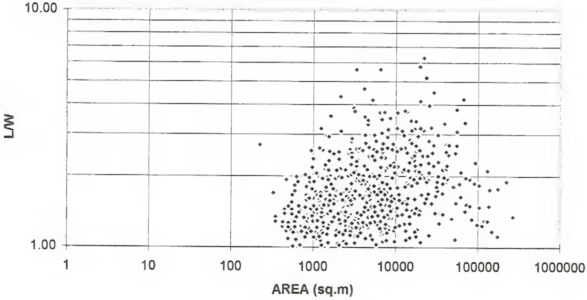

BRANFORD (97A)

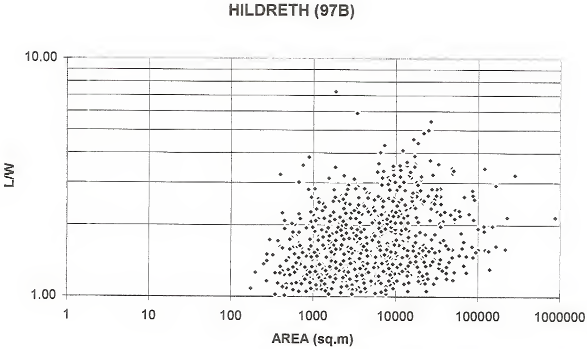
HILDRETH (97B)

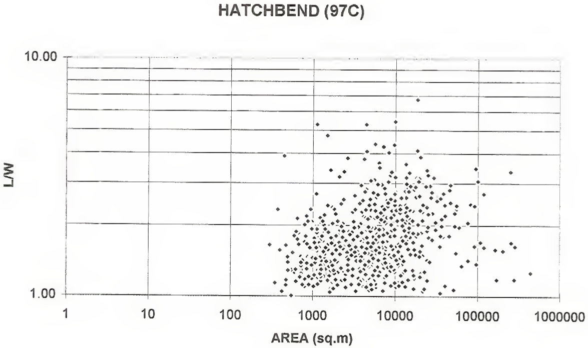
HATCHBEND (97C)

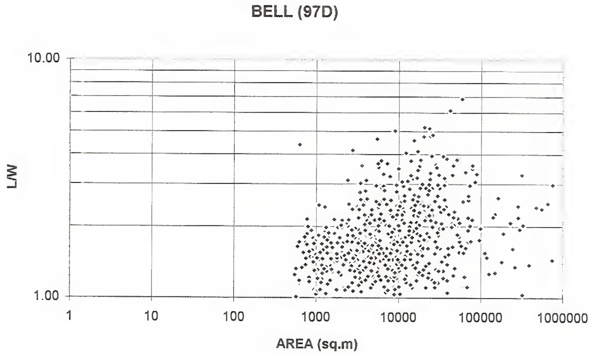
BELL (97D)
10.00
1.00
L/W
1
10
100
1000
10000
100000
1000000
AREA (sq.m)

APPENDIX B

DEPRESSION LENGTH AND WIDTH RELATIONSHIPS FOR TOPOGRAPHIC QUADRANGLES

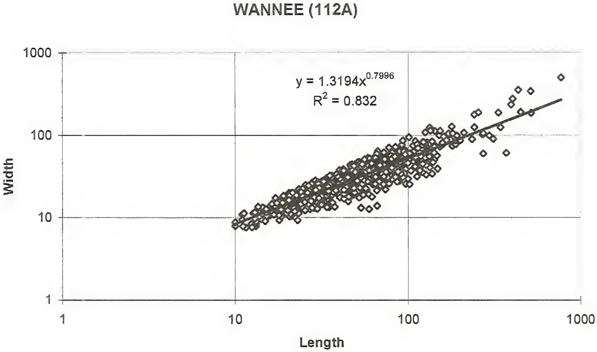

WANNEE (112A)

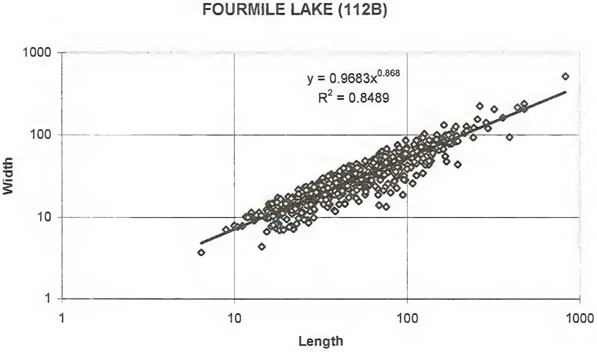

FOURMILE LAKE (112B)

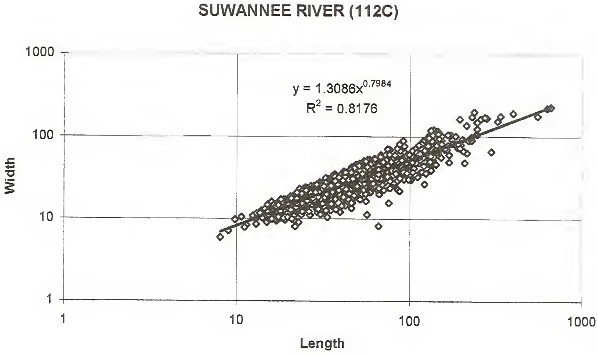
SUWANNEE RIVER (112C)
y = 1.3086x^0.7984
R^2 = 0.8176
Width
Length
1000
100
10
1
1
10
100
1000

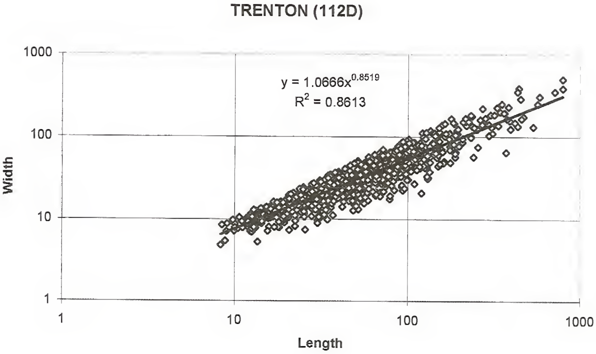
TRENTON (112D)
y = 1.0666x^0.8519
R^2 = 0.8613
Width
Length
1000
100
10
1
1
10
100
1000

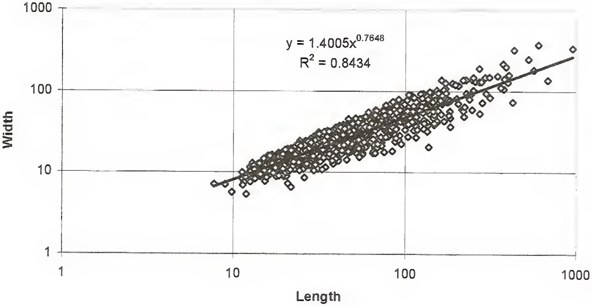
MANATEE SPRINGS (122A)

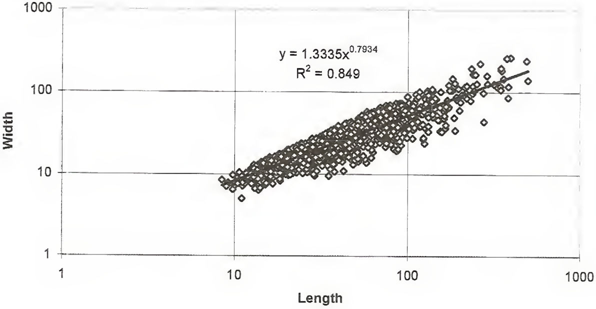
CHIEFLAND (122B)

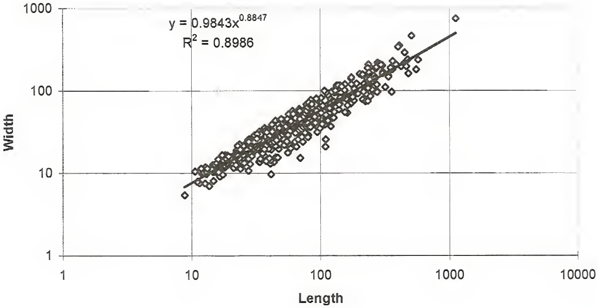
LEE (59B)

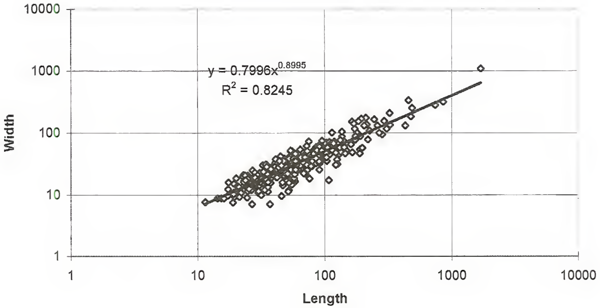
MADISON SE (59D)

ELLAVILLE (60A)

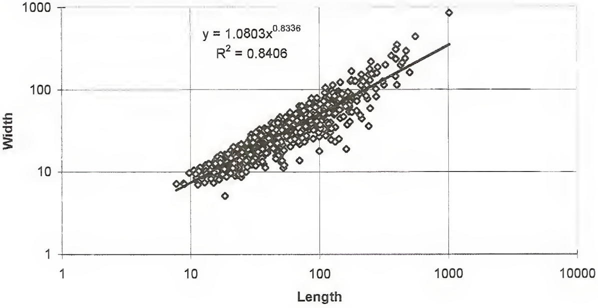

FORT UNION (60B)

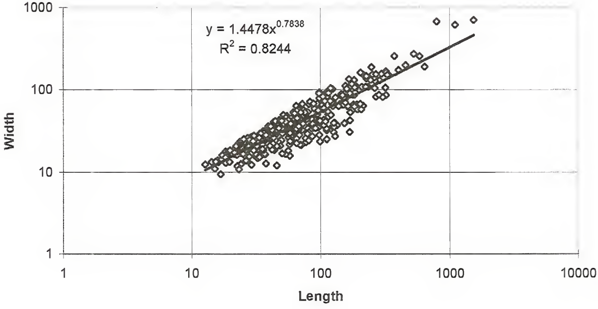

FALLMOUTH (60C)

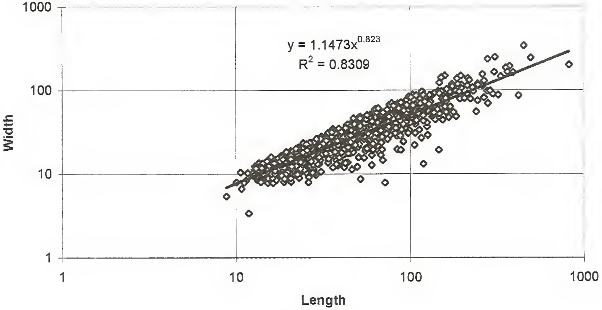

LIVE OAK WEST (60D)

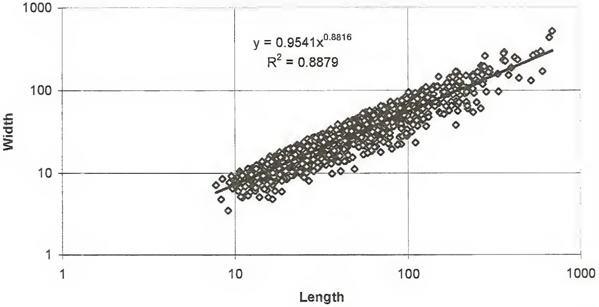

HILLCOAT (61A)

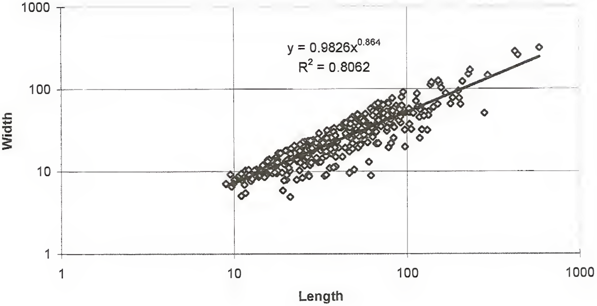

DAY (78B)

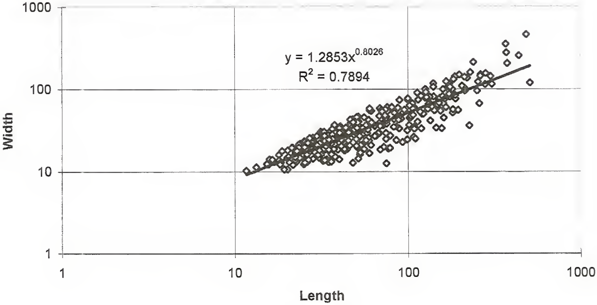

DOWLING PARK (79A)

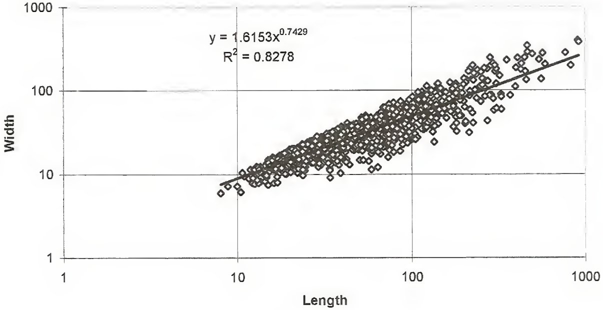

MAYO NE (79B)

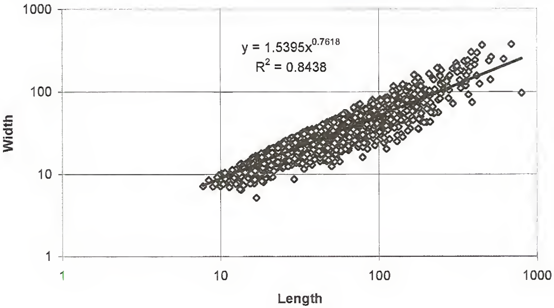

MAYO (79C)

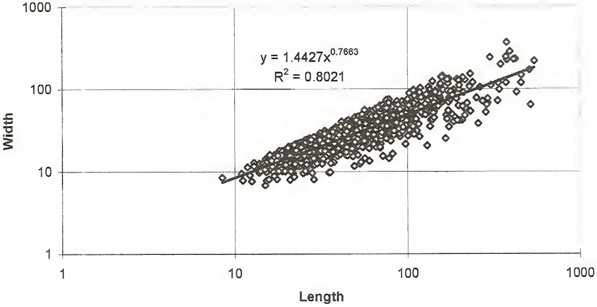

MAYO SE (79D)

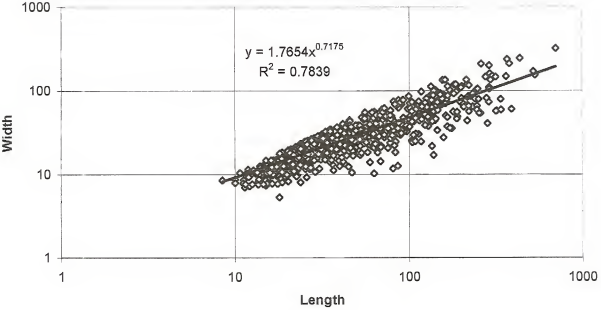

O'BRIEN SE (80D)

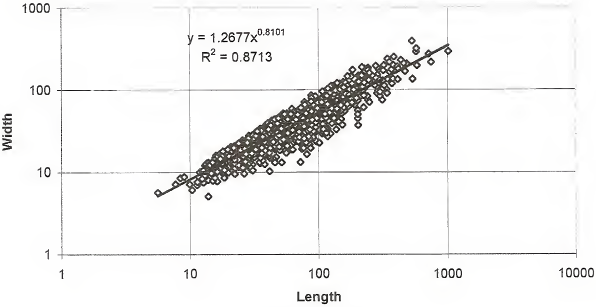

BRANFORD (97A)

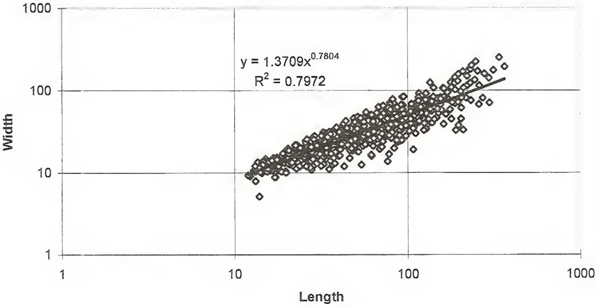

HILDRETH (97B)

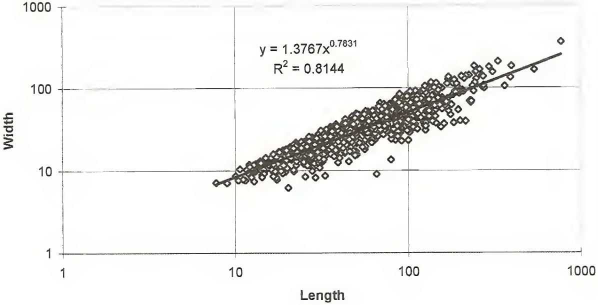

HATCHBEND (97C)

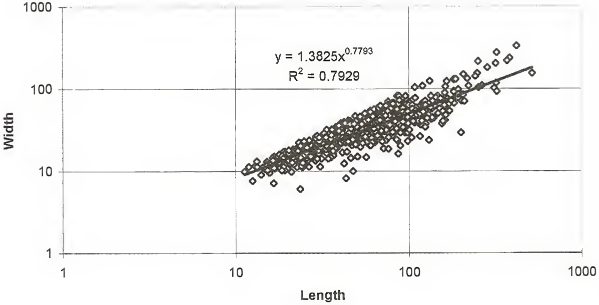

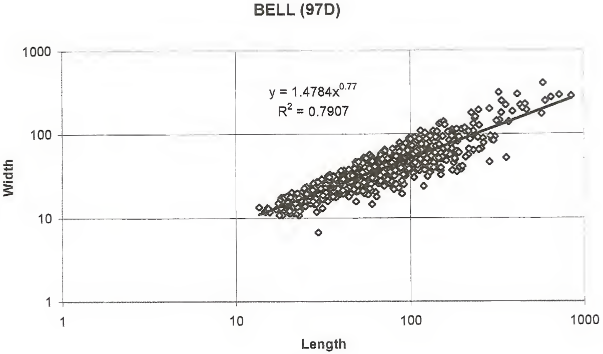
BELL (97D)
y = 1.4784x^0.77
R^2 = 0.7907
Width
1000
100
10
1
1
10
100
1000
Length

APPENDIX C
FLOW DURATION CURVES

Long term flow duration curve for Ellaville, Upper Suwannee

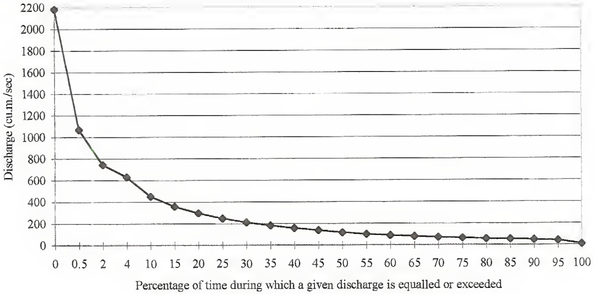

Long term flow duration curve for Fort White, Santa Fe

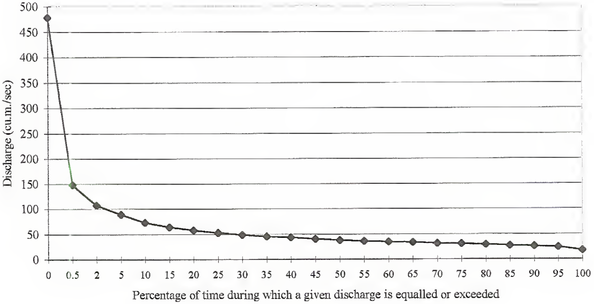

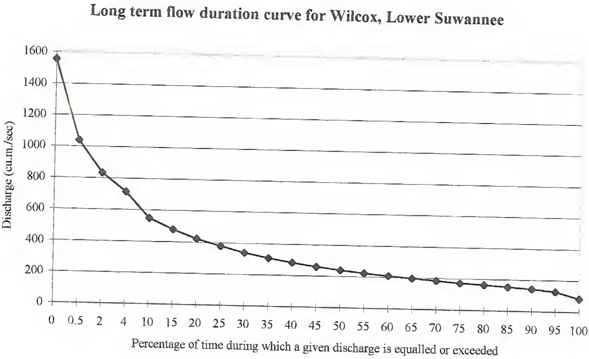

Long term flow duration curve for Wilcox, Lower Suwannee

APPENDIX D
ALLOMETRIC RELATIONSHIPS FOR ELEVATION RANGES AND MARINE TERRACES

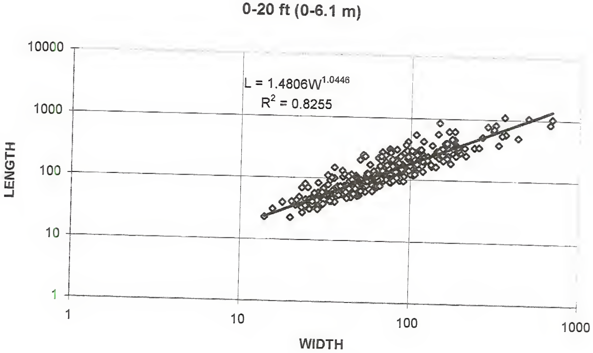
0-20 ft (0-6.1 m)
L = 1.4806W$^{1.0446}$
R^2 = 0.8255
LENGTH
10000
1000
100
10
1
WIDTH
1
10
100
1000

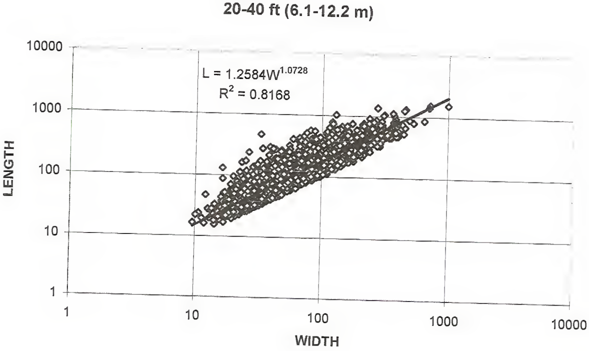
20-40 ft (6.1-12.2 m)
L = 1.2584W$^{1.0728}$
R^2 = 0.8168
LENGTH
10000
1000
100
10
1
WIDTH
1
10
100
1000
10000

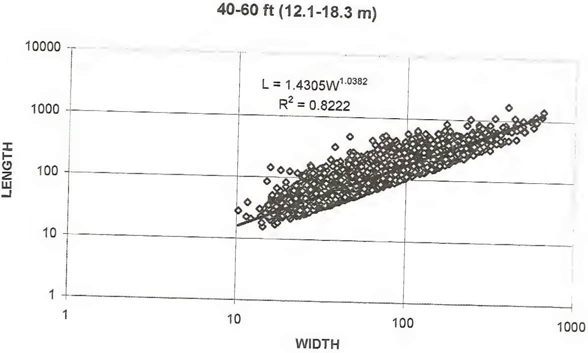

40-60 ft (12.1-18.3 m)

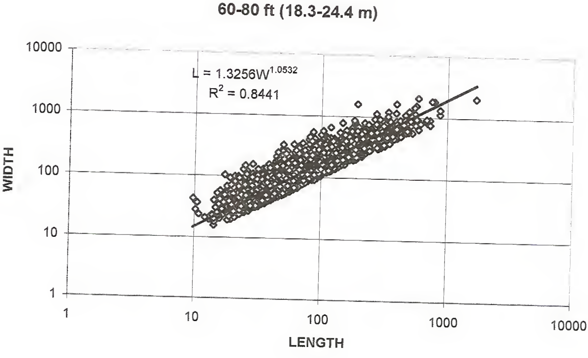

60-80 ft (18.3-24.4 m)

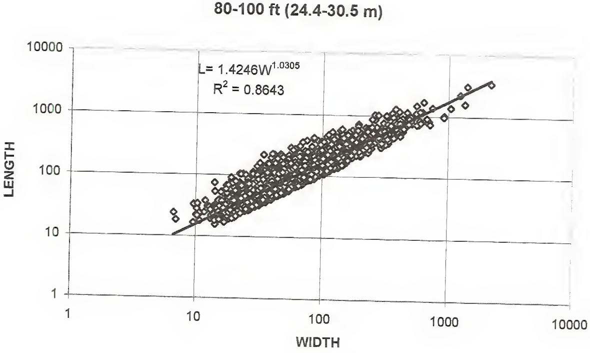
80-100 ft (24.4-30.5 m)
L= 1.4246W^1.0305
R^2 = 0.8643
LENGTH
10000
1000
100
10
1
1
10
100
1000
10000
WIDTH

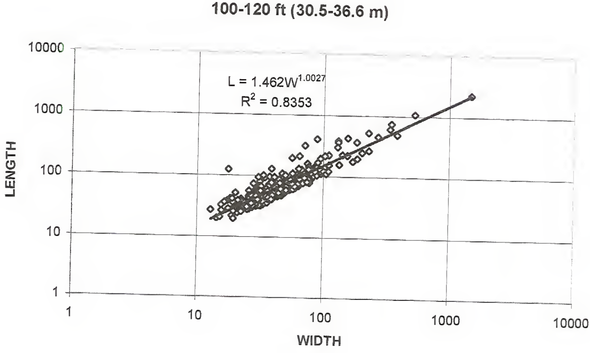
100-120 ft (30.5-36.6 m)
L = 1.462W^1.0027
R^2 = 0.8353
LENGTH
10000
1000
100
10
1
1
10
100
1000
10000
WIDTH

120-140 ft (36.6-42.7 m)

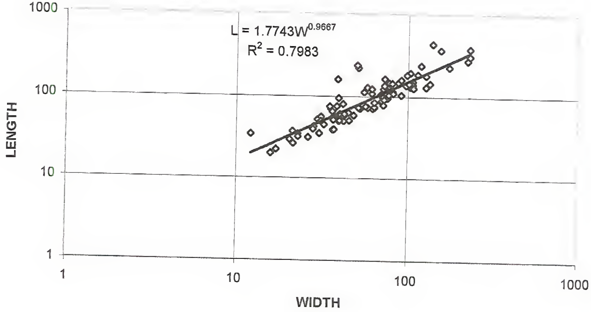

140-160 ft (42.7-48.8 m)

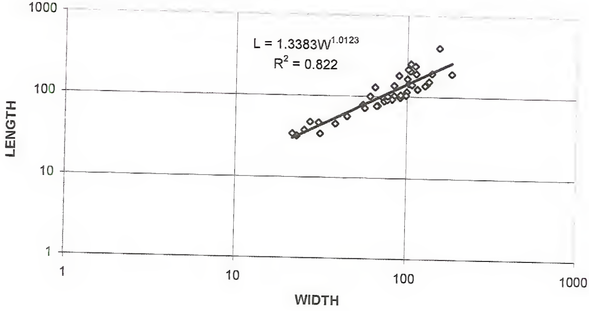

PAMLICO TERRACE

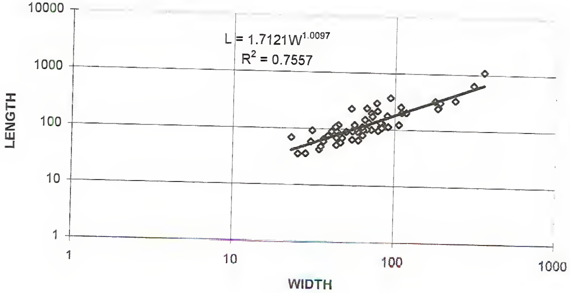

TALBOT TERRACE

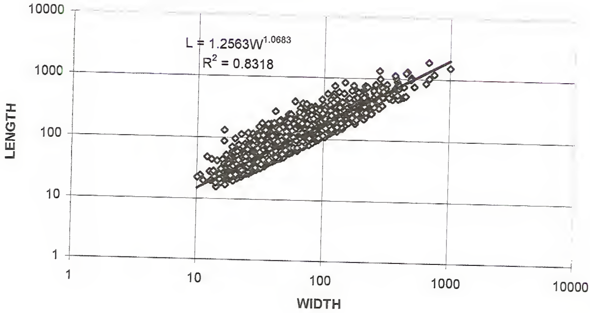

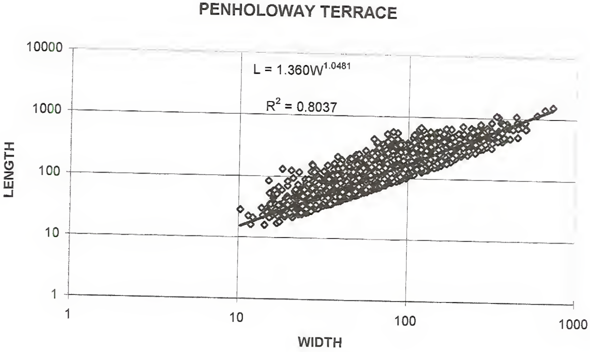
PENHOLOWAY TERRACE
L = 1.360W^1.0481
R^2 = 0.8037
LENGTH
10000
1000
100
10
1
1
10
100
1000
WIDTH

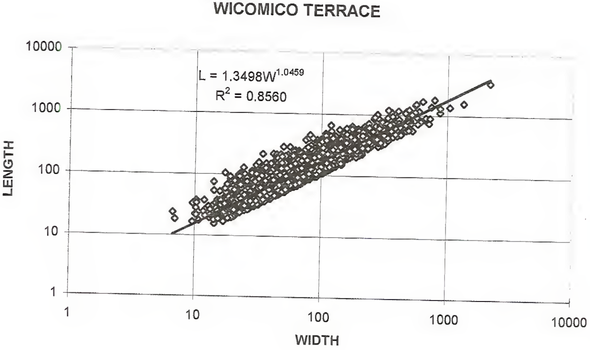
WICOMICO TERRACE
L = 1.3498W^1.0459
R^2 = 0.8560
LENGTH
10000
1000
100
10
1
1
10
100
1000
10000
WIDTH

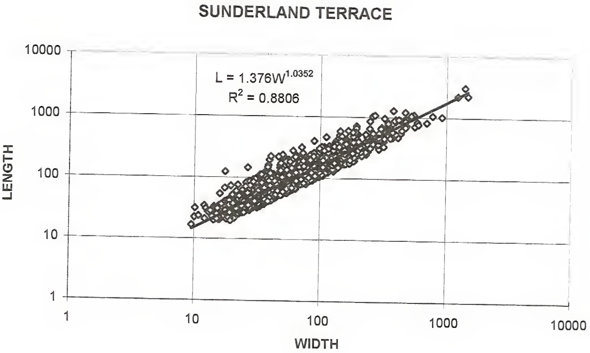
SUNDERLAND TERRACE
L = 1.376W^1.0352
R^2 = 0.8806
LENGTH
10000
1000
100
10
1
1
10
100
1000
10000
WIDTH

APPENDIX E
L/W RATIO AND AREA RELATIONSHIP WITHIN ELEVATION RANGES

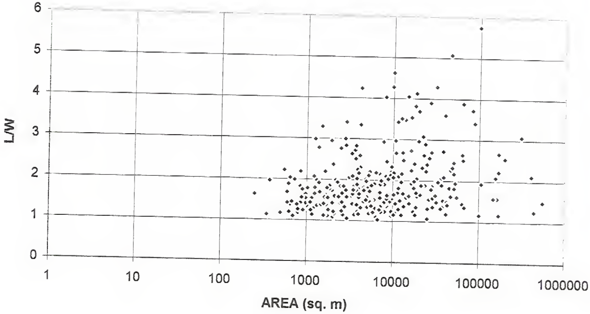

0-20 ft (0-6.1 m)

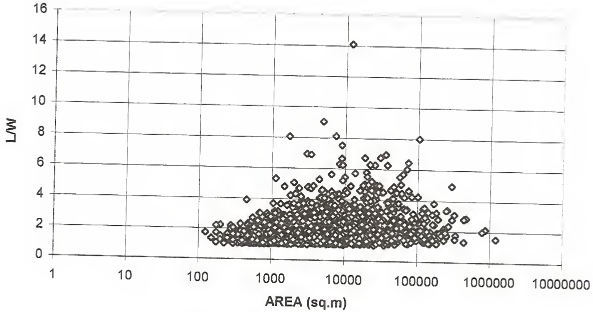

20-40 ft (6.1-12.2 m)

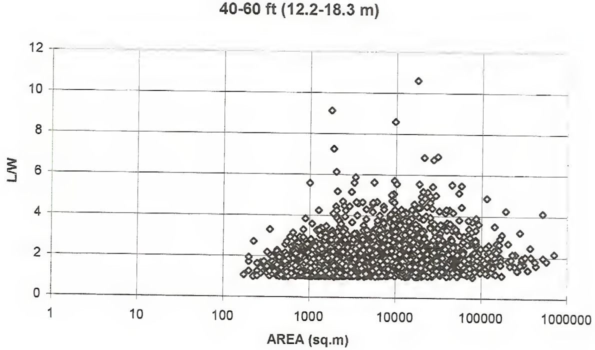
40-60 ft (12.2-18.3 m)
12
10
8
6
4
2
0
L/W
1
10
100
1000
10000
100000
1000000
AREA (sq.m)

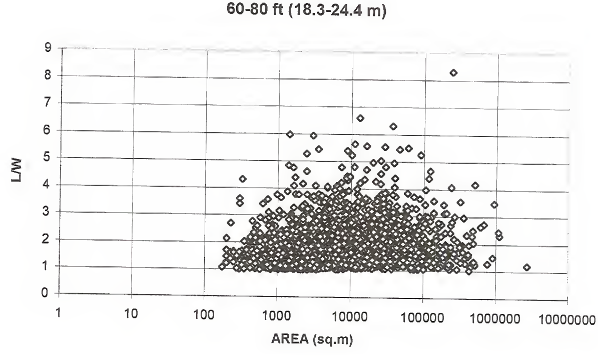
60-80 ft (18.3-24.4 m)
9
8
7
6
5
4
3
2
1
0
L/W
1
10
100
1000
10000
100000
1000000
10000000
AREA (sq.m)

80-100 ft (24.4-30.5 m)

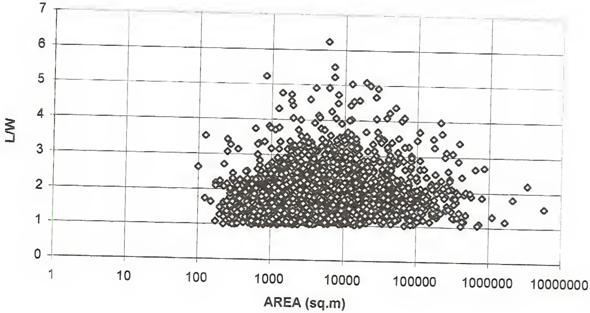

100-120 ft (30.5-36.6 m)

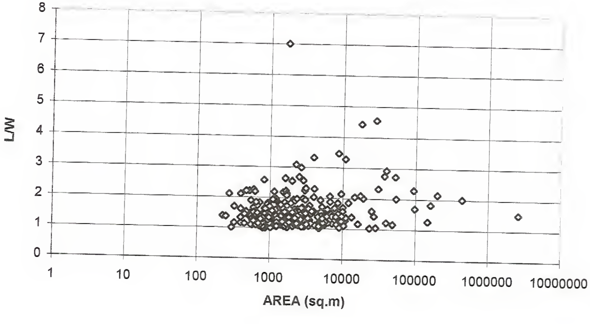

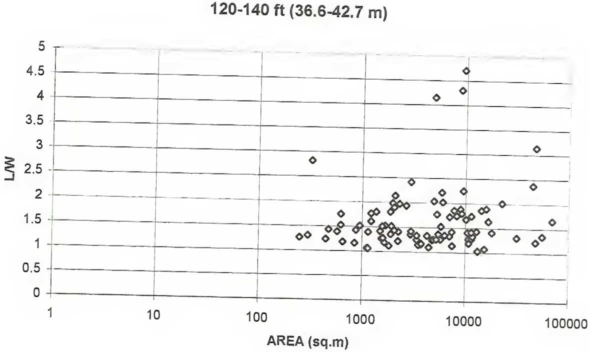
120-140 ft (36.6-42.7 m)
L/W
0
0.5
1
1.5
2
2.5
3
3.5
4
4.5
5
1
10
100
1000
10000
100000
AREA (sq.m)

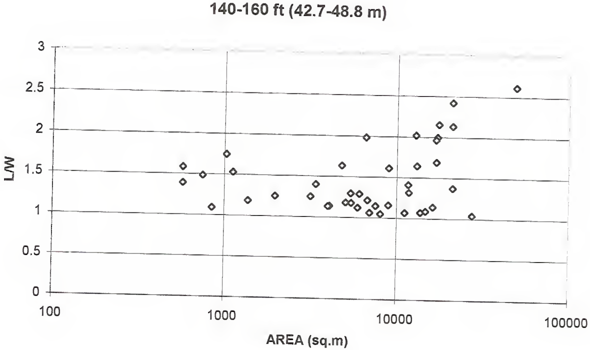
140-160 ft (42.7-48.8 m)
L/W
0
0.5
1
1.5
2
2.5
3
100
1000
10000
100000
AREA (sq.m)

LIST OF REFERENCES

Abrahams, A.D., 1972, Environmental constraints on the substitution of space for time in the study of natural channel networks: Geol. Soc. America Bull., v. 83, pp. 1523-1530.

Alt, D., and Brooks, H.K., 1965, Age of the Florida marine terraces: Journal of Geology v. 72, pp. 406-411.

Applin, P.L., 1951, Preliminary report on buried pre-Mesozoic rocks in Florida and adjacent states: U.S. Geological Survey Circular no. 91, 28 p.

Aubert, D., 1967, Estimation de la dissolution superficielle dans le Jura, Bull. Soc. Vaud.: Sci. nat., v. 69, pp. 365-376.

Aubert, D., 1969, Phenomenes et formes du karst jurassien: Ecl. Geol. Helv., v. 62, pp. 325-399.

Back, W.B., Hanshaw, J.S., Herman, and Van Driel, J.N., 1986, Differential dissolution of a Pleistocene reef in the ground-warer mixing zone of coastal Yucatan, Mexico: Geology, v. 14, pp. 137-140.

Bahtijarevic, A., 1989, Sinkhole density of the Forest City Quadrangle: In Engineering and Environmental Impacts of Sinkholes and Karst. Proceedings of the Third Multidisciplinary Conference on Sinkholes and the Engineering and Environmental Impacts of Sinkholes and Karst, Beck, B.F., (ed.), Rotterdam, A.A. Balkema, pp. 75-82.

Bahtijarevic, A., 1996, Karst landforms in Florida: geomorphological analysis: M.Sc. Thesis, University of South Florida, Tampa, Florida, 159 p.

Balazs, D., 1971, Intensity of the tropical karst development based on caves of Indonesia: Karst es Barlangkutatas, Hungarian Speleo. Soc., v. 6, pp. 1-67.

Bates, R.L., and Jackson J.A. (eds.), 1987, Glossary of geology: American Geological Institute, Alexandria, Virginia, p. 788.

Bauer, F., 1964, Kalkabtragungsmessungen in den Osterreichischen: Erdkunde, v. 18, pp. 95-112.

Beck, B.F., 1986, A generalized genetic framework for the development of sinkholes and karst in Florida, U.S.A.: Environ. Geol. Water Sci., vol. 8, no. 1 / 2. 5-18, pp. 5-18.

Beck, B.F., and Arden, D.D., 1983, Hydrogeology and geomorphology of the Dougherty Plain, Southwest Georgia-Guidebook for Field Trip, Southeastern Geological Society of America, Tallahassee, Florida: Americus, GA, Georgia Southwestern College.

Beck, B.F., Ceryak, R., Jenkins, D.T., Scott, T.M., and Spangler, D.P., 1984, Field guide to some illustrative examples of karst hydrology in central and northern Florida: Sinkhole Research Inst., University of Central Florida, report no. 84-85-2, 43 p.

Beck, B.F., and Jenkins, D.T., 1985, Morphometric analysis of a mantled karst plain, Nirth Florida, USA: Abstract of papers, Spencer, T., (ed.) First International Conference on Geomorphology, Manchester, Englans, 15-21 September, 1985. pp. 3.

Beggs, T., and Ruth, B.E., 1984, Factors affecting the collapse of cavities: In Sinkholes: Their geology, engineering, and environmental impact, edited by B. F. Beck, Rotterdam: A.A. Balkema, pp. 183-188.

Brooks, H.K., 1966, Stops 5-8. Geologic history of the Suwannee river: In Geology of the Miocene and Pliocene series in the North Florida-South Georgia area. Guidebook for the 12th Annual Field Conference of the Southeastern Geological Society, pp. 37-45.

Brooks, H.K., 1967, Rate of solution of limestone in the karst terrane of Florida: Gainesville, Water Resources Research Center, University of Florida, 67 p.

Bull, W.B., 1975, Allometric change of landforms: Geol. Soc. of America Bull., v. 86, pp. 1489-1498.

Ceryak, R., Knapp, M.S. and Burnson, T.Q., 1983, The geology and water resources of the Upper Suwannee River basin: Florida Geological Survey Report of Investigation. no. 87, 165 p.

Clark, P.J., and Evans, F.C., 1954, Distance to nearest neighbor as a measure of spatial relationships in populations: Ecology, v. 35, pp. 445-453.

Cooke, C. White, 1945, Geology of Florida: Florida State Geol. Surv., Geol. Bull., no. 29, 339 p.

Corbel, J., 1957, Les Karsts du nord-ouest de l'Europe: Mem. Inst. Etudes Rhodaniennes, v. 12.

Corbel, J., 1959, Erosion en terrain calcaire: Ann. Geogr,. v. 68, pp. 97-120.

Corbel, J., 1965, Karsts de Yougoslavie et notes sur les Karsts tcheques et polonias: Rev. Geogr. de l'Est. v.5 pp. 245-294.

Corbel, J., 1971, Les Karsts des regions chaudes (des deserts aux zones tropicales humides): Studia Geomorphologica Carpatho-Balcanica, v. 5, pp. 49-74.

Cramer, H., 1941, Die Systematik der Karstdolinen: Neues Jb. Miner. Geol. Palaont., v. 85, pp. 293-382.

Cvijic, J., 1893, Das Karstphanomen. Versuch einer morphologischen Monografie: Geogr. Abhandl., v.5, p. 218-329.

Dalgleish, J., and Alexander, E.C.Jr., 1984, Sinkhole distribution in Winona county, Minnesota: : In Sinkholes: Their geology, engineering, and environmental impact, edited by B. F. Beck, Rotterdam: A.A. Balkema, pp. 79-85.

Davies, W.E., and LeGrand, H.E., 1972, Karst of the United States: In Karst, Important Karst Regions of the Northern Hemisphere by Herak, M. and Stringfield, V.T. (eds.), Elsevier, Holland.

Davis, R.C.Jr., 1997, Geology of the Florida coast: In Geology of Florida by Randazzo, A.F. and Jones, D.S. (eds.), University Press of Florida, pp. 155-168.

Day, M.J., 1982, The influence of some material properties on the development of tropical karst terrain: Trans. Brit. Cave. Res. Assoc. v. 9(1), pp. 23-37.

Day, M. J., 1983, Doline morphology and development in Barbados: Annals of the Association of American Geographers, v. 73(2), pp. 206-219.

Drake, J., and Ford, D.C., 1972, The analysis of growth patterns of two generation populations; the example of karst sinkholes, Can. Geog. v. 16, pp. 381-384.

EPA (United States Environmental Protection Agency), 1985, DRASTIC: A standardized system for evaluating ground water pollution potential using hydrogeologic settings: EPA/600/2-85/018.

Faulkner, H., 1974, An allometric growth model for competitive gullies: Zeitschr. Geomorphologie, Suppl. bd. 20.

Fellers, J., 1993, Typical surface water quality: Department of Water Resources, Suwannee River Water Management District, p. 112.

Feeney, C.M., 1977, The karstification of drainage: a morphometric approach: MA thesis, University of Auckland.

Fermor, J., 1972. The dry valleys of Barbados: a critical review of their origin and pattern: Trans. Inst. Brit. Geogr. v. 57, pp. 153-165.

Fernald, E.A., and Patton, D.J., eds., 1984, Water resources atlas of Florida. Tallahassee: Florida State University, 291 p.

Fisk, D.W., 1977, Water balance for the Suwannee River Water Management District: Suwannee River Water Management District Information Circular 3, Live Oak, Fl.

Ford, D.C., 1964, Origin of closed depressions in the central Mendip Hills: 20th Internat. Geog. Congr., London, Abtracts, pp. 106-106.

Ford, D.C., and Williams, P.W., 1989, Karst geomorphology and hydrology: Unwin and Hyman, London, 601 p.

Gams, I., 1969, Ergebnisse der neueren Forschungen der Korrosien in Slowenien (NW Jugoslavien): Problems of the Karst Denudation, Studia Geographica, (Brno), v. 5 pp. 9-19.

Gams, I., 1972, Effects of runoff on corrosion intensity in the northwestern Dinaric karst, Trans. Cave Res. Gp. Gt. Br., v. 14, pp. 78-83.

Gunn, J., 1981, Limestone solution rates and processes in the Waitomo district, New Zealand: Earth Surf. Proc. Landforms, v. 6, pp. 427-445.

Hanshaw, B.B., and Back, W.B., 1979. Major geochemical processes in the evolution of carbonate aquifer systems: Journal of Hydrology, v. 43, pp. 278-312.

Hirten, J.J., 1996, Geochemical and hydraulic dynamics of the Suwannee river and Upper Floridan Aquifer system near Branford, Florida: Gainesville, Florida, University of Florida, M.S. Thesis, 101 p.

Hisert, R.A., 1994, A multiple tracer approach to determine the ground water and surface water relationships in the Western Santa Fe river, Columbia County, Florida: Gainesville, Florida, University of Florida, Doctoral Dissertation, 215 p.

Hull, J.P.D.Jr., 1962, Cretaceous Suwannee Strait, Georgia, and Florida: Bulletin of the American Association of Petroleum Geologists, v.46, pp. 118-22.

Hunn, J.D., and Slack, L.J., 1983, Water resources of the Santa Fe river basin, Florida: U.S. Geological Survey Water-Resources Investigations report, no. 83-4075, 105 p.

Jakucs, l., 1973, The role of climate in quantitative and qualitative control of karstic corrosion: Symposium on Karst Morphogenesis, Intl. Geogr. Union, European Regional Conf. Hungary, pp. 122-152.

Jennings, J.N., 1972a, Observations at the Blue Waterholes, March '65 – April '69 and limestone solution on the Cooleman Plain, N.S.W.: Helictite, v. 10, pp. 1-46.

Jennings, J.N., 1972b, The Blue Waterholes, Cooleman Plain, N.S.W., and the problem of karst denudation rate determination: Trans. Cave. Res. Gp. Gt. Br., v. 14, pp. 109-117.

Kemmerly, P.R., 1976, Definitive doline characteristics in the Clarksville qudrangle, Tennessee: Geol Soc. Amer. Bull., v. 87, pp. 42-46.

Kemmerly, P.R., 1980, A time-distribution study of doline collapse: framework for prediction: Environ. Geol., v. 3, pp. 123-130.

Kemmerly, P.R., 1982, Spatial analysis of a karst depression population: clues to genesis: Geol Soc. Amer. Bull., v. 93, pp. 1078-1086.

Kemmerly, P.R., 1986, Exploring a contagion model for karst-terrane evolution: Geol Soc. Amer. Bull., v. 97, pp. 619-625.

Kemmerly, P.R., and Towe, S.K., 1978, Karst depressions in a time context: Earth Surf. Proc. v. 35, pp. 355-362.

Kincaid, T.R., 1994, Groundwater and surface water relationships in the Ginnie Springs area, High Springs, Florida: Gainesville, Florida, University of Florida, M.S. Thesis, 186 p.

La Valle, P., 1967, Some aspects of linear karst depression development in South Central Kentucky, Annals of the Assoc. Am. Geographers, v. 57, pp. 49-71.

La Valle, P., 1968, Karst depression morphology in South Central Kentucky, Geog. Annler, v. 50A, pp. 94-108.

Lehman, H., 1964, States and tasks of research on karst phenomena: Erdkunde, v. 16, pp. 81-83.

Littlefield, J.R., Culbreth, M.A., Upchurch, S.B., and Stewart, M.T., 1984, Relationship of modern sinkhole development to large-scale photolinear features: In Sinkholes:

Their geology, engineering, and environmental impact, edited by B. F. Beck, Rotterdam: A.A. Balkema, pp. 189-95.

MacNeil, F.S., 1949, Pleistocene shorelines in Florida and Georgia: U.S. Geological Survey Professional Paper no. 221-F, pp. 95-106.

Magdalene, S., and Alexander, C.E.Jr., 1995, Sinkhole distribution in Winona County, Minnesota revisited: In Karst GeoHazards, Beck, B.F. (ed.), Balkema, Rotterdam. pp. 43-51.

Miller, J.A., 1986, Hydrogeologic framework of the Floridan aquifer system in Florida and parts of Georgia, Alabama, and South Carolina: U.S. Geological Survey Professional paper no. 1403-B, 91 p.

Ogden, A.E., and Reger, J.P., 1977, Morphometric analysis of dolines for predicting ground subsidence, Monroe County, West Virginia: In Hydrologic Problems in Karst Regions by Dilamarter, R.R., and Csallany, S,C. (eds.), West Ky. Univ, Bowling Green, Ky., pp. 130-139.

Opdyke, N.D., Spangler, D.P., Smith, D.L., Jones, D.S., and Lindquist, R.C., 1984, Origin of the epeirogenic uplift of Pliocene-Pleistocene beach ridges in Florida and development of the Florida karst: Geology, v. 12, pp. 226-228.

Palmer, M.V., and Palmer, A.N., 1975, Landform development in the Mitchell Plain of southern Indiana: origin of a partially karsted plain: Z. Geomorph. N. F. v. 19(1), pp. 1-39.

Palmquist, R., 1979, Geologic controls on doline characteristics in mantled karst: Z. Geomorph. Supp. Band, v. 32, pp. 90-106.

Pirkle, E.C., and Brooks, H.K., 1959, Origin and hydrology of Orange Lake, Santa Fe Lake, and Levys Prairie Lake of north-central peninsular Florida: Journal of Geology, v 67, n.3, pp. 302-317.

Pitty, A.F., 1968, The scale and significance of solutional loss from a limestone tract of the south Pennines: Proc. Geol. Ass. Lond., v. 79, pp. 153-177.

Price, D.J., 1984, Karst progression: In Sinkholes: their geology, engineering, and environmental impact, Beck, B.F. (ed.), Rotterdam, A.A. Balkema, pp. 17-21.

Pulina, M., 1968, The eastern Siberian karst: Geographica Polonica, v. 14, pp. 109-117.

Pulina, M., 1971, Observations on the chemical denudation of some karst areas of Europe and Asia: Studia Geomorphologica Carpatho-Balcanica, v. 5, pp. 77-92.

Puri, H.S., and Vernon, R.O., 1964, Summary of the geology of Florida and guidebook to classical exposures: Florida Geological Survey Special Publication no. 5 (revised), 312 p.

Randazzo, A.F., 1997, The sedimentary platform of Florida: Mesozoic to Cenozoic: In Geology of Florida by Randazzo, A.F. and Jones, D.S. (eds.), University Press of Florida, pp. 39-56.

Randazzo, A.F. and Bloom, J.I., 1985, Mineralogical changes along the freshwater/saltwater interface of a modern aquifer: Sedimentary Geology, v. 43, pp. 219-239.

Rosenau, J.C., Faulkner, G.L., Hendry, W. Jr., and Hull, R.W., 1977, Springs of Florida (revised): Florida Geological Survey Bulletin no. 31, 461 p.

Runnels, D.D., 1971, Chemical weathering of the Biscayne Aquifer, Dade County, Florida: Southeastern Geol., v. 13, pp. 167-174.

Safko, P.S. and Hickey, J.J., 1992, A preliminary approach to the use of borehole data, including television surveys, for characterizing secondary porosity of carbonate rocks in the Floridan aquifer system. U.S. Geological Survey, Water Resources Investigations Report no. 91-4168. 70 p.

Schmidt, W., 1997, Geomorphology and physiography of Florida: in Geology of Florida by Randazzo, A.F. and Jones, D.S. (eds.), University Press of Florida, pp. 1-12.

Schmidt, W., and Scott, T.M., 1984, Florida karst – Its relationship to geologic structure and stratigraphy, In Sinkholes: Their geology, engineering, and environmental impact, edited by B. F. Beck, Rotterdam: A.A. Balkema, pp. 11-16.

Scott, T.M., 1997, Miocene to Holocene history of Florida: in Geology of Florida by Randazzo, A.F. and Jones, D.S. (eds.), University Press of Florida, pp. 57-68.

Scott, T.M. and MacGill, Peter L., 1981, The Hawthorn Formation of central Florida; Part I, Geology of the Hawthorn Formation in central Florida: Fla. Bur. Geol., Report of Investigations, n. 91, 32 p.

Smith, D.I., 1969, Solutional erosion in the area around Maldon and Maroon Town, Jamaica, J. Brit. Speleo. Ass., VI, v. 43 / 44, pp. 120-133.

Smith, D.I., 1970, The residual hypothesis for the formation of Jamaican bauxite –a consideration of the rate of limestone erosion: J. Geol. Soc. Jamaica, v. 11, pp.3-12.

Smith, D. I., 1972, The solution of limestone in an Arctic environment: Inst. Brit. Geogr. Spec. Pub., v. 4, pp. 187-200.

Smith, D.I., and Atkinson, T.C., 1976, Process, landforms and climate in limestone regions: In Geomorphology and Climate, E. Derbyshire (ed.), 369-409. London: Wiley.

Soto, A.E., and Morales, W., 1984, Collapse sinkholes in the blanket sands of the Puerto Rico karst belt: In Sinkholes: their geology, engineering, and environmental impact, Beck, B.F. (ed.), Rotterdam, A.A. Balkema, pp. 143-146.

Strahler, A.N., 1957, Quantitative analysis of watershed geomorphology: Am. Geophys. Union Trans., v. 38, pp. 913-920.

Sweeting, M.M., 1964, Some factors in the absolute denudation of limestone terrains, Erdkunde, v. 18, pp. 92-95.

Troester, J. W., White, E.L., and White, W.B., 1984, A comparison of sinkhole depth frequency distributions in temperate and tropical karst regions: In Sinkholes: their geology, engineering, and environmental impact, Beck, B.F. (ed.), Rotterdam, A.A. Balkema, pp. 65-73.

Upchurch, S.B., 1989, Karst of Florida. In The Lithostratigraphy and Hydrostratigraphy of the Floridan Aquifer system in Florida, Field Trip Guidebook no. T185. 28th International Geological Congress, American Geophysical Union, pp. 46-55.

Upchurch, S.B., and Lawrence, F.W., 1984, Impact of ground-water chemistry along a retreating scarp: In Sinkholes: their geology, engineering, and environmental impact, Beck, B.F. (ed.), Rotterdam, A.A. Balkema, pp. 189-195.

Upchurch, S.B., and Littlefield, J.R.Jr., 1987, Evaluation of data for sinkhole-development risk models: In Karst Hydrogeology: Engineering and Environmental Applications, Beck, B.F., and Wilson, W.L., (eds.), Rotterdam, A.A. Balkema, pp. 359-364.

Vernon, R.O., 1951, Geology of Citrus and Levy counties, Florida: Florida Geological Survey, Geological Bulletin no. 33, 256 p.

Welch, D.M., 1970, Substitution of space for time in a study of space development: Jour. Geology, v. 78, pp. 5-18.

White, W.A.., 1958, Some geomorphic features of central peninsular Florida: Florida Geological Survey, Geological Bulletin no. 41, 92 p.

White, W.B., Culver, C.D., Herman, J.S., Kane, T.C, and Mylroie, J.E., 1995, Karst lands: American Scientist, v. 83, pp. 450-459.

White, E.L., and White, W.B., 1979, Quantitative morphology of landforms in carbonate rock basins in the Appalachian Highlands: Geol Soc. Amer. Bull., v. 90, pp. 385-396.

Wigal, J.M., 1948, A study of the lower Greenbrier group and some geologic controls on cavern development within Greenbrier County, West Virginia: M.Sc. Thesis, West Virginia University, p. 168.

Williams, P.W., 1966, Morphometric analysis of temperate karst landforms: Irish Speleol., v. 1., pp. 23-31.

Williams, P.W., 1971, Illustrating morphometric analysis of karst with examples from New Guinea: Zeit. Fur Geom., v. 15, pp. 40-61.

Williams, P.W., 1972, Morphometric analysis of polygonal karst with examples from New Guinea, Bull. Geol. Soc. Amer. Bull., v.83, pp. 761-796.

Williams, P.W., 1983, The role of subcutaneous zone in karst hydrology: Journal of Hydrology, v.61, pp. 45-67.

Wilson, W.L., 1995, Sinkhole and buried sinkhole frequencies in karsts of Northwest Peninsular Florida: In Karst GeoHazards, Beck, B.F. (ed.), Balkema, Rotterdam. pp. 79-91.

Wilson, W.L., and Beck, B.F., 1992, Hydrogeologic factors affecting new sinkhole development in the Orlando area, Florida: Ground Water, v. 30, no. 6, pp. 918-930.

Winston, G.O., 1976, Florida's Ocala Uplift is not an uplift: Bulletin of the American Association of Petroleum Geologists. v. 62, pp. 121-127.

BIOGRAPHICAL SKETCH

Can Denizman was born in Ankara, Turkey, and graduated from the Hacettepe University, where he received his B.Sc. and M.S. in hydrogeology. After working for the International Research and Application Center for Karst Water Resources, Ankara, Turkey, he moved to Gainesville in 1991 and attended the graduate school at the University of Florida.

I certify that I have read this study and that in my opinion it conforms to acceptable standards of scholarly presentation and is fully adequate, in scope and quality, as a dissertation for the degree of Doctor of Philosophy.

Anthony F. Randazzo

Anthony F. Randazzo, Chairman
Professor of Geology

I certify that I have read this study and that in my opinion it conforms to acceptable standards of scholarly presentation and is fully adequate, in scope and quality, as a dissertation for the degree of Doctor of Philosophy.

Douglas L. Smith
Professor of Geology

I certify that I have read this study and that in my opinion it conforms to acceptable standards of scholarly presentation and is fully adequate, in scope and quality, as a dissertation for the degree of Doctor of Philosophy.

Daniel P. Spangler

Daniel P. Spangler
Associate Professor of Geology

I certify that I have read this study and that in my opinion it conforms to acceptable standards of scholarly presentation and is fully adequate, in scope and quality, as a dissertation for the degree of Doctor of Philosophy.

Jonathan B. Martin

Jonathan B. Martin
Assistant Professor of Geology

I certify that I have read this study and that in my opinion it conforms to acceptable standards of scholarly presentation and is fully adequate, in scope and quality, as a dissertation for the degree of Doctor of Philosophy.

Joann Mossa
Associate Professor of Geography

This dissertation was submitted to the Graduate Faculty of the Department of Geology in the College of Liberal Arts and Sciences and to the Graduate School and was accepted as partial fulfillment of the requirements for the degree of Doctor of Philosophy.

May, 1998

Dean, Graduate School